


2009

Optimization of the microprecipitation procedure for nuclear forensics applications

Lyndsey Renee Kelly
University of Nevada Las Vegas

Follow this and additional works at: <https://digitalscholarship.unlv.edu/thesesdissertations>

 Part of the [Analytical Chemistry Commons](#), [Criminology Commons](#), [Evidence Commons](#), [Law Enforcement and Corrections Commons](#), [Nuclear Commons](#), and the [Radiochemistry Commons](#)

Repository Citation

Kelly, Lyndsey Renee, "Optimization of the microprecipitation procedure for nuclear forensics applications" (2009). *UNLV Theses, Dissertations, Professional Papers, and Capstones*. 166.
<https://digitalscholarship.unlv.edu/thesesdissertations/166>

This Thesis is protected by copyright and/or related rights. It has been brought to you by Digital Scholarship@UNLV with permission from the rights-holder(s). You are free to use this Thesis in any way that is permitted by the copyright and related rights legislation that applies to your use. For other uses you need to obtain permission from the rights-holder(s) directly, unless additional rights are indicated by a Creative Commons license in the record and/or on the work itself.

This Thesis has been accepted for inclusion in UNLV Theses, Dissertations, Professional Papers, and Capstones by an authorized administrator of Digital Scholarship@UNLV. For more information, please contact digitalscholarship@unlv.edu.

OPTIMIZATION OF THE MICROPRECIPITATION PROCEDURE FOR NUCLEAR
FORENSICS APPLICATIONS

by

Lyndsey Renee Kelly

Bachelor of Science
Louisiana State University
2007

A thesis submitted in partial fulfillment
of the requirements for the

Master of Science in Health Physics
Department of Health Physics and Diagnostic Sciences
School of Allied Health Sciences
Division of Health Sciences

Graduate College
University of Nevada, Las Vegas
December 2009



THE GRADUATE COLLEGE

We recommend that the thesis prepared under our supervision by

Lyndsey Kelly

entitled

Optimization of the Microprecipitation Procedure for Nuclear Forensics Applications

be accepted in partial fulfillment of the requirements for the degree of

Master of Science

Health Physics

Ralf Sudowe, Committee Chair

Steen Madsen, Committee Member

Phillip Patton, Committee Member

Vernon Hodge, Graduate Faculty Representative

Ronald Smith, Ph. D., Vice President for Research and Graduate Studies
and Dean of the Graduate College

December 2009

ABSTRACT

Optimization of the Microprecipitation Procedure for Nuclear Forensics Applications

by

Lyndsey Kelly

Dr. Ralf Sudowe, Advisory Committee Chair
Assistant Professor of Health Physics and Radiochemistry
University of Nevada, Las Vegas

Microprecipitation has become one of the most widely used sample preparation techniques for alpha spectroscopy. Many factors during the precipitation process can affect the yield and energy resolution by adding unwanted mass to the sample. Current applications in nuclear forensics call for an optimization of energy resolution and yield in order to improve identification and quantify specific radionuclides. The purpose of this research is to determine the optimal parameters used for microprecipitation. The optimal solution temperature, precipitation time, carrier amount, and hydrofluoric acid amount are used to investigate the influence of varying the type of carrier, as well as, the addition of hydrochloric acid and other radionuclides. The determined optimal parameter was 0.0125mg of cerium with 1mL of hydrofluoric acid at room temperature for 30 minutes. The optimal carrier concentration for lanthanum was 0.005mg while neodymium was 0.0025mg. A multinuclide solution had no impact on the results; however the addition of 20 mL of HCl should be reduced before performing microprecipitation. The homogeneity of the radionuclides deposited onto the source sample was determined by using autoradiography. The optimal parameters of microprecipitation, in addition to the deposition pattern of the radionuclide, can be used to improve identification and quantification of radionuclides for nuclear forensics applications.

AWKNOWLEDGEMENTS

First and foremost, I would like to thank my advisor, Dr. Ralf Sudowe, for his continuous patience, guidance, and support throughout my graduate studies. His willingness to provide never ending advice, direction, and expertise allowed me to grow academically and professionally. I consider myself extremely fortunate for the opportunity to master the field of Health Physics while gaining laboratory skills and knowledge of Radiochemistry. I am truly appreciative and honored to have worked for a professor who has encouraged me to do my best, pushed me to my limit, and instill confidence that I may have never gained. I have learned more through Dr. Sudowe than I ever thought possible. Thank you for never giving up on me.

I would also like to extend my appreciation to the many people that have helped me through my master's degree. I would like to thank my graduate committee, Dr. Steen Madsen, Dr. Phillip Patton, and Dr. Vernon Hodge, for all of the scientific expertise and assistance during my coursework and thesis preparation. Thank you to the radiochemistry gang for being brave enough to be my safety partner while using HF and volunteering your time to show me laboratory etiquettes and pipetting techniques: Chris Klug, Sherry Stock Faye, Ashlee Crable, and Megan Bennett. Also, I would like to give thanks to the UNLV Institute for Security Studies providing a grant to fund my research project.

I would like to thank the faculty and staff at the Louisiana State University for the immense support, generosity, and assistance throughout the years. Thank you, Ms. Yvonne Thomas, for all of your help throughout my education and for your happy smiles and conversations. Thank you, Dr. Erno Sajo, Dr. Kenneth Matthews, and Dr. L. Max Scott, for your incredible teaching and opening my eyes to the field of Health Physics.

Thank you, Dr. Lorraine Day, for simply brightening my day. Thank you for the years of dedication to the Deep South Chapter. You have a true passion for Health Physics and I admire you. I would like to truly thank the students, faculty, and staff at the Radiation Safety Office. Thank you all for teaching me the fundamentals of Health Physics, field work, instrumentation, lab surveying, and organizing the tons of paper work! I would like to give a special thanks to Ms. Mary Haik for being a strong, dedicated female professional that I could always go to for help even on a personal level. I have always looked up to you. You have worked so hard and have always looked out for the best interest of the office and students. Thank you to Mr. Richard Teague for teaching me instrumentation and for always willing to teach me everything you know—which is A LOT! Thank you, thank you, thank you! Without all of your help and encouragement, I would not be where I am today.

Last but certainly not least, a special thanks to Dr. Wei-Hsung Wang for hiring me at the Radiation Safety Office under his one condition: he will *try* to change my major from Medical to Health Physics (and of course, he succeeded). I truly could not have done my master's degree without you, Dr Wang. You always believed in me and cared about me academically and personally. Thank you for always giving me moral support and guidance throughout the years—even when I am 1,771 miles away. Thank you for willingly lending me your ear for complaining, a shoulder for crying, and a phone call for day-to-day laughing. You may believe that there could be no bigger shoes to fill than your advisor, Dr. Herman Cember, but I believe you have. Thank you for being my professor, my advisor, my boss, my therapist, my life coach, my mentor, and especially, my friend. Thank you for simply being you. Thank you for... everything!

LIST OF TABLES

Table 1.1	^{241}Am and ^{230}Th with varying Fe^{3+} carrier amounts	11
Table 1.2	La^{3+} on the ^{241}Am coprecipitation	12
Table 1.3	LaF_3 precipitate standing time on ^{241}Am	14
Table 1.4	Effects of temperature on the yield of ^{241}Am	15
Table 3.1	Varying the carrier with 1mL of HF	34
Table 3.2	Varying the amount of HF with 0.0125mg of cerium carrier	36
Table 3.3	Varying cerium carrier and hydrofluoric acid simultaneously	38
Table 3.4	Various precipitation temperatures	40
Table 3.5	Various precipitation times	42
Table 3.6	Various lanthanum concentrations.....	44
Table 3.7	Various neodymium concentrations	45
Table 3.8	Various concentrations of cerium with 20 mL of HCl	47
Table 3.9	Multinuclide solution containing ^{241}Am and ^{239}Pu	49
Table 3.10	Varying cerium with 20 mL of HCl in multinuclide solution	51

LIST OF FIGURES

Figure 2.1	Single Filtration Setup.....	17
Figure 2.2	Millipore Sampling Manifold.....	18
Figure 2.3	Exposing samples to film in cassette.....	30
Figure 3.1	FWHM verses the amount of Cerium with 1mL of HF	35
Figure 3.2	Yield verses the amount of Cerium with 1mL of HF.....	35
Figure 3.3	FWHM with varied HF and 0.0125mg of cerium carrier.....	37
Figure 3.4	Yield with varied HF and 0.0125mg of cerium carrier	37
Figure 3.5	FWHM of cerium and HF varying simultaneously	39
Figure 3.6	Yield of cerium and HF varying simultaneously	39
Figure 3.7	FWHM verses different precipitation temperatures	41
Figure 3.8	Yield verses various precipitation temperatures.....	41
Figure 3.9	FWHM verses various precipitation times	43
Figure 3.10	Yield verses various precipitation times.....	43
Figure 3.11	FWHM for various concentrations of La, Ce, and Nd	45
Figure 3.12	Yield for various concentrations of La, Ce, and Nd.....	46
Figure 3.13	FWHM varying cerium with 20 mL of HCl.....	47
Figure 3.14	Yield varying cerium with 20 mL of HCl	48
Figure 3.15	FWHM for ^{241}Am and ^{239}Pu verses the cerium concentration	49
Figure 3.16	Yield for ^{241}Am and ^{239}Pu verses the cerium concentration.....	50
Figure 3.17	FWHM for multinuclide solution with 20 mL of HCl	51
Figure 3.18	Yield for multinuclide solution with 20 mL of HCl.....	52
Figure 3.19	Autoradiographic visuals of various cerium concentrations	53
Figure 3.20	Autoradiographic visuals of 0.0025 and 0.05mg of La, Nd, Ce.....	54

TABLE OF CONTENTS

ABSTRACT.....	iii
ACKNOWLEDGEMENTS.....	iv
LIST OF TABLES.....	vi
LIST OF FIGURES.....	vii
CHAPTER 1 INTRODUCTION.....	1
Nuclear Forensics.....	1
Alpha Spectroscopy.....	2
Literature Review.....	9
Objective of Proposal.....	15
CHAPTER 2 METHODOLOGY.....	16
Materials.....	16
Experimental Apparatus.....	16
General Method.....	18
Scope of Research.....	19
Investigated Parameters.....	22
Liquid Scintillation Counting.....	26
Alpha Spectroscopy.....	27
Radiometric Phosphor Imager.....	28
CHAPTER 3 RESULTS AND DISCUSSION.....	31
Data Analysis.....	31
Parameter Discussion.....	33
Visual Interpretations.....	52
Results.....	54
CHAPTER 4 ERROR ANALYSIS.....	61
Data Error.....	61
Experimental Error.....	62
Instrumentation Error.....	65
CHAPTER 5 CONCLUSION.....	68
CHAPTER 6 FUTURE RESEARCH.....	74
APPENDIX I MATERIALS, CHEMICALS, AND CHEMICAL FORMULAS.....	75
APPENDIX II TABLES.....	76
BIBLIOGRAPHY.....	103

VITA..... 105

CHAPTER 1

INTRODUCTION

1.1 Nuclear Forensics

The events of September 11, 2001 revealed the weaknesses in the United State's defense. In response to these events, national security efforts have focused on ensuring the safety and protection of nuclear and radioactive sources that could potentially be utilized by terrorists to construct a improvised nuclear devise (IND) or radiological dispersement device (RDD). In the case of a radiological incident, the nation must be prepared to analyze environmental samples quickly and efficiently to determine the identification and quantification of all radionuclides of interest present within each sample. With newly developing interests, the field of "nuclear forensics" has been established to assess the origins of the nuclear and radioactive material resulting from nuclear smuggling or trafficking in hopes to prevent any future terrorist attacks against the country.

Nuclear forensics is defined by the IAEA as "the analysis of intercepted illicit nuclear or radioactive matter and any associated material to provide evidence for nuclear attribution" (Kristo 2009). Today, nuclear forensics concentrates on discovering the origins of a nuclear bomb or RDD via databases, libraries, and sample archives that contain a detailed, specific list of nuclear and radioactive material that each country possesses. As a result, the need to improve sample analysis for identification and quantification of radionuclides has increased, in particularly, the analysis of alpha

emitters. After a nuclear or RDD incident, signatures from alpha emitting particles will be one of the key identifiers used to indict a responsible party.

Whether preparing for prevention or investigating the aftermath of a nuclear or RDD attack, interest has increased to advance the methods used for alpha spectroscopy for nuclear forensics applications. A reliable method to identify and quantifying alpha emitters needs to be enhanced by optimizing the current parameters used for source preparation. In addition, the time to analyze samples should also be considered especially in emergency response situations. Improving the identification and quantification of alpha emitting radionuclides in environmental samples is not only essential for emergency response applications but can also be used in other fields of nuclear science such as nuclear waste management, site decontamination and decommissioning, and environmental assessment. However, the improvement for alpha spectroscopy techniques is especially vital for the field of nuclear forensics.

1.2 Alpha Spectroscopy

The interaction of radiation with matter depends on the charge of the particle, type and energy of radiation, and the density and atomic number of the absorbing material. Compared to other types of radiation, alpha particles are massive and carry a charge of +2 which causes the particle to interact readily with the surrounding material through columbic forces. As alpha particles pass through matter, the interactions between the positive charge of the alpha particles ionizes or excites the negatively charged electrons found in material. Because of the numerous interactions encountered, an alpha particle readily loses energy along its path as it passes through matter. The more interactions the particles encounter, the faster the particles loses energy. When the alpha particle slows to

a complete stop, the energy deposited increases due to the increase of ionizations occurring. In air, alpha particles can travel only a few centimeters; while in the body, alpha particles can penetrate only a few layers of tissue.

The investigation of alpha emitting radionuclides is of great public concern due to the health hazards that alpha particles pose. Alpha emitters are one of the most damaging radionuclides for humans if taken up by the body via absorption, inhalation, injection, or ingestion. Since alpha particles have a short emission range, the energy will be deposited locally within the tissue of the body. The uptake of alpha emitters has been shown to cause cellular DNA damage; however, humans are often at greater risk from the short-lived daughter products originating from the parent. Once the radionuclide is deposited within the body, the parent radionuclide will decay to daughter atoms that may cause continuous radiological damage to the cells for tens to thousands of years depending on the half-life of the mother nuclide. The public's fear of health hazards associated with radiation, in particularly cancer, has triggered an additional need for more reliable analytical techniques for detecting alpha particles.

For environmental sample analysis, alpha emitters must be separated from all other foreign materials present in the sample. Ideally, alpha emitting nuclides should be evenly distributed onto a flat surface as thin as possible to avoid any attenuation. If a monatomic layer is not achieved, the alpha particle may become attenuated by the surrounding material which will lead to energy loss by the material found in the sample. This process is known as "self absorption." If any attenuation occurs, the particles will not directly reach the detector causing a decrease in count rates and energy. Attenuation is not only due to the contaminants within the sample but can occur in the space between the source

and the detector via interactions with air molecules. The latter attenuation can be fixed simply by applying a vacuum within the detector chamber. Any attenuation that may occur from energy loss will result in a broadening of the peak spectrum, ultimately causing a decrease in energy resolution and a decrease in yield. As the energy resolution decreases, the potential for overlap between energy peaks will also increase. If the sample being analyzed has more than one radionuclide present, the increase in the full width half maximum, FWHM, may be too wide to distinguish each individual radionuclide energy peak. Thus, misidentification of the radionuclides can occur.

One of the largest difficulties is detecting low activity concentrations of alpha emitting radionuclides in an environmental sample. Because of the sensitivity required, no interference should occur in order to achieve an accurate count rate. If any attenuation occurs, the resulting count rate will show a dramatic decrease. Consequently, many scientists will count the sample for a longer period of time in order to obtain the best possible yield and counting statistics. In the case of a nuclear incident, time should be reduced as much as possible while achieving the best possible energy resolution and yield of the sample.

Alpha spectroscopy has many controllable factors that could be optimized to give better results; although, some optimizations may result in a less desirable product. First, in order to get source samples as thin as possible, the sample could be spread evenly over a wider area. However, as the area gets larger, the counting efficiency decreases and the peak will acquire tailing at lower energies. The tailing is caused by the large angle between the source and the detector. Ultimately, the peaks will not look monoenergetic but will have characteristics of a spectrum of energy that may cause misidentification and

quantification. The source should be spread evenly over a reasonable size area to avoid any tailings. Secondly, the amount of air between the source and the detector could be reduced to decrease the probability of the alpha particle interacting with an air molecule. If the alpha particles interact with the air molecules, attenuation will occur resulting in a decrease in counts. However, decreasing the air thickness would also increase the potential of recoil contamination within the detector due to less absorbance from the air molecules. The density of air between the detector and source should be thin enough to avoid attenuation; yet, thick enough to avoid recoil atom to contaminate the detector. Next, increasing the distance between the source and the detector would allow only the particles traveling in a straight path to reach the detector instead of the scattered particles. Yet, increasing the distance will decrease the counting efficiency. Lastly, the windows to the detector should be as thin as possible to allow alpha particles to enter. Nevertheless, scientists should look at all factors that can be controlled in order to optimize the procedure used for alpha spectroscopy.

1.2.1 Methods of Source Preparation for Alpha Spectroscopy

To prevent poor energy resolution characterized by wide peaks, many different methods can be used to prepare the sample source in order to achieve a homogenous, thin surface. The three methods used most commonly for source preparation are electrodeposition, evaporation, and microprecipitation. The evaporation method simply heats all of the components of the sample onto a planchet; while, electrodeposition and microprecipitation samples undergo various chemical and physical transformations to eliminate any extra mass that may cause attenuation. In any case, the goal is to achieve the thinnest possible surface thickness. However, each of the methods relies on different

separation techniques that result in different mounting techniques of the substrates, such as filters or metal disks. Separation along with purification is necessary especially in cases with low activity to reduce radiochemical interferences. Deciding on a suitable source preparation method is one of the most critical steps in the analysis of alpha emitters. When determining the best method, the strengths and weaknesses of each method along with the detection method should be considered.

One of the most common and widely used source preparation methods is electrodeposition. The method begins with a solution containing a radionuclide, which is then added to an electrolytic solution. The solution undergoes an electrochemical process through which the radionuclides are deposited onto a metal planchet once a voltage is applied for a given time. This process is known as “nonspontaneous” electrochemical process (MARLAP). The radionuclides can also be deposited onto the planchet “spontaneously” without an applied voltage depending on the electrode potential between the ion and electrode (MARLAP). As a result, electrodeposition produces a thin, uniform layer of deposited radionuclides on the planchet which is required for alpha spectroscopy.

However, several disadvantages discourage scientists from using electrodeposition as a preferred preparation method. First, interferences within the electrolyte solution or any interferences resulting from an incomplete separation prior to source preparation may potentially be deposited onto the planchet. Examples of interferences include metals, in particularly iron, rare earth elements, or organic material. Increasing mass onto the planchet results in an increasing potential for attenuation. Secondly, some requirements must be met to use electrodeposition. Samples cannot be massive, typically less than 100nm, because a thick deposition layer will accumulate onto the planchet (Pollanen

2006). Also, stainless-steel planchets cannot be used due to the corrosiveness of the electrolytic solution. The use of platinum planchets is preferred but can be expensive. Reuse of the planchet is not only time consuming but the probability of cross contamination can also increase if the planchet is not cleaned properly. Lastly, the apparatus of electrodeposition is difficult to maintain and can have many problems with the overall set up. One of the most common problems is leakage of cells that may cause a loss in sample and contamination onto the apparatus. Other problems that may occur are current fluctuations and pH changes during electroplating which can lead to low isotope recovery. Because of the possible problems associated with electrodeposition, large variations occur in the results. Without consistent results, reproducibility is difficult to achieve.

If good energy resolution is not a major necessity for the measurement, simple evaporation can be used for sample preparation. Evaporation is extremely easy, fast, and adequate for preparing samples. The entire sample amount is transferred to a stainless steel planchet and evaporated to dryness under a heat lamp or in an oven. To minimize the amount of solids present on the planchet, the planchet can be flamed over a burner. However, some volatile radionuclides will be lost during flaming. Once the sample has cooled, the sample can be weighed and counted.

Some problems are associated with evaporating solids. The major problem associated with evaporation is that the entire sample contents are dried onto the planchet. Without eliminating the other interferences found in the sample, more mass will remain with the sample resulting in poor energy resolution. Another problem encountered with evaporation is that the solids form a ring around the edge of the planchet which causes

the sample to not be uniform. To help with the uniformity problem, some techniques can be employed before evaporation to prevent sample loss. Some additives include a wetting agent, such as tetraethylene glycol or a 5% insulin solution, freeze-drying the sample, or precipitation (Friedlander 1981). Before the sample is put onto the planchet, a wetting agent can be pipetted onto the planchet and then be removed.

1.2.2 Microprecipitation

Microprecipitation is another source preparation method that has gained favor compared to evaporation and electrodeposition. Microprecipitation is a type of coprecipitation that uses a soluble component combined with a nonisotopic carrier to form a precipitate. In many environmental samples, concentrations of radionuclides are usually too low to precipitate directly. This is due to the fact that the solubility constant is not exceeded. Since it is impossible to increase the concentration of the element above the solubility constant to form a precipitate, the radionuclide needs to be separated from the solution by introducing an alternative insoluble compound. Other isotopic forms of the element can increase the total concentration of the element to form a precipitate. This is known as a “carrier.” A carrier can be either isotropic or nonisotropic. An isotopic carrier is a compound of the same element as the radionuclide of interest in the sample. On the other hand, nonisotopic carriers are different elements with chemical and physical property characteristics similar to the radionuclide of interest. When analyzing environmental samples, nonisotopic carriers are preferred since isotopic carriers interfere with the counting statistics. Nonisotopic carriers are particularly used to separate radionuclides to retain high specific activity (Moody 2005). In addition, some

radionuclides do not have stable isotope. Therefore, isotopic carriers cannot be used for such elements. Examples include polonium and astatine.

Many advantages are associated with microprecipitation, making it a preferred method compared to evaporation and electrodeposition. First, small amounts of manipulation are performed on the source. Even though a carrier is used, only “micro” amounts of the carrier will remain with the sample. As a result, high yields and good peak resolutions are achieved. Secondly, due to the little manipulation, the process is faster yet more reliable compared to electrodeposition. Consistency is a necessity in the case of a nuclear incident where a large number of samples needs to analyze accurately. Also, microprecipitation does not require sophisticated equipment. A simple filtration system can be acquired from any laboratory inventory.

1.3 Literature Review

During the 1980s, microprecipitation was first introduced by Sill as an alternative to electrodeposition as the premier source preparation method (Sill 1981). In his studies, Sill showed that lanthanide carriers such as cerium gave better results than smaller ions such as iron or zirconium. Comparable results were also obtained for lanthanum and neodymium. However, the use of cerium became more desirable than that lanthanum and neodymium because of its additional oxidation state which made it easier to purify (Sill 1981).

In addition, Sill investigated several other parameters relevant to the preparation of sources for alpha spectroscopy (Sill 1987). First, he investigated the type of different filter substrates and the influence of flow rate. For the majority of his earlier studies, a polysulfone filter, Tuffryn HT-100, with a pore size of 0.1 μm was used. Because the

filters were discontinued, Sill switched to polysulfone membrane filter with 0.2 μm pores which resulted in poor energy resolution and yield. Sill believed that the sample loss was due to either the pores being too large or the flow rate of 5 mL/minute being too high. He switched to a polypropylene membrane filter with 0.1 μm pores size which gave him excellent energy resolution and yield. However, the polypropylene filters have a low melting point and care must be taken so that the filters do not curl or melt (Sill 1987).

A number of recent studies in the peer-reviewed literature have focused on improving the method performance of microprecipitation. However, the majority of these studies did not focus on a general method of optimization. Instead, the parameters that were investigated were unique to a specific application. For instance, the carriers used for precipitating ^{241}Am and ^{239}Pu varied depending on the author. In most cases, a cerium carrier was used to precipitate actinides (Hindman 1983); however, in other cases, the use of lanthanum (Joshi 1985) and neodymium (Hindman 1983) was preferred. A quantitative comparison of the performance of different carriers was not performed nor did any of the references discuss why a certain carrier was preferred. An investigation of the different types of carriers needs to be performed to determine the optimal carrier type.

Extensive research has been performed comparing the different amounts of carrier used for microprecipitation along with varying the temperature and time available for the precipitate to form. One study by Lozano varied the amount of Fe carrier, used to form a $\text{Fe}(\text{OH})_3$ substrate, at 30 μg and 45 μg while also alternating the temperature of the precipitation from 100 $^{\circ}\text{C}$ to room temperature (Lozano 1997). The precipitation time was held constant at 30 minutes (See Table 1.3.1). The results show that at higher carrier amounts, the yield and energy resolution became worse compared to lower amounts of

carrier (Lozano 1997). In addition, the results of the precipitation temperature study showed that the yields were comparable to each other and the energy resolution improved at room temperature compared to 100°C. Lozano stated that better results at room temperature were obtained because the “precipitation at room temperature may have produced finer particles than in a hot process” (Lozano 1997). However, additional data points are needed to determine the optimal precipitation temperature, time, and amount of carrier.

Table 1.1 The FWHM and yield of ^{241}Am and ^{230}Th with varying Fe^{3+} carrier amounts, filter sizes, and precipitation temperatures (Lozano 1997).

Nuclide	Carrier (μg)	Filter size (μm)	Precipitation ^a ($^{\circ}\text{C}$)	Yield ^b (% decimal)	FWHM ^b (keV)
^{241}Am	30	0.1	100	99.9 ± 3.2	63 ± 4
	30	0.1	Room-temp	100.8 ± 3.3	42 ± 3
	45	0.2	100	98.2 ± 3.0	76 ± 6
^{230}Th	45	0.2	Room-temp	97.8 ± 2.9	66 ± 4
	45	0.2	100	98.3 ± 3.0	65 ± 5
	45	0.2	Room-temp	96.8 ± 2.8	59 ± 4

^a Digestion was done at 100°C

^b Mean values of three measurements plus minus two standard deviations

Another study performed by Jia optimized a number of parameters. The first parameter investigated was the amount of lanthanum carrier used for the precipitation of ^{241}Am . The precipitation time was kept constant at 30 minutes and the precipitation was performed at room temperature. The results are shown in Table 1.3.2.

Table 1.2 The effects of the amount of La^{3+} on the ^{241}Am coprecipitation (Jia 1994).

La^{3+} (μg)	LaF_3 (μg)	LaF_3 ($\mu\text{g}/\text{cm}^2$)	^{241}Am Yield ^a (%)	FWHM ^a (keV)
10	14.1	4	87.6 ± 8.2	39.4 ± 6.2
25	35.2	10	97.2 ± 1.4	49.6 ± 3.2
30	42.3	12.1	98.4 ± 2.1	51.6 ± 5.2
40	56.4	16.1	93.6 ± 3.0	46.4 ± 4.8
50	70.5	20.1	101.0 ± 1.3	50.0 ± 4.4
80	113	32.3	95.6 ± 2.1	67.4 ± 4.2
120	169	48.3	100.6 ± 0.5	89.5 ± 8.7

^aMean values of three measurements plus minus two standard deviations

The results show that as the amount of lanthanum carrier increases, the yield improves while the energy resolution gets worse especially for carrier amounts greater than $80\mu\text{g}$.

To determine the best possible yield and energy resolution, smaller amounts of carrier should be evaluated, in particular, carrier amounts below $50\mu\text{g}$ (Jia 1994).

Secondly, the effect of varying the amount of hydrofluoric acid on the precipitation of ^{241}Am was also investigated by Jia. The amount of carrier used was kept at $50\mu\text{g}$ of lanthanum with a 30 minute standing time for the precipitate to form at room temperature. The results, reported in Table 1.3.3, show that the yield increased as the amount of HF increased. At least 0.2 mL of HF is needed to achieve yields greater than 92%. Once the hydrofluoric acid has exceeded 0.2 mL, the yield of ^{241}Am begins to plateau and reaches an average of roughly 93%. The study did not discuss the energy resolution for each amount of HF. To determine the optimal HF amount, a study of HF with constant carrier needs to be performed. In addition, a study of fractionating simultaneously the amount of HF and carrier together should also be performed. The

optimal HF and carrier amount should be determined based on the results from both the yield and energy resolution (Jia 1994).

A similar study performed by Stock tested the amount of cerium and hydrofluoric acid needed for optimization along with experiments that showed the effect of fractionation of cerium and hydrofluoric acid. The results showed that the optimal concentration of cerium was $1.98\text{E-}4$ mol of Ce^{3+} . The FWHM and yield at the optimized carrier concentration of $1.98\text{E-}4$ mol of Ce^{3+} was 27 ± 2 keV and $98 \pm 6\%$. Lastly, the study tested the minimal amount of hydrofluoric acid required to get comparable results. The conclusion of the study showed that reducing the amount of hydrofluoric acid to 3.11 mol of F improved the results; however, an optimal amount was never determined (Stock 2007).

Lastly, the effect of the precipitation time and temperature was investigated. During a precipitation study by Jia, constant amounts of $30\mu\text{g}$ of lanthanum carrier and 0.3mL of HF were used. The precipitation times investigated were 3, 10, 20, 30, 60, and 1440 minutes at room temperature. Results are seen in Table 1.3.4. According to this study, at least 20 minutes is needed for the precipitate to form. However, if the solution is left for longer than 1440 minutes, the yield decreases. A more thorough investigation between 20 and 1440 minutes should be performed to determine the optimal precipitation time (Jia 1994). The energy resolution should also be included into the results along with the yields to determine the optimal procedure.

Table 1.3 Effect of LaF₃ precipitate standing time on ²⁴¹Am using 30 μg of La and 0.3 mL of Hydrofluoric acid (Jia 1994).

Standing Time (min)	²⁴¹ Am Yield ^a (%)
3	82.6 ± 11.4
10	91.9 ± 5.0
20	96.1 ± 7.1
30	93.4 ± 3.0
60	95.2 ± 2.8
1440	68.9 ± 19.7

^aMean values of three measurements plus minus two standard deviations

Another study performed by Stock took into account both energy resolution and yield during a precipitation time study. The study evaluated the microprecipitation technique as described by Eichrom (Eichrom 2004). The time for the precipitate to form was varied between 10, 20, 30, 40, 50, and 60 minutes. The results showed that 30 minutes was the optimal time for the precipitate to form considering both the optimal yield and energy resolution (Stock 2007).

In addition to the precipitation time study, an experiment conducted by Jia evaluated the effects of the precipitation temperature with a 30 minute precipitation time. The temperatures evaluated were 10, 13, 20, 26, 30, 36, and 50°C. The results are seen in Table 1.3.5. The yields in the table are comparable to each other; however, temperatures above 30°C are more consistent. To determine the optimal parameter, an investigation including the energy resolution should also be conducted (Jia 1994).

Table 1.4 Effect of temperature on the yield of ^{241}Am at a precipitation time of 30 minutes (Jia 1994).

Temperature (°C)	^{241}Am yield (%)
10	92.9
13	100.2
20	93.9
26	93.2
30	96.8
36	99.4
50	97.9

1.4 Objective of Proposal

The objective for this research is to optimize the procedure used for microprecipitation as a sample preparation method for alpha spectroscopy. The parameters investigated are the amount and type of carrier, amount of hydrofluoric acid, temperature, and precipitation time. Other influences such as precipitation from larger sample volumes and multinuclide solutions will also be investigated. The goals for the research will focus on obtaining the best spectral resolution and yield while also achieving both in the least amount of time. Ultimately, the results from the research will be confirmed visually by assessing the filters using an autoradiographic instrument to determine the homogeneity of the radionuclide deposition, and an optical and scanning electron microscope to determine the homogeneity of the carrier deposition.

CHAPTER 2

EXPERIMENTAL

2.1 Materials

The materials used for all the experiments are listed in Appendix I

2.2 Experimental Apparatus

2.2.1 Single Filtration Apparatus

One apparatus used for the filtration of single samples during the microprecipitation experiments consisted of a Gelman filtration system that included a polycarbonate base with a metal grid screen inserted on top of the base. The grid screen is used to hold the 0.1 micron 25mm diameter polypropylene Resolve filter in place. A 25mm diameter polysulfone, twist-lock funnel, which could hold a maximum of 50mL volume of liquid, is tightened on top of the Gelman apparatus. Before tightening, the filter is placed on the metal grid which lies between the funnel and the base. A rubber stopper is placed at the bottom of the Gelman apparatus to connect it to a 500 mL polypropylene flask which catches the sample filtrate. The rubber stopper also guarantees no leakage of solution and restricts air flow while vacuum is applied to the flask. A second flask is connected to the first flask via rubber tubing and serves as a “trap” to catch any solution that may possibly have leaked from the primary flask before it can enter the vacuum pump. Without the second flask, contamination could potentially spread into the vacuum system. Lastly, a vacuum is applied to ensure a continuous, consistent suction through the filtration system.



Figure 2.1 Single Filtration Setup (Stock 2007)

2.2.2 Multi Filtration System Apparatus

An alternative to the single filtration system is the use of a multiposition filtration system. Such a system allows the filtration of multiple samples in parallel and would definitely be required for emergency response scenarios where quicker and/or numerous sample preparation is desired. The Millipore Model 1225 Sampling Manifold was used in this work to filter up to twelve samples at one time. With the addition of the Millipore manifold, it was possible to obtain more data in a smaller amount of time.

The Millipore sampling manifold is composed of a round canister containing a test tube rack that can hold up to twelve 15mL test tubes, approximately 125mm x 16 mm diameter (Millipore 2000). The test tubes are placed in the rack to catch the filtrate once the sample solution has been filtered. A support plate, containing 12 support screens is placed on top of the chamber. Each screen lines up with a particular test tube underneath

it. The filters are placed onto the support screen and held tightly by a top plate, which has 12 corresponding sample cups used to funnel the solution. The apparatus is tightened using a screw and nut which holds all of the components together as seen in Figure 2.2. Vacuum can then be applied to the system.

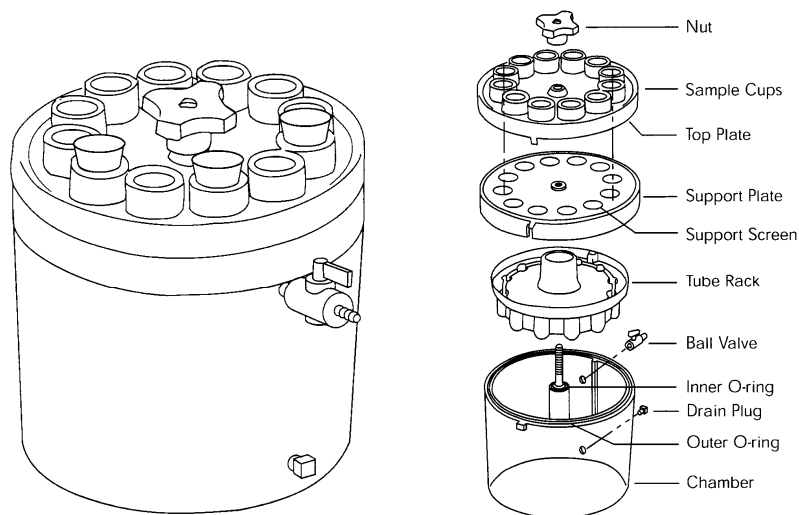


Figure 2.2 Millipore Sampling Manifold (Millipore 2000).

2.3 General Method

Once the apparatus is correctly set up, an initial rinse with ethanol (C_2H_5OH) is needed to open the filter pores and allow the solution to flow through the filter. The filter is then rinsed with DI water to ensure that the sample can be properly filtered through the filter without any leakage occurring. The filter may need to be rinsed again if too much time has passed before filtering the sample solution. The longer the filters sit, the more likely it becomes that the filter will dry out and the pores will close. If there are any signs

of leakage from the system when the DI water is applied, the leakage will need be controlled before pouring the sample into the funnel. Without testing for leaks, contamination onto the outside of the filtration system and sample loss could be possible.

For microprecipitation, a carrier is introduced to a sample solution containing an alpha emitting radionuclide. Only “micro” amounts of the carrier are added to the solution to minimize the mass on the filter. After the carrier is added, hydrofluoric acid is introduced to the solution and a precipitate forms immediately. The precipitate is left to form for a given length of time and the solution is then passed through one of the filtration systems as described above. The funnel is rinsed with DI water to ensure that the entire sample is removed from the edges. Lastly, the filter is rinsed with ethanol to replace any water that may be left on the filter. The filter is then placed in a petri dish and dried under a heat lamp. Once the filter is dry, it is taped onto a 25 mm stainless steel planchet using double sided tape to be assayed by alpha spectroscopy. Until it is counted, the planchet is stored in a petri dish. The lid of the dish is labeled to clearly identify the sample contained within each.

2.4 Scope of Research

There are different parameters that can affect the performance of the microprecipitation procedure, in particular the yield and energy resolution that can be achieved. These parameters include the amount of carrier, the amount of hydrofluoric acid, the ratio of carrier to hydrofluoric acid amount, temperature, time allowed for the precipitate, and the type of carrier. Other influences affecting the method performance can stem from the separation steps that precede the source preparation. Such influences include the solution matrix in which the sample is present, e.g. acids or organic

complexants, the volume of solution and/or the presence of other radionuclides. The parameters affecting the microprecipitation directly as well as these additional influences need to be evaluated to determine the optimal conditions for microprecipitation.

The first parameter investigated would be the influence of the amount of carrier. For this purpose the amount of cerium carrier would be varied while holding the amount of hydrofluoric acid constant. Each experiment will be performed using 700 μ L of ^{241}Am . Once the optimal amount for cerium is obtained, the influence of the amount of hydrofluoric acid will be determined by varying the amount of acid while keeping the amount of carrier constant at the optimal value obtained in the first study. A third set of experiments will be performed to determine the dependence on the ratio between the amounts of cerium and hydrofluoric acid. Once the optimal amounts of cerium and hydrofluoric acid are known, the time and temperature dependence on the formation of the precipitate will be explored.

Once the optimal parameters for the single radionuclide microprecipitation from pure solutions using cerium as a carrier have been acquired, then the influence of other factors will be investigated. First, a comparison between the different types of carriers will be carried out. The carriers examined will be lanthanum and neodymium due to the fact that these carriers are all in the same group of elements as cerium known as the lanthanide series. Due to the similarities in oxidation state and ionic radius, lanthanides will easily form a precipitate with tri and tetravalent actinides such as ^{241}Am or ^{239}Pu .

Next, the influence of sample volume and matrix will be considered. Microprecipitation from hydrochloric acid will be investigated in particular, because this acid is a common matrix for the elution of ^{241}Am after successful chemical separation.

The amounts of hydrochloric acid will be adjusted to typical amounts used in common chemical separation procedures.

Another concern with environmental samples is the impact of other radionuclides that might be present in solution during the precipitation. The simultaneous precipitation of multiple radionuclides is of special interest in cases where chemical separation is not required or not possible. For this purpose, precipitations from a combined solution of ^{241}Am and ^{239}Pu will be investigated. The alpha energies of these two nuclides are sufficiently different to allow their simultaneous determination. The optimal parameters obtained for the single radionuclide solution containing ^{241}Am will be used to determine the influence of the ^{239}Pu added to the solution. Finally, samples containing both a multinuclide solution as well as larger volumes of hydrochloric acid will be evaluated.

Finally, the homogeneity of the radionuclide deposition onto the filter will be determined using autoradiography. The theory of autoradiography acquires an image by accumulating emissions of radiation decays. The image obtained from the filters will determine how and where the radionuclide is deposited. Additionally, an image of optimal parameters will show which deposition pattern results in high energy resolution and yield.

The optimal parameter for all experiments will be based on the best possible energy resolution and yield while considering the time required to perform each assessment. The energy resolution is based on the FWHM of the peak. The FWHM needs to be as small as possible to facilitate easy peak-to-peak identification of radionuclides and to prevent the overlap of multiple peaks in the spectra. On the other hand, the yield should be as high as possible in order to minimize the counting time required to obtain statistically valid results.

The optimal set of parameters can therefore depend strongly on the ultimate application and three different categories will be considered: parameters used for identification of the radionuclides, parameters used for quantification of radionuclides, and a combination of both identification and quantification of radionuclides.

2.5 Investigated Parameters

2.5.1 Amount of Cerium with Constant Hydrofluoric Acid

The process of microprecipitation requires a certain amount of carrier to be present in order to form a precipitate. If not enough carrier is present, the radionuclides will precipitate only partially or not at all and will therefore still be present in the supernate. If too much carrier is present in the solution, then the carrier will add more mass to the filter and decrease the count rate through attenuation affecting both yield and energy resolution. The carrier cerium was evaluated at different concentrations to determine the amount needed to give the best yield and energy resolution. The concentrations used were 0.0025, 0.005, 0.0125, 0.025, 0.05 mg. The amount of hydrofluoric acid was held constant at 1mL.

2.5.2 Amount of Hydrofluoric Acid with Constant Cerium

In addition to the optimal amount of carrier, the optimal amount of hydrofluoric acid was determined by using 0.0125mg of cerium and varying the amount of acid. The investigated volume of acids were 250, 500, 750, 1000, and 1250 μ L. If not enough hydrofluoric acid is present, the volume of acid will not be enough to form the precipitate of AmF₃ and CeF₃. Unlike cerium, large volumes of hydrofluoric acid should not affect the energy resolution and yield. From the breakdown of hydrofluoric acid, the fluoride

ion will readily react with the cerium and americium; however, any extra HF will remain in the filtrate.

2.5.2 Varying Cerium and Hydrofluoric Acid Simultaneously

Once the optimal amounts of cerium and hydrofluoric acid had been determined, then the influence of the relative amounts of cerium to hydrofluoric acid was evaluated. The ratio of cerium and hydrofluoric acid was held constant; however, the amount of cerium and hydrofluoric acid was varied simultaneously. The evaluated concentrations of cerium and hydrofluoric acid, respectively, were: 0.0025mg with 50 μ L, 0.005mg with 100 μ L, 0.0125mg with 250 μ L, 0.025mg with 500 μ L, and 0.05mg with 1000 μ L.

2.5.3 Temperature Study

As soon as hydrofluoric acid is added to the solution, the precipitate begins to form. The temperature of the solution can affect precipitate formation. The influence of temperature on microprecipitation will be evaluated by holding the precipitation time constant at 30 minutes. A water bath was used to adjust the temperature and hold it constant over the course of the experiment. Precipitations were carried out at 25, 30, 35, 40, 45, 50°C.

2.5.4 Time Study

Once the optimal temperature had been determined, the time that the precipitate was allowed to form was evaluated. If too little time is given from the time HF is added into the sample solution to the time of filtration, the precipitate will not form. This means that the radionuclide will remain in the supernate. If too much time is elapsed, the formation of AmF₃ may breakdown. Ultimately, this may transport the americium back into the supernate before filtration occurs. In any case, timing is important for optimization of the

procedure for microprecipitation. The different precipitation times used were 10, 20, 30, 45, and 50 minutes, and 1, 2, 4, 8, 16, and 24 hours.

2.5.5 Carrier Study

Lanthanide elements are preferred as carriers for the microprecipitation of actinide elements because they share many structural and chemical characteristics. Members of both series readily form fluoride compounds when hydrofluoric acid is introduced, e.g. americium and cerium will form CeF_3 and AmF_3 , respectively. However, there are other lanthanide elements that can be used as carrier besides cerium. In addition to cerium, lanthanum and neodymium were evaluated as carriers as well. These two elements were studied using the same amounts that were used for cerium, namely 0.0025, 0.005, 0.0125, 0.025, 0.05 mg. The optimal parameters for the amount of hydrofluoric acid, time, and temperature previously determined in the cerium studies were used.

2.5.6 Interference of Hydrochloric Acid

Before the preparation of counting sources can occur, most environmental samples will undergo chemical separations to eliminate any interfering matrix elements or to separate one radionuclide from another. The main techniques used for chemical separations are co-precipitation, liquid-liquid extraction, ion exchange and extraction chromatography. As a result of these processes, the sample will have a finite volume before microprecipitation and different mineral acids are added to the sample solution. One of the standard separation procedures for ^{241}Am results in an elution fraction of approximately 20 mL of 4 M hydrochloric acid (Eichrom 2000). To determine the influence of the additional sample volume and to evaluate the effect of the acidic sample matrix, microprecipitations were carried out using a sample solution of 20 mL of 4 mL

hydrochloric acid using 0.0025, 0.005, 0.0125, 0.025, 0.05, 0.1, 0.2, 0.3, 0.4, 0.5, and 0.6 mg of cerium carrier. The amount of hydrofluoric acid, precipitation time, and precipitation temperature were held constant at the optimal values determined earlier.

2.5.7 Interference of Multi Radionuclide Solution

Typical environmental samples, in particular those taken after an incident involving a IND or RDD, there may be more than one radionuclide of interest. For example, the environmental sample submitted for analysis may contain both the alpha emitting nuclides ^{241}Am and ^{239}Pu . Therefore the precipitation from a solution containing multiple radionuclides was studied. The sample solution contained equal activities of ^{241}Am and ^{239}Pu and 0.0025, 0.005, 0.0125, 0.025, 0.05 mg of carrier solution were used respectively. The optimal amount of hydrofluoric acid, precipitation time, and precipitation temperature determined earlier was used.

2.5.8 Multi Radionuclide Solution Plus Addition of Hydrochloric Acid

If an environmental sample contains ^{241}Am and ^{239}Pu , they will both be subject to chemical separation treatments. Consequently the interference of hydrochloric acid on the precipitation from a multinuclide solution was investigated as well. As in earlier experiments, an additional amount of 20 mL of 4 M hydrochloric acid was added to the stock solution containing ^{241}Am and ^{239}Pu . The amount of cerium carrier was varied between 0.0025, 0.005, 0.0125, 0.025, 0.05 mg. The optimal parameters determined earlier for the amount of hydrofluoric acid, precipitation time, and precipitation temperature were used.

2.6 Liquid Scintillation Counting

Liquid scintillation was used to determine the net count rate of the stock solutions used. This information is needed to calculate the deposition yield for each sample. The activity of the Am²⁴¹ and ²³⁹Pu stock solutions was assayed using a Perkin Elmer model 3100TR liquid scintillation counter. Each sample solution was counted for 60 minutes with the count mode set to “normal”, pre-count delay set to “0”, and the low CPM threshold was set to “off” due to the high CPM from each sample. A 2 sigma % terminator was used for each sample. The background subtraction feature was set to “off” on the liquid scintillation counter. The window settings were set to encompass the peaks for both Am-241 and Pu-239. Each 700µL of the stock solution was counted separately in different scintillation vials to determine the counts rate for each radionuclide. Instead blanks were also counted under the same parameters and subtracted manually from each sample.

2.6.1 General Counting Procedure

During liquid scintillation counting, the sample was dissolved within a scintillation cocktail in either plastic or glass vials. The vials were closed tightly and shaken before loaded into a cassette. The vials were positioned into the cassette from left to right starting with the blank sample, then the standard solution, following the evaluated samples. The cassette was placed onto the moving belt of the counter. The samples are automatically removed from the cassette and placed into a “light-tight enclosure” where the light output from the sample is then determined by two photomultiplier tubes (PMTs) in coincidence. The count rate, count time, and quench determined for each sample was printed as a report. For alpha particles, the counting efficiency is assumed to be 100%

due to the high energy and the short range of the alpha particles. The blank is subtracted from the samples to obtain the net count rate for each sample.

2.7 Alpha Spectroscopy

Before beginning alpha spectroscopic measurements, an energy calibration was performed on each detector. The alpha spectrometer was calibrated using an electroplated, mixed radionuclide source that contained ^{nat}U , ^{239}Pu , and ^{241}Am . The isotope and energy for the calibration source as well as the corresponding channel numbers in each calibration spectrum can be found in Appendix I Table A. In addition an efficiency calibration was performed using a single nuclide standard prepared by electrodepositing ^{241}Am onto a stainless steel disk. The activity of the standard was 1.044 E4 dpm dated on July 26, 2007 at 12:00 EST.

Each of the filters prepared was assayed using a Canberra Alpha Analyst model 7200-04 consisting of eight counting chambers marked 1A, 2A, 3A, 4A, 1B, 2B, 3B, and 4B. Each chamber contained a Canberra Passivated Implanted Planar Silicon (PIPS) detector with an active area of 450mm^2 . Once the samples were placed into the chamber, an Edwards 2 stage pump was used to apply vacuum to the system to reduce the amount of energy loss from the alpha particle in air. The software used for analyzing the spectra obtained from each sample was Canberra's GENIE 2000 alpha analyst.

2.7.1 General Procedure

The filters obtained from each set of experiments were taped onto a lipped stainless steel planchet and were analyzed on the fourth shelf from the top, approximately 15mm away from the detector. The fourth shelf was used for each measurement based on the solid angle covered between the sample and the detector. The distance from source to

detector was far enough to give acceptable energy resolution yet close enough to still give adequate detector efficiency. Each sample was counted for at least 10,000 counts under each peak area in order to obtain 1% or less counting error. From the accumulation of the spectra, the area under the peak, time of count, and the full width half maximum (FWHM) was recorded to later determine the yield and energy resolution for each sample.

2.8 Radiometric Phosphor Imager

A Perkin Elmer Cyclone Plus Storage Phosphor System was used to determine the distribution of radionuclides over the sample. The system was used to give a qualitative image of the activity distribution on the filter, it could not be used to perform an exact quantification. The filter samples were exposed to a phosphor screen for a given amount of time. The screen contains Eu^{2+} ions in a crystal lattice which are ionized to Eu^{3+} when the screen comes in contact with radiation. The electrons freed by the ionization move within the conduction band and are then trapped in excited states by the vacancies stemming from the bromine ions in the material. The electrons return to ground state via the conduction band once a laser light of 633nm is scanned over the screen (Raccio 2006). A photon is released at 390nm which is detected by a PMT (Raccio 2006). The intensity of the light output recorded is proportional to the activity found on the sample. The results are electronically transferred to a computer and recorded for further analysis. Qualitative images are produced and color coded based on the different intensities of the light emitted.

There are three options for screen sensitivity: multisensitive (MS), super resolution (SR), and tritium sensitive (TR) (Raccio 2006). The MS storage phosphor screens are

more commonly used for “durability, high sensitivity, and good resolution.” On the other hand, the SR storage phosphor screen has a much smaller grain size which makes it ideal for obtaining the best resolution. Unlike the MS and SR storage phosphor screens, the TR screen is uncoated which makes it more sensitive to tritium and other radionuclides. Each screen type was tested in order to determine the best screen to be used for imaging the samples.

2.8.1 General Procedure

Before the screens were exposed to the filter samples, the screen was erased by using a white light box without any interferences of UV light. This is due to the fact that the screens may accumulate background radiation when not in use. The screens were erased by simply placing the screen faced down on top of the white light box for roughly 15 seconds. Once the screens were erased, the filter samples containing the radionuclide were placed directly onto the screens and placed together in a light-tight shut cassette for a given length of time (See Figure 3.1). Trial experiments were performed with each screen to determine the optimal time for imaging. After the exposure, the screen was removed from the cassette and placed onto the carousel for imaging. A laser was passed over the screen and the image was transferred to the computer screen. The image can be changed from a black and white image to a more vivid image of color. The red pixels corresponded to the highest intensity of radiation and the blue corresponded to the least amount of radiation. White on the filter corresponded to no radiation. Filters obtained with varying amounts of cerium carrier were imaged. In addition, images were taken using filters prepared with the highest and lowest amounts of cerium, lanthanum, and neodymium carrier and compared to each other.

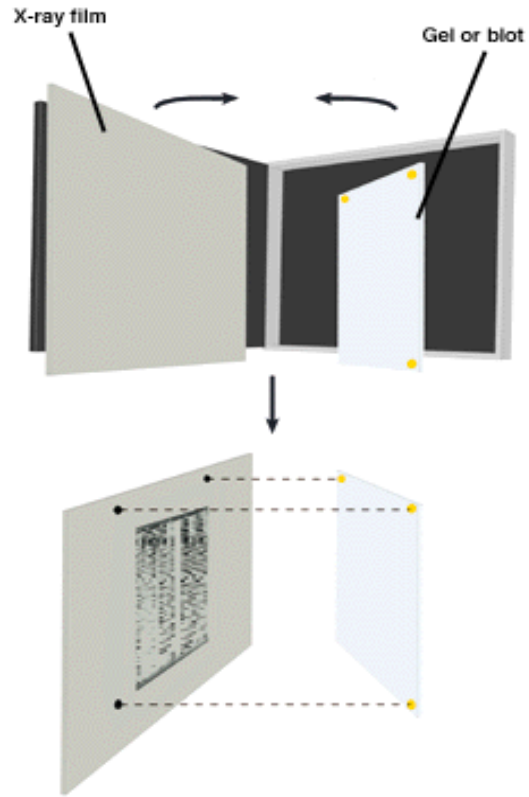


Figure 2.3 Exposing samples to film in cassette (Raccio 2006).

CHAPTER 3

RESULTS AND DISCUSSION

3.1 Data Analysis

3.1.1 Alpha Spectroscopy

Before samples could be evaluated using the Canberra Analyst, an energy calibration needed to be performed. A mixed source composing of natural uranium, ^{239}Pu , and ^{241}Am was placed into the vacuum chamber. Once the spectrum was accumulated, the channel number correlating to each peak positions were determined and a calibration curve was established. The calibration curve was used to determine the energy range of the evaluated alpha emitting radionuclides.

Each alpha chamber contains a fixed detector with twelve different sampling shelf positions. The distance between shelves is approximately 2.5 mm. To determine the best position to measure the prepared filters the efficiency and energy resolution was determined for every other shelf starting at shelf #2 and ending with shelf #12 using the electrodeposition ^{241}Am standard described in Chapter 2. The results can be seen in Appendix I Table B. By taking into account both the efficiency and FWHM, shelf #4 was determined to be the best position for the analysis of the samples. Each sample was counted for a sufficient amount of time until the counts under the peak reached a minimum of 10,000 counts. The exact counting time for each sample depended therefore on the activity present on each sample. A 24 hour background spectrum was obtained for each chamber at least once a month to ensure that no interfering background contamination was present on the detector or the walls of the chamber.

3.1.2 Deposition Yield

After microprecipitation, the filters were counted using the Canberra Alpha Analyst to determine the amount of radioactivity present on the surface of each filter. By taking into account the sample counts, live time for the sample counts, and detector efficiency for the given shelf number, the disintegration per second, DPS, can be calculated by using Equation 3.1.

$$\text{DPS of Sample} = \frac{\text{CPS of the Sample}}{\varepsilon \times \text{yield}} \quad \text{Equation 3.1}$$

where CPS = the counts under the peak divided by the time in seconds
 ε = the detector efficiency at the specific detector shelf

The efficiency of the PIPs detector was determined to be 10.35% for shelf #4. Even though ^{241}Am decays 100% by alpha decay, the region of interest set for the alpha spectroscopy only accounts for 99.4% of the ^{241}Am peak. The yield % for ^{241}Am in all of the experiments was 99.4%. The DPS of the stock solution can be obtained from the printout results from the liquid scintillation counters. Since the energies for alpha emitters are typically in MeV range and their range is very short, the detector efficiency for liquid scintillation detection can be assumed to be 100% for the stock solution. From the calculated DPS of both the sample and stock solution, the deposition yield of the sample can be determined by the following equation:

$$\text{Sample Yield} = \frac{\text{DPS of Sample}}{\text{DPS of Stock Solution}} \quad \text{Equation 3.2}$$

The experiments that used ^{239}Pu had a radiation yield of 100%. All of the sample yields were determined using the same calculation. In order to achieve the best possible results, the sample yields should be as high as possible.

3.1.4 Energy Resolution

In addition to the deposition yield, the energy resolution was determined for each filter. The GENIE 2000 software takes the channel ratio and set the energy to the corresponding channel number. The energy resolution for a given sample is determined for each peak. Once the spectrum was accumulated, the FWHM, time, and counts were recorded. The time and counts under the peak were used to determine the yield as mentioned in the previous section; while, the FWHM was used to determine the energy resolution for each sample. To achieve the best possible results, the FWHM should be as small as possible.

3.2 Parameter Discussion

3.2.1 Optimal Parameters

The different parameters affecting the performance of the microprecipitation were evaluated to determine the conditions that resulted in the best possible energy resolution and deposition yield. The parameters that were investigated were the amount of carrier with constant HF, the amount of HF with constant carrier, the relative amounts of carrier and hydrofluoric acid, precipitation temperature, precipitation time, and different types of carrier elements that can be used to form the precipitate. In addition to the parameter affecting the microprecipitation directly, other interferences added to the sample during the preceding separation may worsen the energy resolution and yield. Examples of interferences include the addition of mineral acids, such as HCl and the presence of other

radionuclides in the sample solution. The effect of the added interferences of hydrochloric acid and other radionuclides present were therefore investigated separately to determine the best possible energy resolution and deposition yield. An additional investigation of the interferences of the hydrochloric acid within a multinuclide solution was investigated. The results obtained from the investigation of the interferences of the hydrochloric acid and the radionuclides were compared to the investigation of the interferences of the hydrochloric acid in a multinuclide solution to determine if any differences occurred.

3.2.2 Varying Cerium with Constant HF

The study of the amount of the cerium carrier was evaluated using a constant 700 μ L amount of ^{241}Am with an activity of 100 Bq/mL and 1 mL of HF. The amounts of carrier used were 0.05, 0.025, 0.0125, 0.005, and 0.0025 mg of cerium. The procedure was repeated at least five times and the standard deviation was determined from each sample set of carrier amounts. The results are shown in Table 3.1. Figure 3.1 shows the FWHM and Figure 3.2 shows the corresponding yields.

Table 3.1 FWHM and deposition yield for varying the carrier amount with 1mL of HF

Amount of Ce (μ L)	Amount of HF (μ L)	Ce (mg)	FWHM (keV)	STD FWHM (keV)	Yield (% decimal)	STD Yield (% decimal)
5	1000	0.0025	38.76	1.64	1.05	0.017
10	1000	0.005	38.93	5.36	1.08	0.0095
25	1000	0.0125	27.32	1.51	0.91	0.014
50	1000	0.025	28.71	1.72	0.94	0.053
100	1000	0.05	36.93	2.42	0.89	0.022

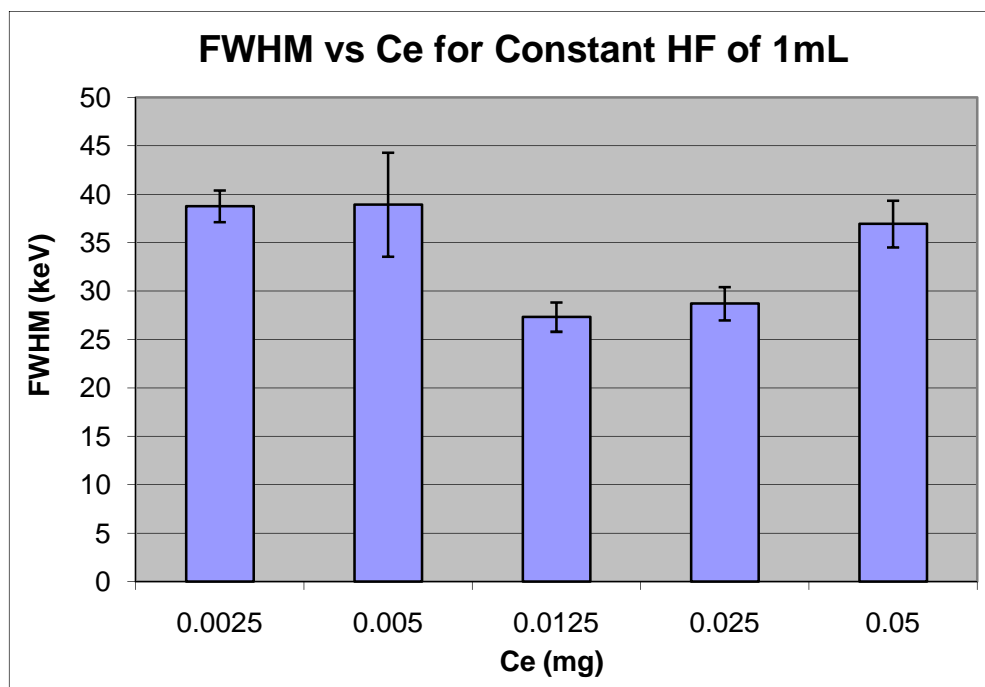


Figure 3.1 Plot of the FWHM versus the amount of Cerium with 1mL of HF

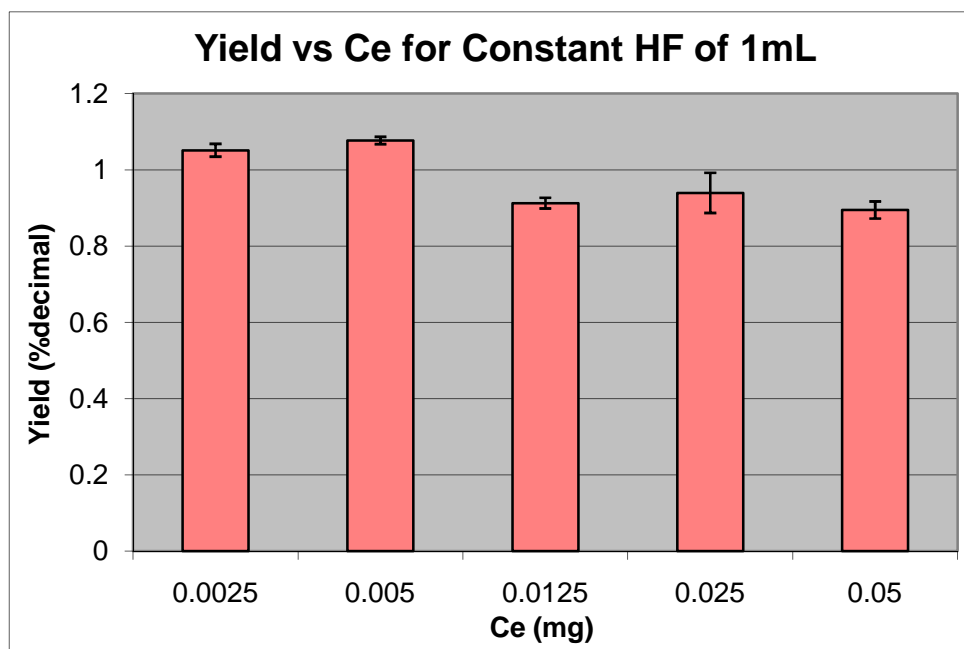


Figure 3.2 Plot of the Yield versus the amount of Cerium with 1mL of HF.

3.2.3 Effect of HF Volume

In a second set of experiments the influence of varying the amount of HF while keeping the amount of carrier constant was investigated. The parameters that were kept constant were the precipitation time of 30 minutes and precipitation temperature of 25°C. The optimal carrier amount determined in the first set of experiments was 0.0125 mg of cerium which gave an optimal FWHM of 27.32 ± 1.51 keV and relative high yields, therefore the amount of carrier during this part of the work was held constant at 0.0125mg of cerium while the volume of hydrofluoric acid was varied. The volumes of hydrofluoric acid used in this study were 250, 500, 750, 1000, and 1250 μ L. The molarity of hydrofluoric acid was held constant at 28 molar. The results for the yield and FWHM are listed in Table 3.2. Plots of the results for yield are shown in Figure 3.3 and the energy resolution is shown in Figure 3.4.

Table 3.2 FWHM and deposition yield for varying the amount of HF while holding the amount of cerium constant at 0.0125mg.

Amount of Ce (μ L)	Amount of HF (μ L)	FWHM (keV)	STD FWHM (keV)	Yield (% decimal)	STD Yield (% decimal)
25	250	69.16	8.33	0.99	0.0066
25	500	33.76	3.086	1.03	0.10
25	750	36.80	2.16	1.03	0.18
25	1000	27.32	1.51	0.91	0.014
25	1250	30.97	1.34	1.06	0.13

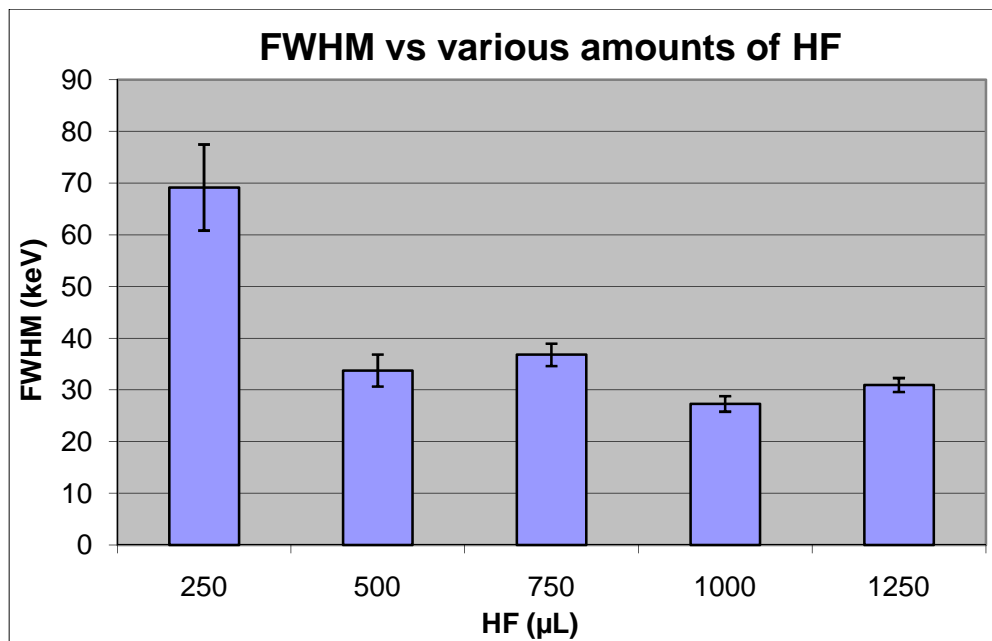


Figure 3.3 Plot of the FWHM versus the amount of HF (Amount of Ce: 0.0125mg)

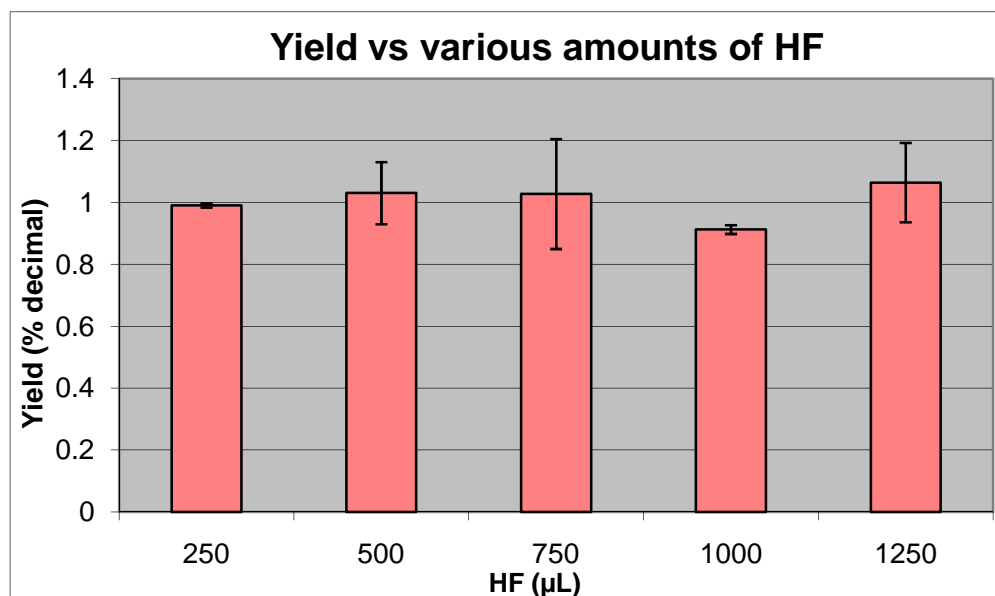


Figure 3.4 Plot of the yield versus the amount of HF (Amount of Ce: 0.0125mg)

3.2.4 Effect of Relative Amounts

In this part of the work the effect of the relative amounts of cerium and HF was investigated. For this study, the amount of cerium and hydrofluoric acid was varied simultaneously; however the ratio of cerium to hydrofluoric acid was kept constant at 0.00005. As the concentration carrier amount increased, the volume of hydrofluoric acid was also increased to maintain the same fraction. For instance, if the amount of cerium was 0.025 mg, the volume of HF used was 500 μ L. The amounts of cerium used were 0.05, 0.025, 0.0125, 0.005, and 0.0025 mg and the corresponding volumes of hydrofluoric acid amounts were 1000, 500, 250, 100, and 50 μ L. The results can be seen in Table 3.3. The FWHM verses the concentration of cerium is plotted in Figures 3.5 while the yield verses the amount of cerium is plotted in Figure 3.6.

Table 3.3 FWHM and deposition yield for varying cerium carrier and hydrofluoric acid simultaneously

Amount of Ce (μ L)	Amount of HF (μ L)	Ce (mg)	FWHM (keV)	STD FWHM (keV)	Yield (% decimal)	STD Yield (% decimal)
5	50	0.0025	45.23	8.06	0.96	0.01
10	100	0.005	44.80	14.74	1.00	0.05
25	250	0.0125	69.16	8.33	0.99	0.01
50	500	0.025	50.93	19.06	1.05	0.04
100	1000	0.05	36.93	2.42	0.89	0.02

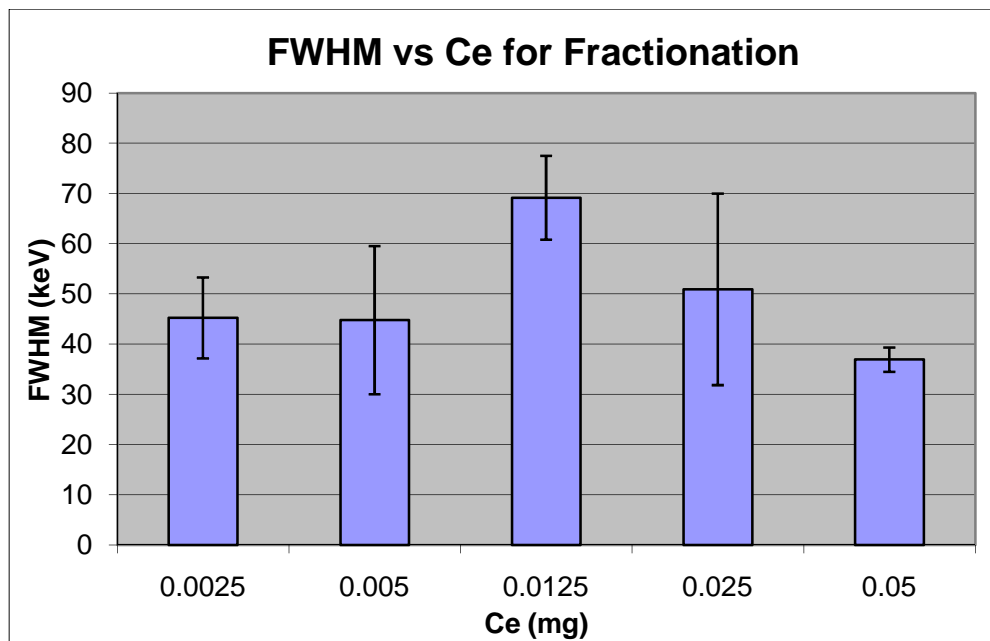


Figure 3.5 Plot of the FWHM versus cerium concentrations. The corresponding volumes of hydrofluoric acid amounts were 1000, 500, 250, 100, and 50 μL , respectively.

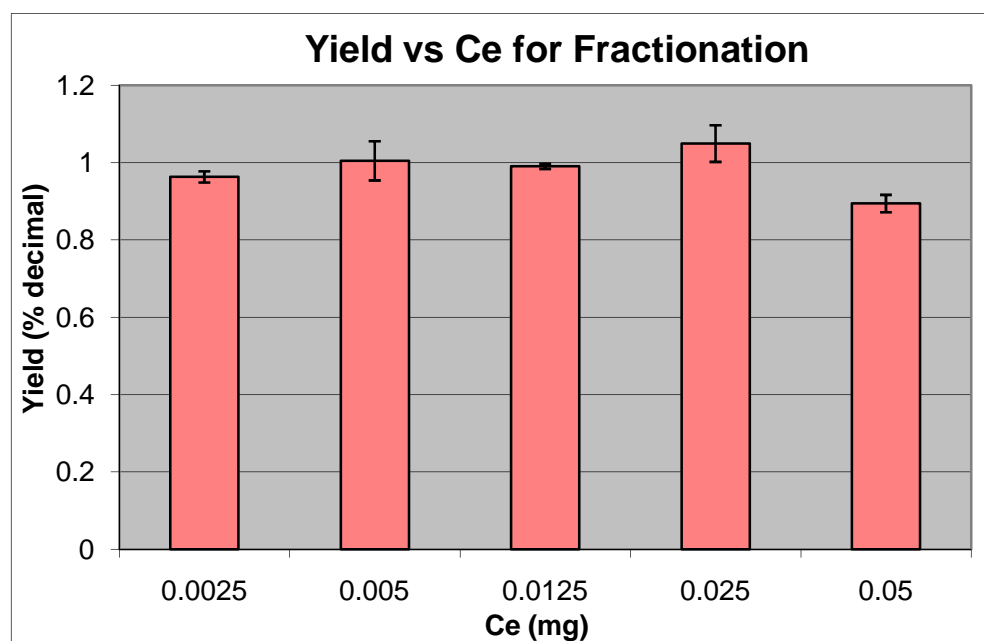


Figure 3.6 Plot of the yield versus cerium concentration. The corresponding volumes of hydrofluoric acid amounts were 1000, 500, 250, 100, and 50 μL , respectively.

3.2.5 Effect of Temperature

In the general procedure for microprecipitation, the precipitate is simply formed at room temperature. The temperature at which the formation occurs can however significantly affect the morphology and properties of the precipitate itself. It was therefore decided to also evaluate the influence of temperature on the procedure. For this purpose the solution was kept at 25, 30, 35, 40, 45, and 50°C, respectively, during the formation of the precipitate. The other parameters were kept as follows: 700 μ L of Am-241 stock solution, 1 mL of HF, and 0.0125 mg of cerium carrier. The temperature was changed by using a water bath for 30, 35, 40, 45, and 50°C. For 25°C, the precipitate was formed at room temperature. The results are listed in Table 3.4, and the FWHM and deposition yield for each temperature are shown in Figure 3.7 and Figure 3.8.

Table 3.4 FWHM and deposition yield for various precipitation temperatures

Precipitation Temperature	FWHM (keV)	STD FWHM (keV)	Yield (% decimal)	STD Yield (% decimal)
0°C	29.04	2.61	0.75	0.33
25°C	27.32	1.51	0.91	0.014
30°C	34.89	3.90	0.98	0.016
35°C	30.77	3.10	0.99	0.017
40°C	29.50	3.24	1.07	0.10
45°C	34.39	1.76	1.16	0.019
50°C	30.42	2.35	1.12	0.013

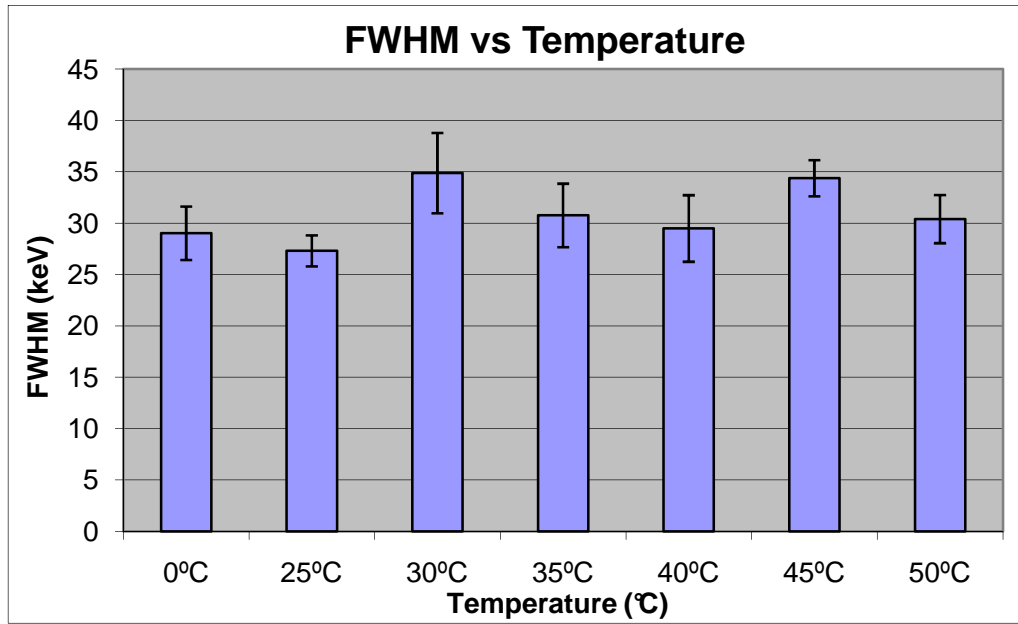


Figure 3.7 Plot of the FWHM verses different precipitation temperatures

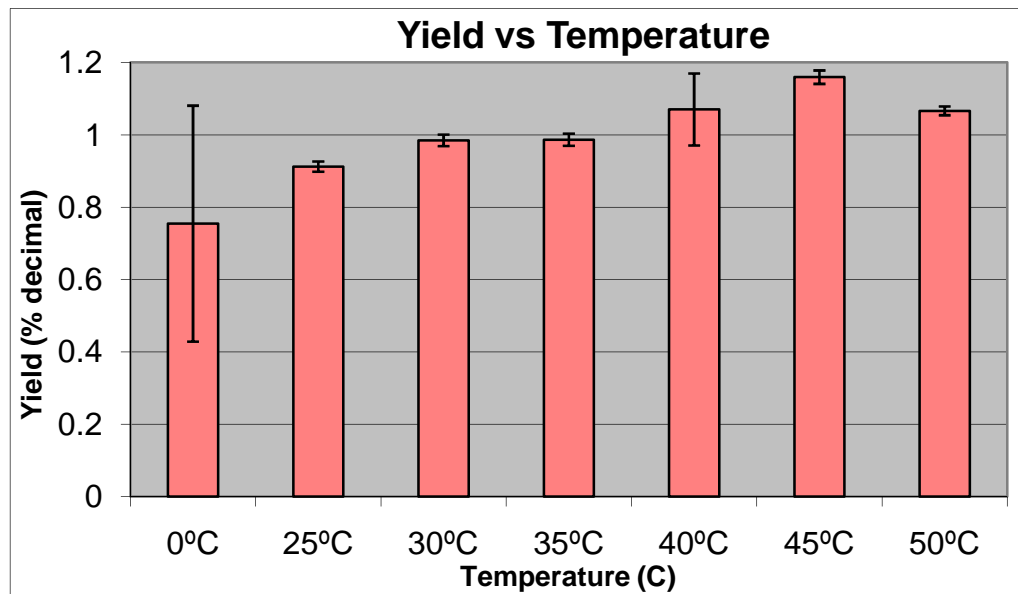


Figure 3.8 Plot of the Yield verses various precipitation temperatures

3.2.6 Effect of Time

Once the hydrofluoric acid is added to the solution, the HF dissociates into hydrogen and fluoride ions. The fluoride ions interact with the americium and cerium ions and a mixed precipitate containing AmF_3 and CeF_3 starts to form. It has been shown that the time that the precipitate is left to form can significantly affect the structure of the precipitate. This is mainly due to the constant dissolution and recrystallization of ions at the surface of the precipitate. Therefore a dedicated set of experiments was carried out to determine the precipitation time that would result in the best possible spectral resolution and yield. The time intervals examined were 10, 20, 30, 45, and 50 mins, and 1, 2, 4, 8, 16, and 24 hours. The amount of carrier was kept constant at 0.0125mg of cerium with 1mL of hydrofluoric acid. The precipitation temperature was constant at room temperature. The results were recorded and can be seen in Table 3.5. Figure 3.9 and Figure 3.10 show the FWHM and yield, respectively.

Table 3.5 FWHM and Yield for various precipitation times

Precipitation Time	FWHM (keV)	STD FWHM (keV)	Yield (% decimal)	STD Yield (% decimal)
10min	35.39	3.76	0.91	0.078
20min	34.85	3.28	0.93	0.054
30min	27.32	1.51	0.91	0.014
45min	28.36	3.15	0.95	0.012
50min	27.59	2.15	0.92	0.048
1hr	33.38	1.18	0.95	0.0068
2hr	31.63	3.39	0.92	0.0038
4hr	31.07	1.60	0.94	0.019
8hr	38.55	4.88	0.95	0.0070
16hr	40.48	1.34	0.95	0.021
24hr	36.77	2.27	0.94	0.0083

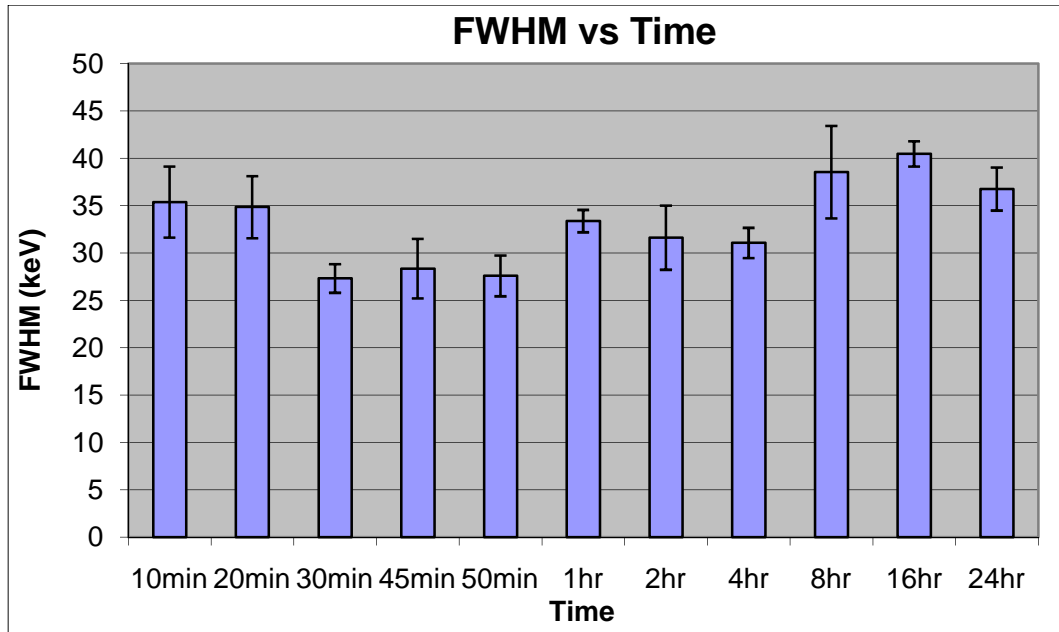


Figure 3.9 Plot of the FWHM for various precipitation times

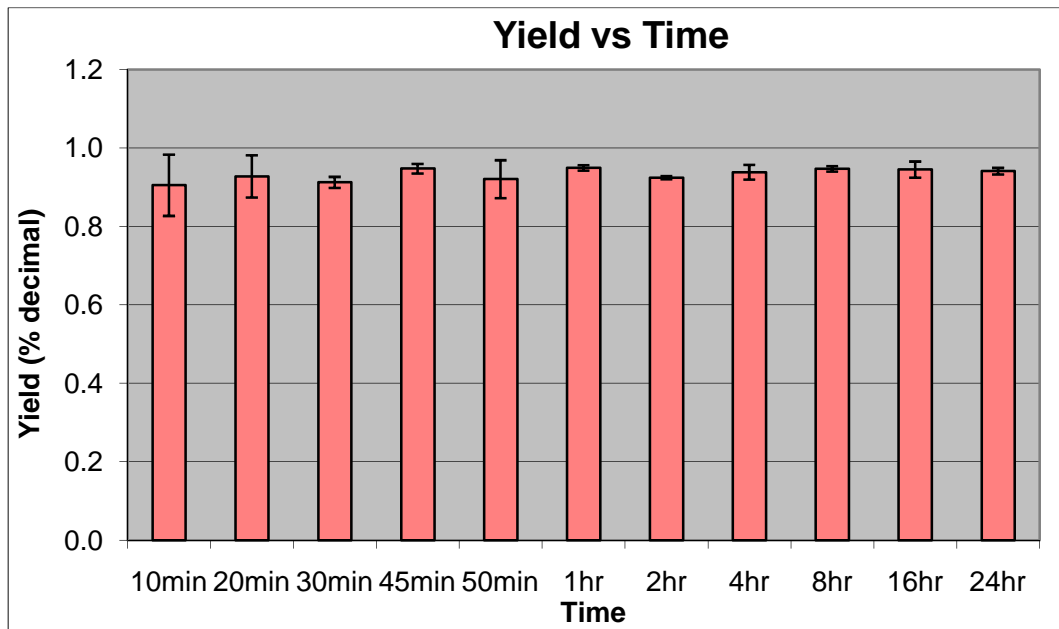


Figure 3.10 Plot of the deposition yield for various precipitation times

3.2.7 Varying Carriers

The general procedure for microprecipitation uses cerium to bring Am-241 out of solution. Due to the similarity in oxidation state and ionic radius, tri- and tetravalent actinides will readily incorporate themselves into the lanthanide fluoride crystal structure. Besides cerium, other lanthanide elements, such as lanthanum and neodymium, have been used as carriers for microprecipitation. For that reason it was decided to contrast the use of lanthanum and neodymium as carrier elements with the use of cerium. Varying amounts of neodymium and lanthanum were added as carrier and their performance was compared to that of cerium. The carrier amounts used were the same as for cerium, namely 0.0025, 0.005, 0.0125, 0.025, and 0.05 mg. The volume of hydrofluoric acid was kept constant at 1 mL. The precipitation temperature was kept at 25 °C and a precipitation time of 30 minutes was used. Table 3.6 lists the results for lanthanum and Table 3.7 shows the results for Neodymium. A comparison of the carrier performance relative to cerium can be seen in Figures 3.11 and 3.12.

Table 3.6 FWHM and Yield for various amounts of carrier

Amount of La (μL)	Amount of HF (μL)	La (mg)	FWHM (keV)	STD FWHM (keV)	Yield (% decimal)	STD Yield (% decimal)
5	1000	0.0025	29.44	1.29	0.92	0.013
10	1000	0.005	26.20	1.53	0.91	0.019
25	1000	0.0125	28.52	3.35	0.92	0.021
50	1000	0.025	32.03	1.63	0.94	0.033
100	1000	0.05	46.14	4.37	0.93	0.019

Table 3.7 FWHM and Yield for various amounts of neodymium carrier

Amount of Nd (μL)	Amount of HF (μL)	Nd (mg)	FWHM (keV)	STD FWHM (keV)	Yield (% decimal)	STD Yield (% decimal)
5	1000	0.0025	28.69	1.10	0.94	0.015
10	1000	0.005	32.02	1.43	0.97	0.048
25	1000	0.0125	35.24	2.06	0.95	0.016
50	1000	0.025	31.14	0.67	0.91	0.025
100	1000	0.05	39.84	0.97	0.93	0.0072

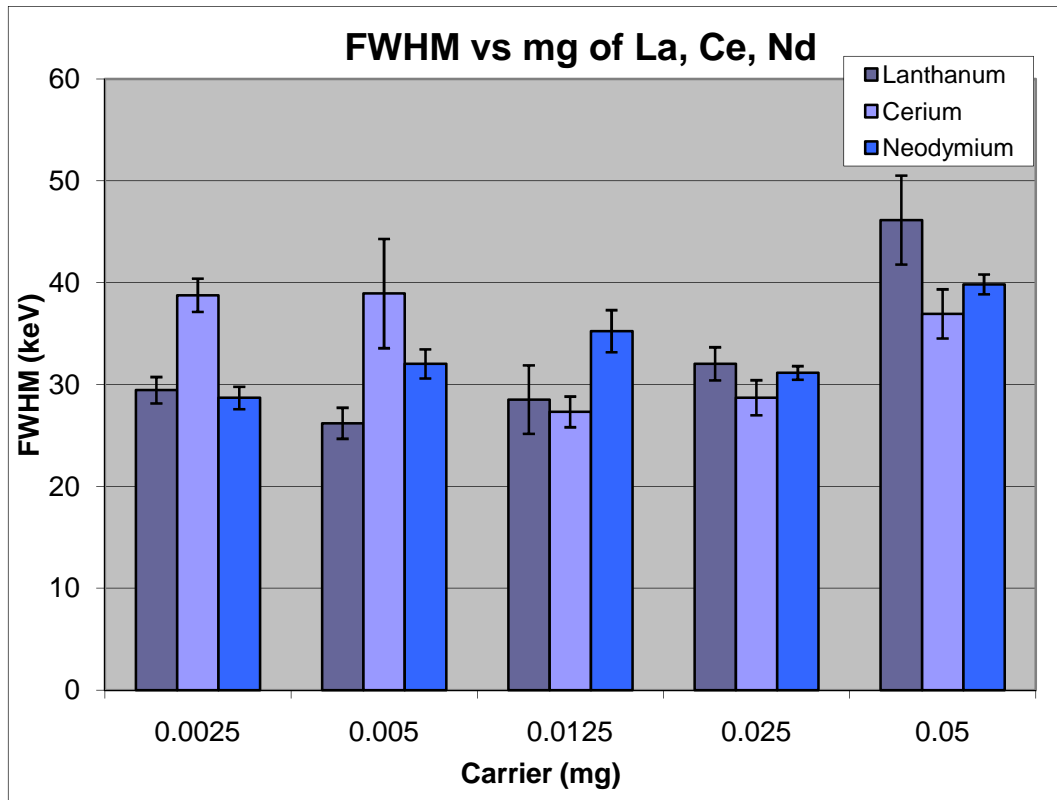


Figure 3.11 Plot showing the FWHM for various amounts of lanthanum, cerium, and neodymium

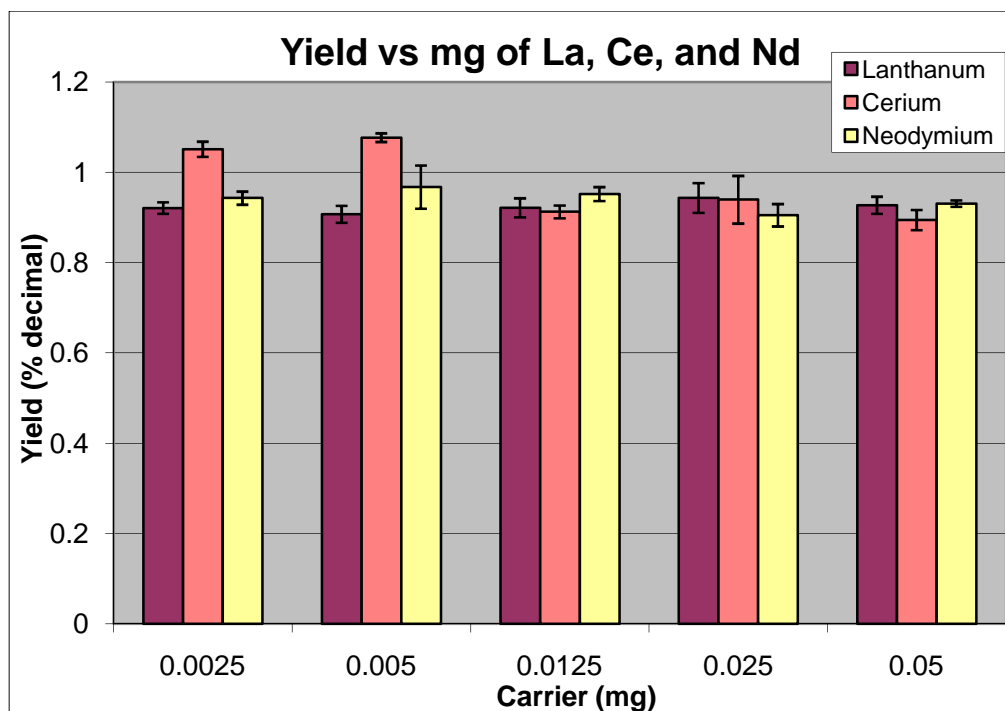


Figure 3.12 Plot showing the Yield for various amounts of lanthanum, cerium, and neodymium

3.2.8 Addition of 20 mL of Hydrochloric Acid

The interference of 20 mL of hydrochloric acid was investigated using the optimal parameters determined earlier. The amount of cerium solution used varied by 0.0025, 0.005, 0.0125, 0.025, and 0.05, 0.1, 0.2, 0.3, 0.4, 0.5, and 0.6 mg along with 1 mL hydrofluoric acid. The precipitation time was 30 minutes at room temperature. The results of introducing 20 mL of hydrochloric acid to the microprecipitation procedure are seen below in Table 3.8. The FWHM verses the amount of cerium concentration can be seen in Figure 3.13. In addition the yield for each cerium concentration is displayed in Figure 3.14.

Table 3.8 Results showing the FWHM and Yield for various concentrations of cerium as 20 mL of hydrochloric acid was added to the sample solution

Amount of Ce (μL)	Amount of HF (μL)	Ce (mg)	FWHM (keV)	STD FWHM (keV)	Yield (% decimal)	STD Yield (% decimal)
5	1000	0.0025	44.51	6.60	0.00032	0.00036
10	1000	0.005	56.23	11.01	0.00028	0.00020
25	1000	0.0125	45.48	5.95	0.0090	0.0074
50	1000	0.025	43.45	6.13	0.0061	0.0046
100	1000	0.05	52.95	12.21	0.39	0.080
200	1000	0.1	76.47	22.89	0.51	0.06
400	1000	0.2	58.63	2.54	0.66	0.059
600	1000	0.3	76.26	2.41	0.69	0.026
800	1000	0.4	92.18	2.45	0.83	0.011
1000	1000	0.5	103.52	4.30	0.89	0.014
1200	1000	0.6	118.42	7.83	0.90	0.020

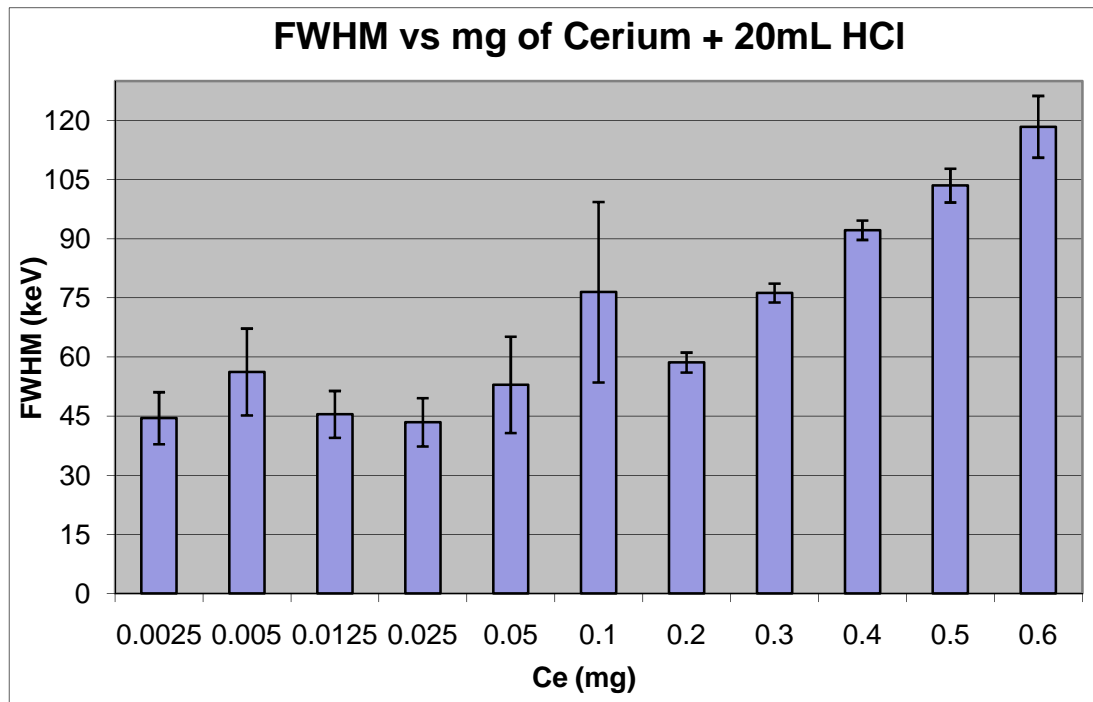


Figure 3.13 Plot showing the FWHM for various concentrations of cerium as 20 mL of hydrochloric acid was added to the sample solution

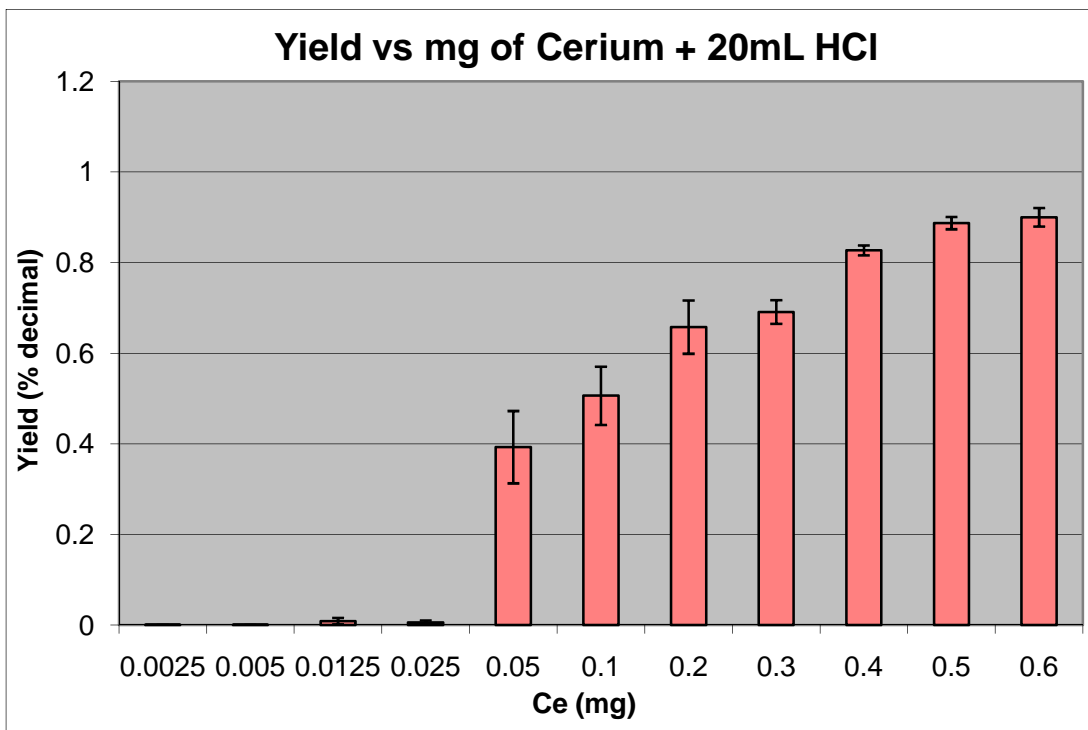


Figure 3.14 Plot showing the yield for various concentrations of cerium as 20 mL of hydrochloric acid was added to the sample solution

3.2.9 Multinuclide Solution of ^{241}Am and ^{239}Pu

In some environmental samples, there may be more than one radionuclide present. The interference of a multinuclide solution was investigated using 700 μL of ^{241}Am plus 700 μL of ^{239}Pu . The parameters used during the experiments were 0.0025, 0.005, 0.0125, 0.025, 0.5mg of cerium solution with 1mL of hydrofluoric acid. The precipitation time was 30 minutes at room temperature. The results for the FWHM and yield of ^{241}Am and ^{239}Pu is reported in Table 3.9. The plot for the FWHM vs the cerium concentration is displayed in Figure 3.15 while the yield vs the cerium concentration is shown in Figure 3.16.

Table 3.9 Results of the FWHM and yield for a multinuclide solution containing ^{241}Am and ^{239}Pu

Ce (mg)	^{241}Am				^{239}Pu			
	FWHM (keV)	STD FWHM (keV)	Yield (% decimal)	STD Yield (% decimal)	FWHM (keV)	STD FWHM (keV)	Yield (% decimal)	STD Yield (% decimal)
0.0025	26.17	0.63	0.90	0.041	31.39	0.76	0.91	0.040
0.005	32.12	1.67	0.92	0.0022	32.47	3.16	0.93	0.0085
0.0125	28.62	0.68	0.93	0.061	32.92	0.85	0.86	0.0610
0.025	28.91	1.54	0.98	0.026	32.39	0.73	0.92	0.0034
0.05	34.76	1.38	0.98	0.013	38.02	0.95	0.89	0.0076

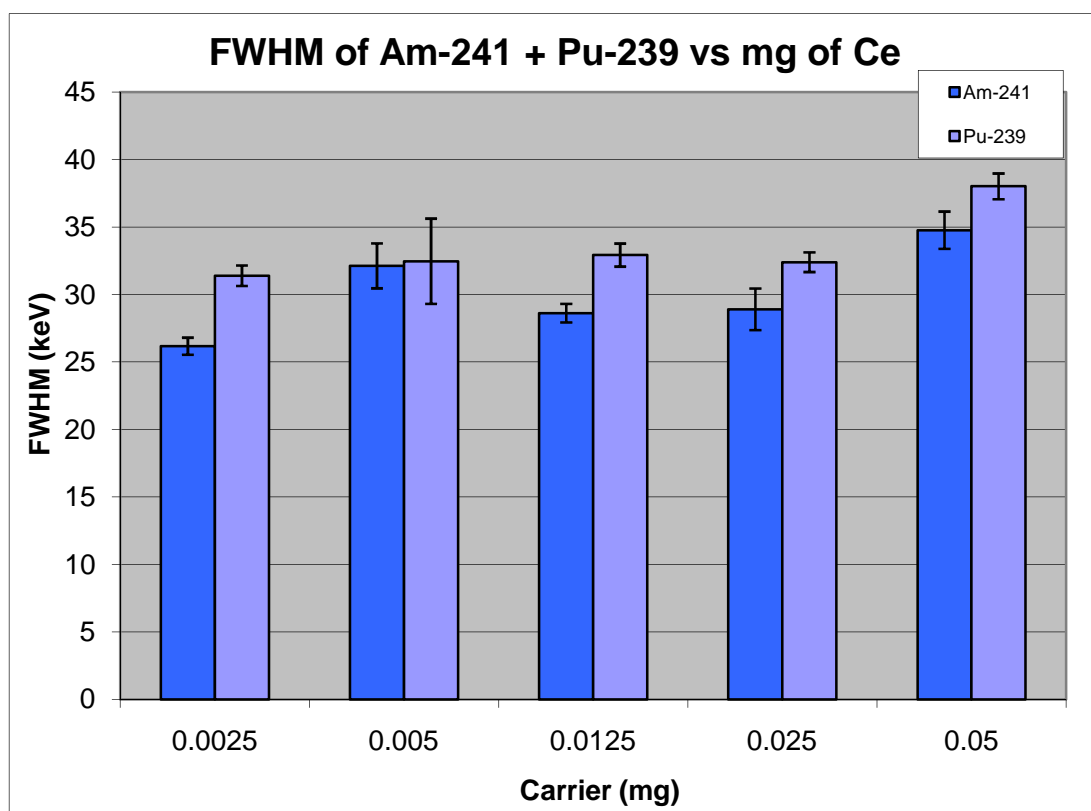


Figure 3.15 Plot showing the FWHM for ^{241}Am and ^{239}Pu verses the cerium concentration

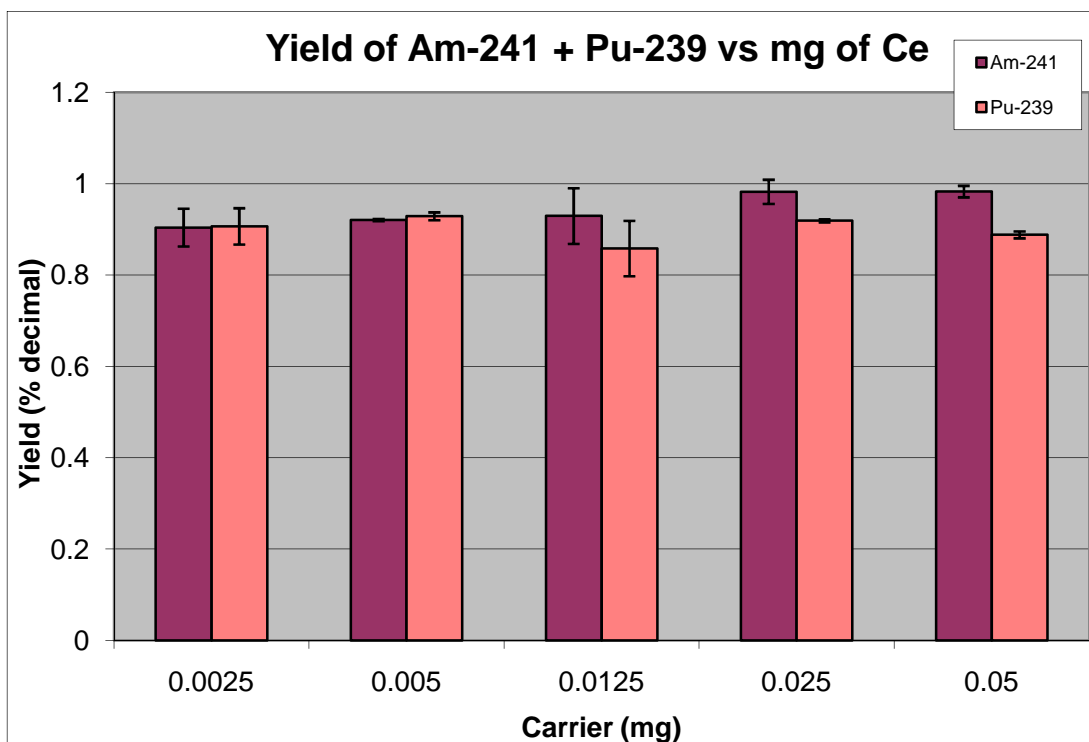


Figure 3.16 Plot showing the yield for ^{241}Am and ^{239}Pu verses the cerium concentration

3.2.10 Multinuclide solution of ^{241}Am and ^{239}Pu with 20 mL HCl

Both the multinuclide solution and the interference of hydrochloric acid were tested earlier. However the interference of both a multinuclide solution plus the hydrochloric acid has not been tested within the same solution. During this experiment, a solution containing both ^{241}Am and ^{239}Pu with 20 mL of hydrochloric acid was investigated. The amount of carrier concentration of cerium varied by 0.0025, 0.005, 0.0125, 0.025, and 0.05mg. The results of yield and FWHM for both ^{241}Am and ^{239}Pu are shown in the Table 3.10. The plot of the yield and FWHM of ^{241}Am and ^{239}Pu are compared in Figures 3.17 and 3.18.

Table 3.10 Results of the FWHM and yield for ^{241}Am and ^{239}Pu with various concentrations of cerium with the addition of 20 mL of hydrochloric acid

Ce (mg)	^{241}Am				^{239}Pu			
	FWHM (keV)	STD FWHM (keV)	Yield (% decimal)	STD Yield (% decimal)	FWHM (keV)	STD FWHM (keV)	Yield (% decimal)	STD Yield (% decimal)
0.0025	69.60	14.00	0.0024	0.002	42.82	3.57	0.0027	0.0037
0.005	62.17	9.69	0.0011	0.0009	42.62	6.02	0.00041	0.00019
0.0125	49.86	35.73	0.0004	0.0002	38.42	3.10	0.0029	0.0018
0.025	32.59	9.24	0.0078	0.01	36.25	3.30	0.093	0.12
0.05	42.81	10.38	0.37	0.081	45.09	10.49	0.66	0.060

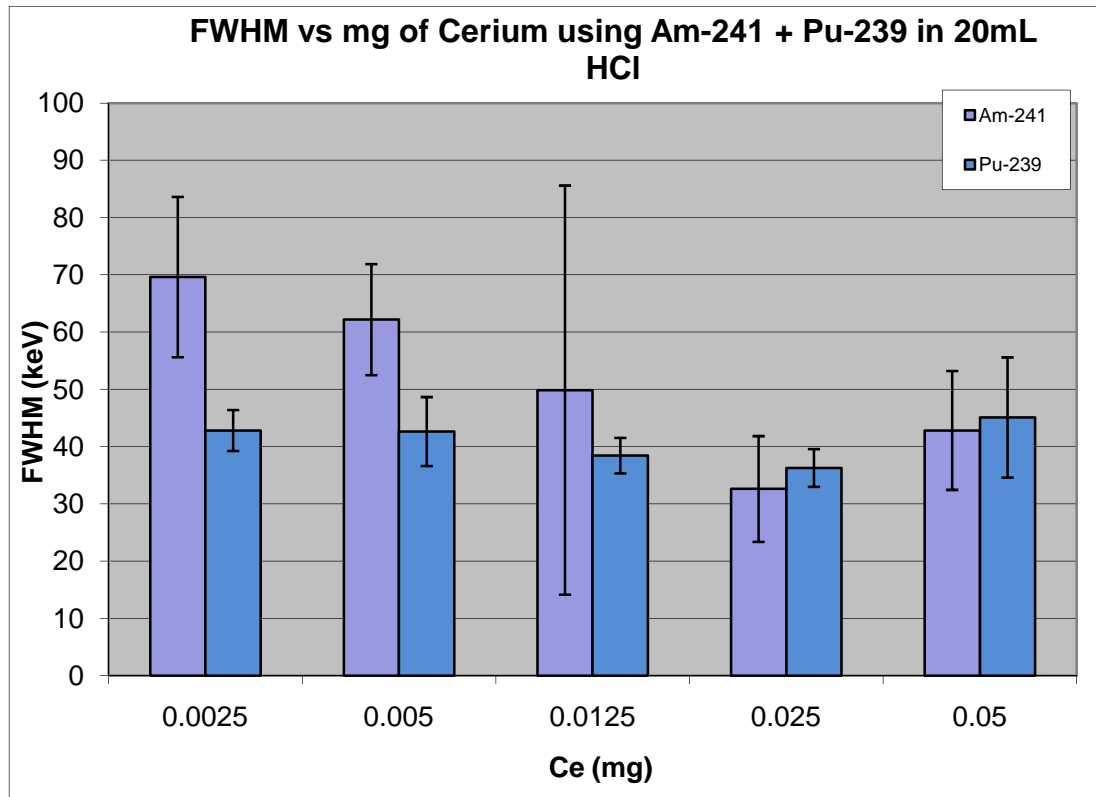


Figure 3.17 Plot of the FWHM for ^{241}Am and ^{239}Pu with various concentrations of cerium with the addition of 20 mL of hydrochloric acid

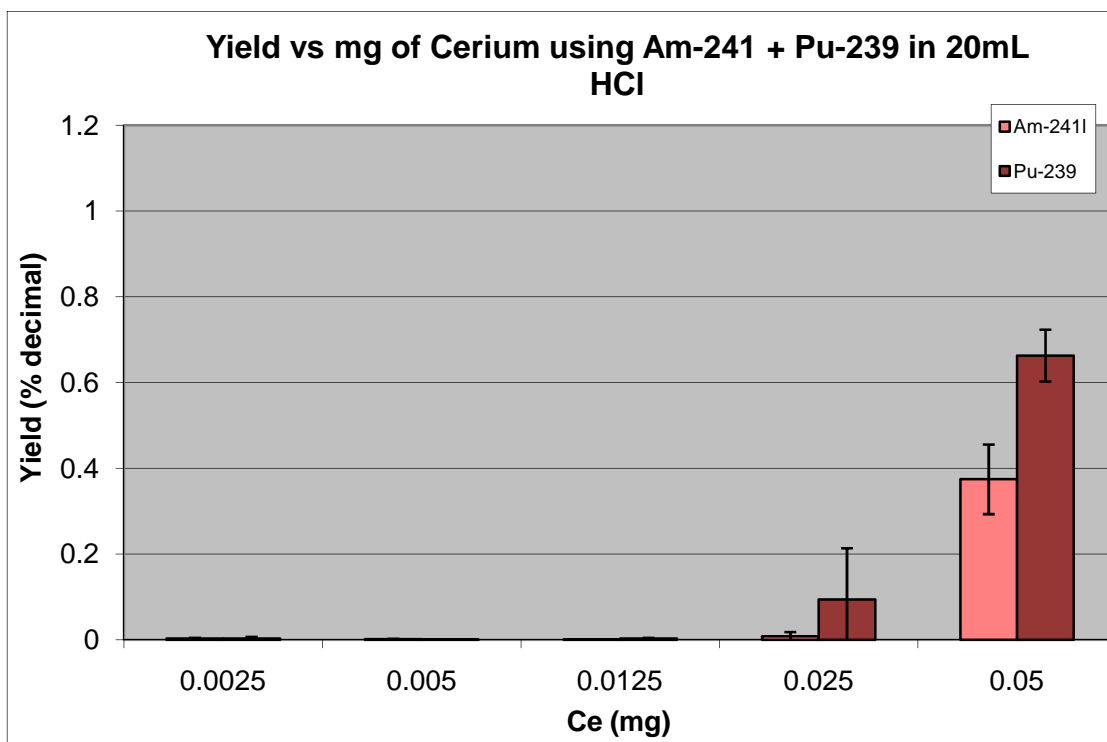


Figure 3.18 Plot of the yield for ^{241}Am and ^{239}Pu with various concentrations of cerium with the addition of 20 mL of hydrochloric acid

3.3 Visual Interpretations

Using the Cyclone Plus audioradiographic instrument, the visuals for the source samples were able to be acquired. The film that produced the clearest visuals was the Super Resolution film (SR). The filter was exposed to the screen for three hours. The first visuals to be obtained were the filters used during the initial study which varied amount of cerium carrier concentration with constant 1mL of hydrofluoric acid. The precipitation time was 30 minutes with a constant precipitation temperature of 25°C. The images are only qualitative and relative to each other. The images are shown in Figure 3.19.

3 Hour Exposure using the Super Resolution Film (SR)

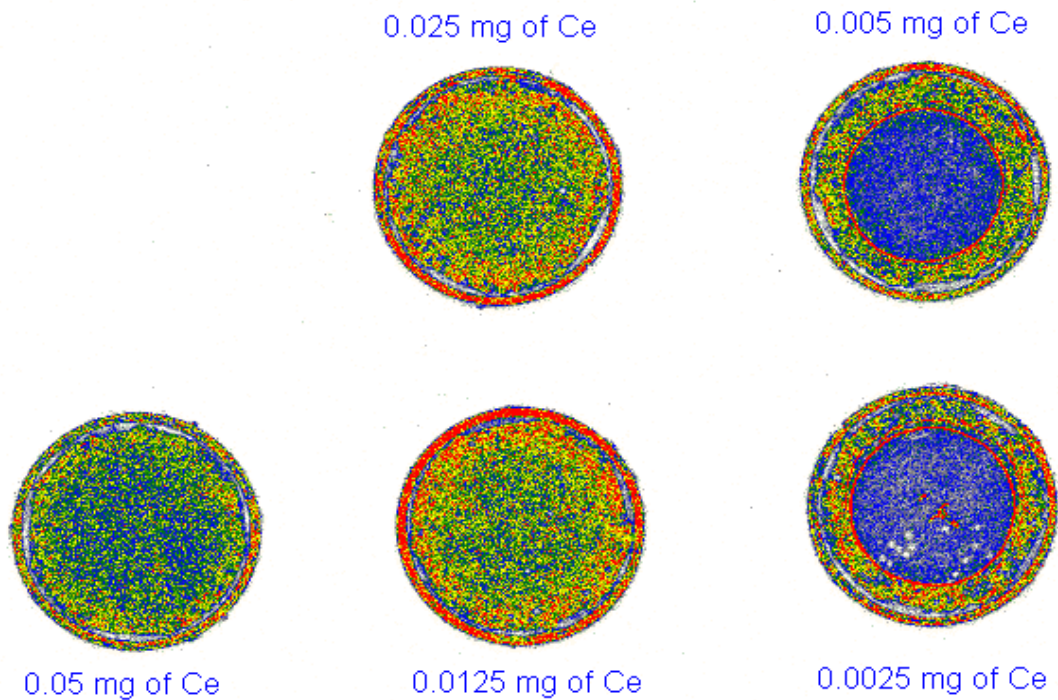


Figure 3.19 Autoradiographic visuals of ^{241}Am distribution during microprecipitation using various cerium concentrations

Using the same parameters for the screens mentioned earlier, the second set of images shown in Figure 3.20 is representative of the lowest and highest amount of carrier solution of cerium, lanthanum, and neodymium. The amount of hydrofluoric was constant at 1mL for each carrier amount. The precipitation time was 30 minutes at room temperature. Each visual of the carrier amount is relative to each other and can only be viewed qualitatively.

3 Hour Exposure using Super Resolution Film (SR)

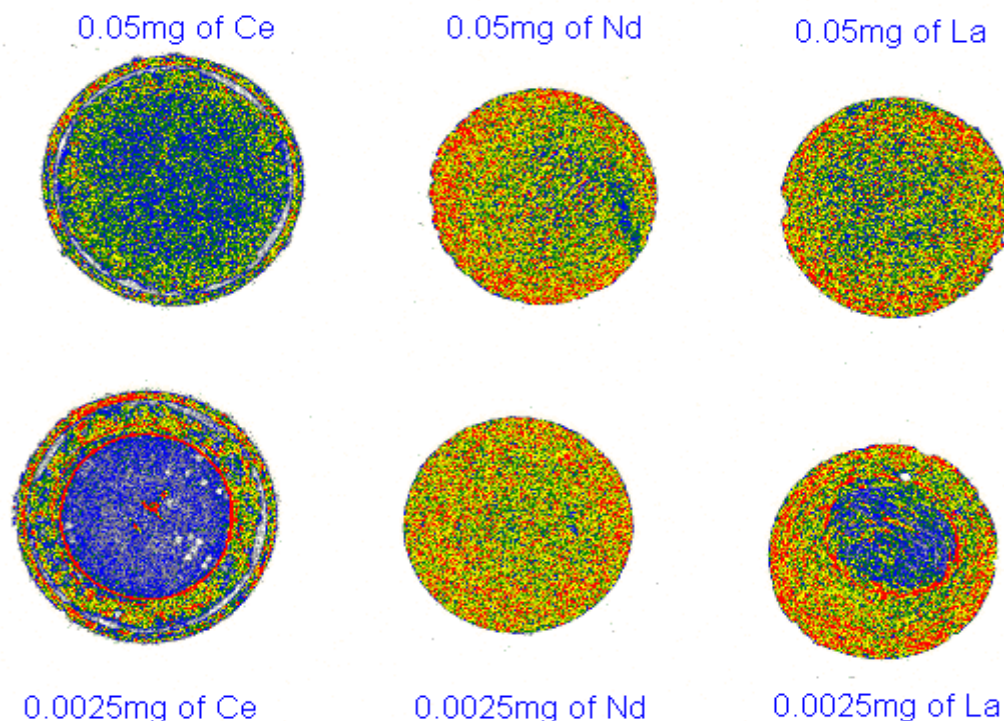


Figure 3.20 Autoradiographic visuals of ^{241}Am distribution during microprecipitation using the highest and lowest concentration of various carriers (La, Nd, Ce).

3.4 Results

3.4.1 Varying Cerium with Constant HF

Data was obtained from the study of varying the carrier amounts of cerium with constant 1mL of hydrofluoric acid. The precipitation time was constant at 30 minutes at room temperature. The results of the energy resolution show that as the cerium carrier concentrations increase, the energy resolution decreases until 0.0125 mg of cerium. Once 0.0125mg of cerium was reached, the energy resolution increased with increasing carrier amount. The data for the energy resolution formed a valley at 0.0125mg of cerium in the

results. The best energy resolution was determined to be 27.32 ± 1.51 keV which corresponded to 0.0125mg of cerium with 1mL of hydrofluoric acid. The yields with increasing carrier amounts were all comparable to each other. The best yield was 107 ± 1 % when 0.005 mg of cerium carrier was used with 1mL of hydrofluoric acid. However, the FWHM that corresponds to the best yield has a poorer energy resolution with large variability compared to the results from the best energy resolution.

3.4.2 Varying the amount of HF with Constant Cerium

The results of varying the amount of HF while keeping the cerium concentration constant at the optimal quantity of 0.0125mg showed that at lower concentration of HF the energy resolution worsened. As the volume of HF increased, the FWHM also decreased to 1000 μ L of HF then increased at 1250 μ L of HF. The optimal volume of HF for 25 μ L of cerium at room temperature with a 30 minute precipitation time was 1000 μ L which had a FWHM of 27.317 ± 1.506 as determined in the previous experiment. The yields for varying the amount of HF with constant 25 μ L of cerium were all comparable to each other; however, majority of the yield values had huge standard deviations.

3.4.3 Varying HF and Cerium Simultaneously

When fractionation of hydrofluoric acid and cerium was tested, an opposite effect of the first experiment was discovered. As the cerium concentrations increased, the FWHM increased to 0.0125mg of cerium then decreased with higher amounts of carrier concentrations. The values of the FWHM formed a peak in the results rather than a valley seen in the first experiment. The best FWHM during the fractionation experiment was 36.93 ± 2.42 keV using the highest concentration of cerium at 0.05mg with 1mL of hydrofluoric acid. The yields for fractionation showed no trend and were comparable to

each other. However, if the fractionation results are compared to the results using constant amount of HF from the previous study, the optimal results for the cerium concentration was using 0.0125mg of cerium with 1mL of HF. Fractionation did not improve the results for energy resolution or yield.

3.4.4 Varying Temperature

From the previous experiments, the optimal concentration of cerium and hydrofluoric acid was 0.0125mg and 1mL, respectively. The experiment was performed with 30 minute precipitation time at room temperature. The optimal results of cerium and hydrofluoric acid were used to evaluate the yield and energy resolution with varying the precipitation temperature. The precipitation time stayed constant at 30 minutes. The results showed that no trend for the FWHM or yield with varying the temperature amount. The best FWHM was 27.32 ± 1.51 keV at 25°C. The yields were roughly 100% however at higher temperatures the yields were better. For simplicity, the best yield compared to the FWHM was determined to be at room temperature.

3.4.5 Varying Time

Using the optimal parameters of 0.0125mg of cerium with 1mL of hydrofluoric acid at room temperature, the precipitation time was varied to determine the optimal time for the precipitate to form. From the results, the best FWHM was between 30 to 50 minutes. The yield did not show any trend and were all comparable to each other at roughly 90%. By comparing the variability of the FWHM and yield, the optimal precipitation time was at 30 minutes since the standard deviation for both the FWHM and yield were smaller compared to 45 and 50 minutes.

3.4.6 Varying Carriers

Once the procedure for microprecipitation has been optimized for cerium carrier, the investigation of other lanthanide carriers was determined. For the carrier of lanthanum, the best FWHM was 26.2 ± 1.53 keV at 0.005mg of lanthanum. The best yield for lanthanum carrier was at the lower concentrations of carrier from 0.0025 to 0.005mg of lanthanum. Comparing the energy resolution and yield, the optimal carrier amount was 0.005mg of lanthanum.

When neodymium carrier amount was varied, the best FWHM was 28.69 ± 1.1 keV at 0.0025mg of neodymium. The best yield was preferred at lower concentrations of neodymium. However, comparing the energy resolution and yield, the optimal parameter of neodymium was at 0.0025mg due to the low FWHM, comparable yields, and low variability.

3.4.7 Addition of 20 mL of Hydrochloric Acid

For most chemical separation procedures, acids are introduced into the environmental samples. During this study, 20 mL of hydrochloric acid was added to the sample solution. The optimized parameters of cerium were used to determine how the addition of acid would interfere with the optimal results for cerium. The optimal parameter used was 0.0125mg of cerium with 1mL of hydrofluoric acid for 30 minute precipitation time at room temperature. From the results, the FWHM and yield increased with increasing carrier amount. The 20mL of hydrochloric acid has a huge impact on the results for microprecipitation and should be reduced in environmental samples to minimize the effects of poor energy resolution and yield.

3.4.8 Multinuclide Solution of ^{241}Am and ^{239}Pu

For some environmental samples, more than one radionuclide may be of interest. The investigation of a varying the carrier concentration of cerium in multinuclide solution containing ^{241}Am and ^{239}Pu was examined. During this study, the concentration of cerium were 0.0025, 0.005, 0.0125mg, 0.025, and 0.05mg of cerium with 1mL of hydrofluoric acid and a 30 minute precipitation time at room temperature. The sample solution contained 700 μL of ^{241}Am and 700 μL of ^{239}Pu . The results showed that ^{239}Pu behaved similarly to ^{241}Am ; however, ^{241}Am gave slightly better results for the FWHM and yield compared to ^{239}Pu . The best results for the FWHM for ^{241}Am was 26.17 ± 0.63 keV at 0.0025mg of cerium. Similarly, the best results for ^{239}Pu was also at 0.0025mg of cerium which was 31.39 ± 0.76 keV. The yields were all comparable to each other.

3.4.9 Multinuclide solution of ^{241}Am and ^{239}Pu with 20 mL HCl

The optimal parameters determined earlier were used to determine the interference of both a multinuclide solution along with 20 mL of hydrochloric acid. The carrier amount of cerium varied while keeping constant 1mL of hydrofluoric acid for 30 minute precipitation time at room temperature. Before performing microprecipitation, a sample solution of 20 mL of hydrochloric acid along with 700 μL of ^{239}Pu was added to the solution of ^{241}Am . The results showed that at low concentration of cerium ^{239}Pu had better FWHM compared to ^{241}Am ; however the yields were extremely low. As the yields began to increase, ^{241}Am began to have better FWHM compared to ^{239}Pu . As shown in the earlier study, the addition of 20 mL of HCl worsened the FWHM and yield. For environmental samples, HCl should be reduced before performing microprecipitation to reduce the additional mass.

3.4.10 Visual Interpretations

A visual for the source filters were obtained using the Cyclone Plus autoradiographic instrument. First, the filters from the first experiment using varied amounts of cerium with 1mL of hydrofluoric acid were imaged. The precipitation time was 30 minutes at room temperature. The images show that at small amounts of carrier the concentration of ^{241}Am concentrates on the outer edge of the filter along with an inner ring of high activity. The center of the filter also shows a high concentration of activity. As the carrier amount increases the ring begins to disappear and the samples activity becomes homogenized over the entire filter. At high concentrations of cerium, the activity is still homogeneous; yet, the activity is decreasing due to the extra mass of the carrier blocking the particles from reaching the detector.

The second set of filters images are the lowest and highest concentration of carrier, which corresponds to 0.005 and 0.05mg of cerium, lanthanum, and neodymium. The objective for this visual is to see if there is a difference between the different carriers and the activity distributed onto the filters. At low amounts of activity for lanthanum, a ring is also observed as seen in the low concentration of the cerium filters. However, the higher concentration of lanthanum does not show the activity as prominent as in the lower concentration of lanthanum. This means that the optimal parameter for lanthanum carrier should be found at the lower concentrations. For the lower amounts of concentration of neodymium, the filter is homogenized with activity with no ring of activity. The higher concentration of neodymium shows a high activity on the outer edge of the filter with the inside of the ring slightly lower in activity as compared to the low concentration of carrier. The low activity maybe due to too much carrier in the center of the filter or

perhaps too much activity located on the outer edge. This explains why the FWHM is worse for higher concentrations of carrier.

CHAPTER 4

ERROR ANALYSIS

4.1 Data Analysis

4.1.1 Standard Deviation

Standard deviation is used to measure the variability within each data set. When only a finite number of measurements can be made, the standard deviation of the sample, s , can be computed by Equation 4.1 rather than the population standard deviation, μ .

$$s = \sqrt{\frac{\sum_i (x - \bar{x})^2}{n - 1}} \quad \text{Equation 4.1}$$

Where s = sample standard deviation
 x = sample value
 \bar{x} = sample mean value
 $n - 1$ = degrees of freedom where n is the total number of samples

Even though the population standard deviation is unknown, the sample standard deviation can be used to make an “unbiased” approximation to the population standard deviation.

However, the sample standard deviation will underestimate the true value of the population standard deviation. The sample standard deviation is used in the experiments to determine the variability of the energy resolution and yields for each data set.

4.1.2 Outliers

Experimental data sets may have an extreme, outlying value that appears to deviate strongly away from the other data set values. These values are known as an outlier. Outliers should not be taken out of the data set unless an explanation is verified for the cause of the outlier. Some causes for possible outliers include errors in sampling, transcription or transmission, data-encoding, instrument malfunction or fluctuations,

spills or sample loss, and contamination. Outliers are not necessarily an incorrect answer but instead could be a result from a flaw in the assumed theory. Outliers should be carefully examined by the researcher for evidence of factual error.

One way to eliminate outliers is to use a statistical test. For small data sets, the Grubbs' test can be used to identify an outlier. The test is done by arranging the data in ascending order from the smallest to largest data point. The suspected outlier will be identified as being the highest data point, X_n , or the smallest data point, X_1 . If the suspected outlier is the highest data point, Equation 4.2 should be used to determine a value of T. On the other hand, if the suspected outlier is the smallest data point, Equation 4.3 should be used to determine a value for T.

$$T = \frac{\bar{X} - X_1}{s} \quad \text{Equation 4.2}$$

$$T = \frac{X_n - \bar{X}}{s} \quad \text{Equation 4.3}$$

For Equation 4.2 and 4.3 \bar{X} is the sample mean and s is the sample standard deviation. The value for T is then compared to the critical value depending on the level of confidence needed for the data. If the calculated value for T is greater than the critical value then the null hypothesis is rejected which implies that the value is suspected of being an outlier. If the null hypothesis is accepted then the value is not an outlier.

4.2 Experimental Error

4.2.1 Human Error

Many errors are associated with the techniques used by researcher for pipetting liquids. First, the pipette tips should be pre-wet with the solution before dispensing. This can be done by aspirating and expelling the solution at least three times before finally

dispensing the liquid into the centrifuge tubes. If the tips are not pre-wetted, sample loss due to evaporation may occur within the tip. Secondly, the researcher should always be aware of bubbles that may form within the tip. If this occurs, the liquid should be expelled and reaspirated. The formation of bubbles can be prevented by paying close attention while the liquid is drawn and not rushing during the aspiration. Another error that can occur is pipetting at an angle. If the pipette is not positioned upright, the pipette can potentially touch the sides of the container which would cause sample loss during aspiration. Also, if the pipette is positioned at an angle as liquid is being suctioned, the angle may cause variation in the amount of volume being drawn. Lastly, if the pipette tips are not fastened tightly to the pipette, variations in the volume will occur due to the inadequate seal. The leakage of air will may result in sample loss.

Sample loss can also occur during rinsing of the centrifuge tubes and the funnel. When the time is reach for the precipitate to form, the centrifuge containing the radioactive solution is poured into the funnel. The centrifuge tubes are rinsed at least twice to ensure that sample loss does not occur. In some cases, the centrifuge tubes may not have been rinsed well enough to remove the entire sample within the centrifuge tubes. This may cause a sample loss to occur. In contrast, if the funnels were not rinsed properly, the sample solution may be contained on the outer rim of the funnel. This may cause cross contamination onto the filter when the next experiment is performed. In any case, care should be taken to ensure that the centrifuge tubes and funnel are properly rinsed.

Another possible source of error during microprecipitation is the possibility of cross contamination onto the filters. The filters may be contaminated from previous

experiments or by other researchers prior to microprecipitation. The filters are packaged to eliminate the possibility for contamination by having a protective paper placed between each filter. However, the tweezers used in the laboratory may have been contaminated from previous experiments which may have contaminated the filter papers. This would lead to additional mass or activity onto the filter papers which would affect the results.

Lastly, error can be seen during the precipitation time. Since the suction of the solution through the filter varies, the precipitation time is not always consistent. The error in time can be as much as 2 minutes longer than expected. However, each sample was suctioned within 2 minutes of pouring the solution into the funnel.

4.2.2 Equipment Error

Error may have occurred with the water bath and the refrigerator temperatures. During the precipitation temperature experiments, a water bath and refrigerator was used to manipulate the temperature of the solution before precipitating. A thermometer was used to determine the outer temperature of the solution. However, for the water bath and the refrigerator, some fluctuations of temperatures did occur. The water bath temperature varied ± 2 degrees. The refrigerator temperature stayed consistent but may have varied by ± 1 degree.

As discussed in the previous section, errors can occur in the pipetting techniques of the researcher. In addition, the setting of the pipette volume may cause error in the amount it dispenses. The two different pipettes used in the experiments were the variable volume VWR pipettor and the set volume Eppendorf pipettor. The accuracy of the VWR

pipettor from 100 to 1000 μ L is ± 0.9 to 0.6% while the accuracy for the 100 μ L Eppendorf pipettor is $\pm 0.6\%$.

Lastly, the errors associated with microprecipitation can also originate from the equipment uncertainties used to prepare the cerium solution. The equipment used during preparation included the mass balance and the 100 mL volumetric flask. The mass balance used to measure the cerium (III) nitrate has a tolerance of ± 0.01 g. The error from the 100 mL volumetric flask is ± 0.08 mL.

4.3 Instrumentation Error

4.3.1 Alpha Spectrometer error

The instrument used to count the sample filters obtained by microprecipitation is the passivated implanted planar silicon (PIPS) detector. The PIPS detector has many advantages compared to the silicon surface barrier (SSB) detectors and diffused junction (DJ) detector. Even though the method of detection has been improved, errors associated with energy lost are still a problem associated with all detectors. The one problem that most people would assume to cause the most error in results would be the noise generated from the preamplifier and other electrical components of the alpha spectrometer. However, only a small portion of the statistical noise contributes to the error. The best energy resolution that can be achieved taking into account statistical noise can be calculated using Equation 4.4.

$$R_{\text{lim}} = 2.35\sqrt{\frac{F}{N}} = 2.35\sqrt{\frac{F\varepsilon}{E}} \quad \text{Equation 4.4}$$

Where F=Fano Factor

N=number of charge carriers per pulse

E=energy of the alpha particle

ε =ionization energy

For alpha particles, the lowest energy resolution achieved under controllable conditions using the PIPS detector was 8 keV. In general, the limiting energy resolution is commercially about 10 keV. For a silicon semiconductor detector, the limiting FWHM of Am-241 can be 3.47 keV taking into account that the Fano factor is 0.11, the ionization energy is 3.62 eV, and the energy of the alpha particle is 5.486 MeV (Knoll 2000).

Factors that cause fluctuations can come from a variety of different phenomenon. For example, the energy of the alpha particle can be transferred to the recoil nucleus instead of the electrons which would cause a lack of electron-hole pair formation. As a result, the energy loss will cause an increase in FWHM. Other factors that can decrease the energy resolution include energy lost within the dead layers of the detector, lattice vibrations within the crystal, damage from crystal, and the inability to collect charge.

4.3.2 Liquid Scintillation error

When the sample of the stock solution is introduced to the liquid scintillation cocktail, the most common problem introduced is quenching. Quenching is defined by Perkin Elmer as the “specific components found in the sample interfere with the production and/or transmission of light, thereby reducing counting efficiency” (TopCount 1993). The two types of quench are chemical and color quenching. Chemical quenching can occur when the chemicals within the sample reduces the number of photons produced. Most commonly, chemical quenching is due to the energy loss that occurs from the solvent to the solute. Color quenching is the optical properties of the sample interfering with the light output. As a result, the photons produced from the solute are

attenuate. To avoid quenching from occurring, samples dissolved in the cocktail should be free from any chemicals and colors that may interfere with the light output.

Noise can also have an impact on the outcome of the results. Noise can originate from the electrons found in the PM tube, scintillator containing long-lived phosphorescence, static from the vials, and/or photoelectron event produced in the absence of radioactivity known as luminescence. In any case, the photon that is produced will generate to a pulse that represents a false decay event. The photon produced from luminescence can occur by the chemicals within the scintillation sample. This is known as chemiluminescence. Also, a photon can be registered as a count if the cocktail is excited by UV light. To prevent noise from occurring, samples should be placed into a dark area to avoid any excitation of the cocktail which could potentially produce a false photon event.

CHAPTER 5

CONCLUSION

With the nation's current focus towards emergency response, the need to improve source preparation methods is becoming more prevalent. In particular, microprecipitation has become more widely used due to its good energy resolution and high yield. In addition, microprecipitation tends to be more reliable than other source preparation methods, such as electrodeposition and evaporation, due to the consistency of the results obtained and the very little variability exhibited. Whether the goal of the analysis is identification or quantification of a radionuclide, the procedure for microprecipitation must be optimized to generate the best possible energy resolution and yield in the least amount of time with the smallest amount of variability. In this study, the main operational parameters for microprecipitation were varied to obtain an optimal procedure for microprecipitation.

Taking into account the general procedure for microprecipitation as described in the literature, cerium was used as the carrier for the initial studies of the operational parameters. The initial studies using cerium also kept the precipitation time constant at 30 minutes and the procedure was carried out at room temperature. In all of the experiments, the amount of the 100 Bq/mL radionuclide stock solution used was held constant at 700 μ L. The parameter that was first varied was the amount of cerium carrier while holding the amount of hydrofluoric acid constant at 1mL. The best FWHM obtained was 27.3 ± 1.5 keV for 0.0125 mg of cerium. On the other hand the best possible yield achieved using the carrier concentration of 0.005mg of cerium which gave a yield of 107

$\pm 1\%$. Overall, the optimal carrier concentration was found to be 0.0125mg because the yields were all comparable at roughly around 90%. Next, the amount of hydrofluoric was varied while keeping the amount of cerium constant at an optimal amount of 0.0125mg. The optimal amount of hydrofluoric acid was 1000 μ L as shown in the previous study. When the amount of hydrofluoric acid deviated from 1000 μ L, the energy resolution worsened and the yields began to exhibit huge variability. After varying hydrofluoric and cerium separately, the next study was to vary both the hydrofluoric acid and cerium simultaneously. The ratio of cerium to hydrofluoric acid was kept constant at 0.0005. From this study of fractionation, the results for energy resolution worsened and showed huge variations in the results. The optimal amounts for cerium and hydrofluoric acid were 0.0125 mg and 1000 μ L, respectively. Using these optimal parameters, the influence of the precipitation temperature was examined. The optimal temperature was determined to be 25°C since it showed the lowest FWHM and reasonable yields of greater than 90%. Once the optimal precipitation temperature was determined, the optimal time to form the precipitate was investigated. From the results, the best energy resolutions were obtained for precipitation times between 30 and 50 minutes. One of the goals of this study was to keep the time required for the method as short as possible; therefore an optimal precipitation time of 30 minutes is suggested.

The initial cerium study took into account the carrier amount, the amount of hydrofluoric acid, fractionation, and the precipitation time and temperature. Using the optimal parameters obtained in this initial study, an investigation of different carrier elements was carried out. The carriers used were lanthanum and neodymium. The amount of the carriers was varied in the same manner as previously for cerium. The other

parameters were as follows: 1000 μ L HF at room temperature for 30 minutes to form the precipitate. The results showed that the optimal amount of lanthanum carrier was 0.005mg which gave a FWHM of 26.2 ± 1.5 keV. The optimal amount of neodymium was 0.0025mg which corresponded to a FWHM of 28.7 ± 1.1 keV. The yields for cerium, lanthanum, and neodymium were all comparable to each and were above 90%.

The final set of experiments took into account other factors, such as the sample volume and the presence of other interferences such as hydrochloric acid or other radionuclides. First, a study was conducted to determine if the optimal parameters would be affected when the sample solution was changed to 20 mL of 4 M HCl. Taking into account the optimal parameters as determined earlier, the amount of cerium carrier required after the addition of the hydrochloric acid was studied. The results showed that the FWHM was the lowest for smaller amounts of cerium; however, the yields were less than 50% for carrier amounts less than 0.1 mg of cerium. As the amount of carrier added to the solution to form the precipitate is increased further, the yields are increasing yet the energy resolution is decreasing. This means that the larger sample volume has a negative effect on the microprecipitation. If the solution consists of larger volumes of HCl, approximately 20mL, the researcher should therefore evaporate as much of the solution as possible before performing microprecipitation to avoid the possibility of poor results due to the added mass. Next, the precipitation from a multinuclide solution was examined to see how the interference of an additional radionuclide would affect the results. 700 μ L of Pu-239 along with the Am-241 was added to the sample solution. The optimal parameters determined from the initial cerium study were used which were 1mL of HF with a precipitation time of 30 at room temperature. From the result of Am-241 and Pu-

239, the energy resolution and yields were both comparable to each other. Am-241 showed slightly better results for both the energy resolution and yield; however, both radionuclides behaved similarly during microprecipitation. Lastly, the precipitation of multiple radionuclides from 20 mL of 4 M HCL was investigated. The optimal parameters were the same as determined in the initial study. The addition of both the 20 mL of HCl and Pu-239 resulted in a huge variability in the energy resolution. The yields, as shown in the HCl study earlier, were extremely low at small amounts of carrier. The Am-241 gave better FWHM compared to Pu-239 for carrier amounts less than 0.0125mg of cerium; however, Pu-239 gave better results for carrier amounts of 0.0125mg and larger. As concluded earlier, solution volume should be reduced as much as possible in order to achieve better energy resolutions and yields with small variability.

Images of the filters prepared were obtained for each amount of cerium with 1mL of HF for 30 minutes of precipitation at room temperature. Based on these images, at low amounts of cerium the activity seems to deposit in a ring pattern around the outer edge of the filter. Since there is not enough cerium to bring the Am-241 to precipitate on top of the filter, the activity remains in the filtrate and is being suctioned through the filter. As the concentration increases, the activity distribution on the filter becomes more homogeneous, in particular for the optimal amount of 0.0125mg. Once the concentration of cerium increases past the optimal concentration, the additional mass of cerium begins to cover the Am-241 and prevents it from reaching the detector. The images prove that 0.0125mg of cerium is the optimal concentration for a solution containing 1mL of HF for 30 minute precipitation time at room temperature.

Another set of images was obtained for filters with the highest and lowest amounts of lanthanum and neodymium carrier, respectively. Comparison of the images for lanthanum showed that at the smallest amount of 0.0025mg, the activity concentrates on the edge as seen for small amounts of cerium. At the higher amount of 0.05mg, the deposition on the filter appears more homogeneous; however, the filters seems to have a lower total activity compared to the filter with a smaller amount of carrier. The optimal concentration for lanthanum should be between 0.0025mg and 0.05mg with a homogeneous distribution on top of the filter. From the study comparing the different carrier types, the optimal concentration of lanthanum is using 0.005mg which is at the lower amount of carrier.

Images were also taken for the largest and smallest amounts of neodymium. From the images, the lowest amount of neodymium appears to result in a homogeneous deposition without a ring formation. This suggests that perhaps amounts smaller than 0.0025mg of neodymium are required for the ring formation to appear. At the highest concentration of neodymium, 0.05mg, the filter also exhibits a homogenous activity distribution; however there seems to be less total activity present compared to the smaller amounts of carrier. This suggests that perhaps the optimal amount of neodymium is towards the lower end of the amounts investigated. Based on the results the optimal amount for neodymium was determined to be 0.0025mg.

From both the images and the spectroscopic data the optimal parameters for microprecipitation were determined. The optimal amount of cerium is 0.0125mg. The optimal volume of hydrofluoric acid is 1000 μ L. A precipitation time of 30 minutes is sufficient for the precipitate to form. The optimal temperature for the precipitate to form

is 25°C, room temperature. If lanthanum is used as a carrier, the optimal amount is 0.005mg. In addition, if neodymium is used as the carrier, the optimal amount is 0.0025mg. In a multinuclide solution, the presence of another radionuclide, such as Pu-239, does not have an effect on the energy resolution or yield. If the sample consists of larger volumes of HCl, the sample solution should be evaporated under a heat lamp or on a hot plate to reduce the volume. This is also true for the precipitation from a multinuclide solution in the presence of larger volumes of HCl.

The overall time of the procedure for microprecipitation can be optimized depending on the volume of the sample. If the sample requires large volumes of filtrate to be acquired, a single filtration system must be used. If microprecipitation is performed with a single filtration system, a total of four samples can be filtered in an hour. However, the process time of microprecipitation can be shortened if the sample filtrate is less than 15mL. In this case, a multi filtration system apparatus, such as the Millipore sampling manifold, can be used to produce 12 samples in an hour. The volume of the sample can be reduced by evaporation which could allow the analyst to use the multi filtration system. For emergency response purposes, a multi filtration system is essential.

CHAPTER 7

FUTURE RESEARCH

Based on the results presented in this work the microprecipitation procedure can be optimized depending on the specific application. However, additional parameters can be considered if a further optimization of the procedure is desired. Future research should focus on the influence of other interferences on the method performance, in particular that of interferences that are found in environmental samples. Examples of such interferences could include elements commonly found in soil or water samples such as phosphates, iron, and calcium. Also, further images of the filter deposits should be obtained using a scanning electron microscope to determine where and how these elements are distributed onto the filter. In addition, a scanning electron microscope and x-ray fluorescence can also be used to determine the distribution of the carrier on the filters, as well. A detailed comparison of the distribution of the carrier and the radionuclide should be performed. Lastly, additional studies should be performed using sample solution volumes representative of those encountered after common chemical separations. Using a more realistic sample volume will ensure that the previously determined optimal parameters result in the best possible energy resolution and yield. With these last studies, a final optimized procedure for microprecipitation will be obtained.

APPENDIX I

MATERIALS, CHEMICALS, AND CHEMICAL FORMULAS

^{241}Am in 1M hydrochloric Acid, 100 Bq mL⁻¹, Isotope Products

Cerium (III) Nitrate Hexahydrate ($\text{Ce}(\text{NO}_3)_3 \cdot 6\text{H}_2\text{O}$), 99.9%, Strem Chemicals

Hydrofluoric Acid (HF), 48-51%, J.T. Baker

Hydrochloric Acid (HCl), 37-38%, J.T. Baker

Deionized Water (DI)

Ethanol

Lipped 25mm stainless steel planchets

Variable volume VWR pipettors

50mL Centrifuge Tubes

15mL test tubes, 125 mm x 16 mm diameter

Gelman filter apparatus

Water Bath

Thermometer

Heat lamp

Petri dishes

Vacuum pump, Dry-fast, model number 2012B-01

Resolve filters 0.1 micron 25 mm polypropylene, Eichrom

Liquid Scintillation Counter, Perkin Elmer Tri-Carb, model 3100TR

Canberra Alpha Analyst Spectrometer, 450 mm² active area PIPS detector

APPENDIX II

Table A. Calibration source data

Isotope	Energy	Channel #
²³⁹ Pu	5.16	383
U-238	4.20	311
U-234	4.78	354
²⁴¹ Am	5.49	407

Table B. Alpha spectrometer calibration data for detectors 1A, 2A, 3A, 4A, 1B, 2B, 3B, and 4B

Detector 1A				
Slot #	Counts	livetime (secs)	FWHM (keV)	Effeciency %
2	10005	303.86	30.70	20.15
4	10006	650.63	22.41	9.41
6	10000	1177.76	27.81	5.20
8	10000	1876.73	25.04	3.26
10	10000	2746.79	21.40	2.23
12	10000	3830.45	20.07	1.60

Detector 2A				
Slot #	Counts	livetime (secs)	FWHM (keV)	Effeciency %
2	10004	313.9	33.23	19.51
4	10000	662.96	23.25	9.23
6	10001	1175.47	27.10	5.21
8	10000	1901.54	29.17	3.22
10	10001	2801.01	22.86	2.19
12	10001	3992.22	13.48	1.53

Detector 3A				
Slot #	Counts	livetime (secs)	FWHM (keV)	Effeciency %
2	10002	310.00	32.14	19.75
4	10002	641.90	26.28	9.54
6	10000	1168.72	21.17	5.24
8	10000	1862.89	28.49	3.29
10	10001	2810.22	21.51	2.18
12	10000	3906.63	21.57	1.57

Detector 4A

Slot #	Counts	livetime (secs)	FWHM (keV)	Effeciency %
2	10001	316.99	33.87	19.31
4	10000	659.77	23.63	9.28
6	10002	1194.41	22.69	5.12
8	10000	1899.13	27.42	3.22
10	10000	2834.77	20.57	2.16
12	10000	3921.02	20.77	1.56

Detector 1B

Slot #	Counts	livetime (secs)	FWHM (keV)	Effeciency %
2	10003	316.63	30.95	19.34
4	10004	649.87	22.20	9.42
6	10000	1193.69	24.29	5.13
8	10000	1875.62	28.81	3.26
10	10000	2780.18	23.96	2.20
12	10001	3935.54	25.94	1.56

Detector 2B

Slot #	Counts	livetime (secs)	FWHM (keV)	Effeciency %
2	10004	306.32	31.39	19.99
4	10003	643.49	27.12	9.51
6	10002	1134.41	13.46	5.40
8	10000	1811.34	28.99	3.38
10	10000	2747.5	22.26	2.23
12	10000	3866.34	23.44	1.58

Detector 3B

Slot #	Counts	livetime (secs)	FWHM (keV)	Effeciency %
2	10008	316.99	33.87	19.32
4	10001	659.77	23.63	8.72
6	10000	1194.41	22.69	4.82
8	10000	1899.13	27.42	3.03
10	10000	2834.77	20.57	2.03
12	10000	3921.02	20.77	1.47

Detector 4B				
Slot #	Counts	livetime (secs)	FWHM (keV)	Effeciency %
2	10005	318.85	29.19	19.21
4	10003	663.37	28.80	9.23
6	10002	1176.10	22.43	5.21
8	10000	1862.06	21.81	3.29
10	10001	2816.09	26.73	2.17
12	10001	3960.62	20.88	1.55

Table C. Efficiencies (%) for Each Detector in Position #2-12

Slot #	1A	2A	3A	4A	1B	2B	3B	4B
2	18.94	18.34	18.56	18.15	18.18	18.79	18.16	18.05
4	8.85	8.68	8.96	8.72	8.86	8.94	8.72	8.68
6	4.89	4.89	4.92	4.82	4.82	5.07	4.82	4.89
8	3.07	3.03	3.09	3.03	3.07	3.18	3.03	3.09
10	2.10	2.05	2.05	2.03	2.07	2.09	2.03	2.04
12	1.50	1.44	1.47	1.47	1.46	1.49	1.47	1.45

Table D. FWHM (keV) for Each Detector in Position #2-#12

Slot #	1A	2A	3A	4A	1B	2B	3B	4B
2	30.70	33.23	32.14	33.87	30.95	31.39	33.87	29.19
4	22.41	23.25	26.28	23.63	22.20	27.12	23.63	28.80
6	27.81	27.10	21.17	22.69	24.29	13.46	22.69	22.43
8	25.04	29.17	28.49	27.42	28.81	28.99	27.42	21.81
10	21.40	22.86	21.51	20.57	23.96	22.26	20.57	26.73
12	20.07	13.48	21.57	20.77	25.94	23.44	20.77	20.88

Table E. Data used for determining the FWHM and yield for 5 μ L of cerium concentration with constant 1mL of HF for 30 minutes precipitation time at room temperature

Detector	Trial #	Counts	Lifetime (sec)	FWHM (keV)	Detector Efficiency (% decimal)	Count rate (cps)	Corrected Counts (dps)	Yield (% decimal)
3A	#1	68323	10800	38.76	0.10	6.33	61.18	1.06
	#2	22619	3600	38.80	0.10	6.28	60.76	1.05
	#3	22779	3600	37.63	0.10	6.33	61.19	1.06
	#4	22956	3600	37.20	0.10	6.38	61.67	1.07
	#5	22023	3600	41.40	0.10	6.12	59.16	1.02
Average FWHM				38.76	Average Yield			1.05
STD				1.64	STD			0.02

Table F. Data used for determining the FWHM and yield for 10 μL of cerium concentration with constant 1mL of HF for 30 minutes precipitation time at room temperature

Detector	Trial #	Counts	Lifetime (sec)	FWHM (keV)	Detector Efficiency (% decimal)	Count rate (cps)	Corrected Counts (dps)	Yield (% decimal)
2B	#1	69629	10800	40.45	0.10	6.45	62.35	1.08
	#2	23108	3600	34.18	0.10	6.42	62.08	1.07
	#3	23235	3600	33.12	0.10	6.45	62.42	1.08
	#4	22891	3599	46.25	0.10	6.36	61.51	1.06
	#5	23462	3600	40.64	0.10	6.52	63.03	1.09
Average FWHM				38.93	Average Yield			1.08
STD				5.36	STD			0.01

Table G. Data used for determining the FWHM and yield for 25 μL of cerium concentration with constant 1mL of HF for 30 minutes precipitation time at room temperature

Detector	Trial #	Counts	Lifetime (sec)	FWHM (keV)	Detector Efficiency (% decimal)	Count rate (cps)	Corrected Counts (dps)	Yield (% decimal)
2A	#1	78930	10799	26.75	0.10	7.3090	70.69	0.91
	#2	26146	3600	27.74	0.10	7.2628	70.24	0.90
	#3	26307	3600	26.56	0.10	7.3075	70.67	0.91
	#4	26317	3600	29.72	0.10	7.3103	70.70	0.91
	#5	27167	3600	25.82	0.10	7.5464	72.98	0.94
Average FWHM				27.32	Average Yield			0.91
STD				1.51	STD			0.01

Table H. Data used for determining the FWHM and yield for 50 μL of cerium concentration with constant 1mL of HF for 30 minutes precipitation time at room temperature

Detector	Trial #	Counts	Lifetime (sec)	FWHM (keV)	Detector Efficiency (% decimal)	Count rate (cps)	Corrected Counts (dps)	Yield (% decimal)
1B	#1	72158	10800	27.94	0.10	6.68	64.62	0.97
	#2	24102	3600	31.36	0.10	6.70	64.75	0.97
	#3	23759	3600	29.51	0.10	6.60	63.83	0.96
	#4	23761	3600	27.36	0.10	6.60	63.83	0.96
	#5	25950	3600	27.37	0.10	7.21	69.71	0.85
Average FWHM				28.71	Average Yield			0.94
STD				1.72	STD			0.05

Table I. Data used for determining the FWHM and yield for 100 μL of cerium concentration with constant 1mL of HF for 30 minutes precipitation time at room temperature

Detector	Trial #	Counts	Lifetime (sec)	FWHM (keV)	Detector Efficiency (% decimal)	Count rate (cps)	Corrected Counts (dps)	Yield (% decimal)
1A	#1	39243	6601.07	39.74	0.10	5.95	57.50	0.86
	#2	22176	3600	36.96	0.10	6.16	59.57	0.89
	#3	22092	3600	35.39	0.10	6.14	59.35	0.89
	#4	22884	3599	33.81	0.10	6.36	61.50	0.92
	#5	22542	3600	38.76	0.10	6.26	60.56	0.91
Average FWHM				36.93	Average Yield			0.89
STD				2.415	STD			0.02

Table J. Data used for determining the FWHM and yield for 25 μL of cerium concentration with 250 μL of HF for 30 minutes precipitation time at room temperature

Detector	Trial #	Counts	Lifetime (sec)	FWHM (keV)	Detector Efficiency (% decimal)	Count rate (cps)	Corrected Counts (dps)	Yield (% decimal)
1B	#1	21245	3600	68.35	0.10	5.90	57.07	0.99
	#2	21136	3600	57.52	0.10	5.87	56.78	0.98
	#3	21353	3600	71.52	0.10	5.93	57.36	0.99
	#4	21504	3600	80.71	0.10	5.97	57.77	1.00
	#5	21397	3600	67.72	0.10	5.94	57.48	0.99
Average FWHM				69.16	Average Yield			0.99
STD				8.33	STD			0.01

Table K. Data used for determining the FWHM and yield for 25 μL of cerium concentration with 500 μL of HF for 30 minutes precipitation time at room temperature

Detector	Trial #	Counts	Lifetime (sec)	FWHM (keV)	Detector Efficiency (% decimal)	Count rate (cps)	Corrected Counts (dps)	Yield (% decimal)
1A	#1	31224	5000	30.62	0.10	6.245	60.40	1.04
	#2	33243	5000	31.11	0.10	6.649	64.30	1.11
	#3	28392	5000	33.52	0.10	5.678	54.92	0.95
	#4	27144	5000	38.01	0.10	5.429	52.50	0.91
	#5	34035	5000	35.52	0.10	6.807	65.83	1.14
Average FWHM				33.76	Average Yield			1.03
STD				3.09	STD			0.10

Table L. Data used for determining the FWHM and yield for 25 μL of cerium concentration with 750 μL of HF for 30 minutes precipitation time at room temperature

Detector	Trial #	Counts	Lifetime (sec)	FWHM (keV)	Detector Efficiency (% decimal)	Count rate (cps)	Corrected Counts (dps)	Yield (% decimal)
1A	#1	11881	1800	37.56	0.10	6.60	63.84	1.10
	#2	11686	1800	33.61	0.10	6.49	62.79	1.09
	#3	12409	1800	38.33	0.10	6.89	66.67	1.15
	#4	11633	1800	37.72	0.10	6.46	62.50	1.08
Average FWHM				36.80	Average Yield			1.11
STD				2.16	STD			0.03

Table M. Data used for determining the FWHM and yield for 25 μL of cerium concentration with 1000 μL of HF for 30 minutes precipitation time at room temperature

Detector	Trial #	Counts	Lifetime (sec)	FWHM (keV)	Detector Efficiency (% decimal)	Count rate (cps)	Corrected Counts (dps)	Yield (% decimal)
2A	#1	78930	10799	26.75	0.10	7.31	70.69	0.91
	#2	26146	3600	27.74	0.10	7.26	70.24	0.90
	#3	26307	3600	26.56	0.10	7.31	70.67	0.91
	#4	26317	3600	29.72	0.10	7.31	70.70	0.91
	#5	27167	3600	25.82	0.10	7.55	72.98	0.94
Average FWHM				27.32	Average Yield			0.91
STD				1.51	STD			0.01

Table N. Data used for determining the FWHM and yield for 25 μL of cerium concentration with 1250 μL of HF for 30 minutes precipitation time at room temperature

Detector	Trial #	Counts	Lifetime (sec)	FWHM (keV)	Detector Efficiency (% decimal)	Count rate (cps)	Corrected Counts (dps)	Yield (% decimal)
1A	#1	23505	3600	30.14	0.10	6.53	63.15	1.09
	#2	18022	3600	30.43	0.10	5.01	48.42	0.84
	#3	24092	3600	30.03	0.10	6.69	64.72	1.12
	#4	24427	3600	33.27	0.10	6.79	65.62	1.14
	#5	24504	3600	30.96	0.10	6.81	65.83	1.14
Average FWHM				30.97	Average Yield			1.12
STD				1.34	STD			0.13

Table O. Data used for determining the FWHM and yield for 10 μL of cerium concentration with 100 μL of HF for 30 minutes precipitation time at room temperature

Detector	Trial #	Counts	Lifetime (sec)	FWHM (keV)	Detector Efficiency (% decimal)	Count rate (cps)	Corrected Counts (dps)	Yield (% decimal)
1A	#1	22606	3599	30.17	0.10	6.28	60.75	1.05
	#2	22895	3599	31.61	0.10	6.36	61.52	1.06
	#3	20286	3599	65.96	0.10	5.64	54.51	0.94
	#4	21133	3599	50.46	0.10	5.87	56.79	0.98
	#5	21226	3599	45.78	0.10	5.90	57.04	0.99
Average FWHM				44.795	Average Yield			1.00
STD				14.738	STD			0.05

Table P. Data used for determining the FWHM and yield for 25 μL of cerium concentration with 250 μL of HF for 30 minutes precipitation time at room temperature

Detector	Trial #	Counts	Lifetime (sec)	FWHM (keV)	Detector Efficiency (% decimal)	Count rate (cps)	Corrected Counts (dps)	Yield (% decimal)
1B	#1	21245	3600	68.35	0.10	5.90	57.07	0.99
	#2	21136	3600	57.52	0.10	5.87	56.78	0.98
	#3	21353	3600	71.52	0.10	5.93	57.36	0.99
	#4	21504	3600	80.71	0.10	5.97	57.77	1.00
	#5	21397	3600	67.72	0.10	5.94	57.48	0.99
Average FWHM				69.16	Average Yield			0.99
STD				8.33	STD			0.01

Table Q. Data used for determining the FWHM and yield for 50 μL of cerium concentration with 500 μL of HF for 30 minutes precipitation time at room temperature

Detector	Trial #	Counts	Lifetime (sec)	FWHM (keV)	Detector Efficiency (% decimal)	Count rate (cps)	Corrected Counts (dps)	Yield (% decimal)
2A	#1	22629	3600	52.57	0.10	6.29	60.79	1.05
	#2	23463	3600	34.85	0.10	6.52	63.03	1.09
	#3	23737	3600	30.87	0.10	6.60	63.77	1.10
	#4	21468	3600	78.04	0.10	5.96	57.67	1.00
	#5	21682	3600	58.31	0.10	6.02	58.25	1.01
Average FWHM				50.927	Average Yield			1.05
STD				19.061	STD			0.05

Table R. Data used for determining the FWHM and yield for 5 μL of cerium concentration with 50 μL of HF for 30 minutes precipitation time at room temperature

Detector	Trial #	Counts	Lifetime (sec)	FWHM (keV)	Detector Efficiency (% decimal)	Count rate (cps)	Corrected Counts (dps)	Yield (% decimal)
	#1	21714	3600	40.54	0.10	6.03	58.33	0.94
	#2	22634	3600	39.69	0.10	6.29	60.80	0.98
	#3	22166	3600	58.68	0.10	6.16	59.55	0.96
	#4	22022	3600	40.35	0.10	6.12	59.16	0.96
	#5	22163	3600	46.90	0.10	6.16	59.54	0.96
Average FWHM				45.232	Average Yield			0.96
STD				8.0617	STD			0.01

Table S. Data used for determining the FWHM and yield for 25 μL of cerium concentration with 1000 μL of HF for 30 minutes precipitation time at 0°C

Detector	Trial #	Counts	Lifetime (sec)	FWHM (keV)	Detector Efficiency (% decimal)	Count rate (cps)	Corrected Counts (dps)	Yield (% decimal)
	#1	23352	3600	25.98	0.10	6.49	62.73	1.02
	#2	10737	3600	28.97	0.10	2.98	28.84	0.47
2B	#3	21682	3600	27.25	0.10	6.02	58.25	0.94
	#4	7766	3600	32.63	0.10	2.16	20.86	0.34
	#5	23198	3600	30.35	0.10	6.44	62.32	1.01
Average FWHM				29.04	Average Yield			0.76
STD				2.61	STD			0.33

Table T. Data used for determining the FWHM and yield for 25 μL of cerium concentration with 1000 μL of HF for 30 minutes precipitation time at 30°C

Detector	Trial #	Counts	Lifetime (sec)	FWHM (keV)	Detector Efficiency (% decimal)	Count rate (cps)	Corrected Counts (dps)	Yield (% decimal)
	#1	26121	3600	31.52	0.10	7.26	70.17	0.99
	#2	26116	3600	32.57	0.10	7.25	70.16	0.99
1A	#3	26190	3600	32.36	0.10	7.28	70.36	1.00
	#4	25939	3600	37.58	0.10	7.21	69.68	0.99
	#5	25191	3600	40.42	0.10	7.00	67.67	0.96
Average FWHM				34.89	Average Yield			0.99
STD				3.90	STD			0.02

Table U. Data used for determining the FWHM and yield for 25 μL of cerium concentration with 1000 μL of HF for 30 minutes precipitation time at 35°C

Detector	Trial #	Counts	Lifetime (sec)	FWHM (keV)	Detector Efficiency (% decimal)	Count rate (cps)	Corrected Counts (dps)	Yield (% decimal)
1B	#1	25293	3600	33.71	0.10	7.03	67.95	0.96
	#2	26215	3600	28.28	0.10	7.28	70.43	1.00
	#3	25882	3600	34.35	0.10	7.19	69.53	0.98
	#4	25925	3600	29.87	0.10	7.20	69.65	0.99
	#5	26478	3600	27.62	0.10	7.36	71.13	1.01
Average FWHM				30.77	Average Yield			0.99
STD				3.10	STD			0.02

Table V. Data used for determining the FWHM and yield for 25 μL of cerium concentration with 1000 μL of HF for 30 minutes precipitation time at 40°C

Detector	Trial #	Counts	Lifetime (sec)	FWHM (keV)	Detector Efficiency (% decimal)	Count rate (cps)	Corrected Counts (dps)	Yield (% decimal)
	#1	25699	3600	30.39	0.10	7.14	69.04	1.12
	#2	26481	3600	29.00	0.10	7.36	71.14	1.15
	#3	26370	3600	27.79	0.10	7.33	70.84	1.15
	#4	25682	3600	35.60	0.10	7.13	68.99	1.12
	#5	25959	3600	26.97	0.10	7.21	69.67	0.94
	#6	25955	3600	27.25	0.10	7.21	69.66	0.94
Average FWHM				29.50	Average Yield			1.07
STD				3.24	STD			0.10

Table W. Data used for determining the FWHM and yield for 25 μL of cerium concentration with 1000 μL of HF for 30 minutes precipitation time at 45°C

Detector	Trial #	Counts	Lifetime (sec)	FWHM (keV)	Detector Efficiency (% decimal)	Count rate (cps)	Corrected Counts (dps)	Yield (% decimal)
2B	#1	27374	3600	32.91	0.10	7.60	73.54	1.19
	#2	26414	3600	32.66	0.10	7.34	70.96	1.15
	#3	26668	3600	36.25	0.10	7.41	71.64	1.16
	#4	26323	3600	33.89	0.10	7.31	70.72	1.15
	#5	26445	3600	36.24	0.10	7.35	71.04	1.15
Average FWHM				34.39	Average Yield			1.16
STD				1.76	STD			0.02

Table X. Data used for determining the FWHM and yield for 25 μL of cerium concentration with 1000 μL of HF for 30 minutes precipitation time at 50°C

Detector	Trial #	Counts	Lifetime (sec)	FWHM (keV)	Detector Efficiency (% decimal)	Count rate (cps)	Corrected Counts (dps)	Yield (% decimal)
	#1	25710	3600	30.40	0.10	7.14	69.07	1.06
	#2	25896	3600	27.12	0.10	7.19	69.57	1.07
	#3	25925	3600	32.82	0.10	7.20	69.65	1.07
	#4	26196	3600	33.36	0.10	7.28	70.37	1.08
	#5	25341	3600	29.65	0.10	7.04	68.01	1.05
	#6	25799	3600	29.14	0.10	7.17	69.24	1.07
Average FWHM				30.42	Average Yield			1.07
STD				2.35	STD			0.01

Table Y. Data used for determining the FWHM and yield for 25 μL of cerium concentration with 1000 μL of HF for 10 minutes precipitation time at room temperature.

Detector	Trial #	Counts	Lifetime (sec)	FWHM (keV)	Detector Efficiency (% decimal)	Count rate (cps)	Corrected Counts (dps)	Yield (% decimal)
	#1	24837	3600	41.77	0.10	6.90	66.66	0.90
	#2	26333	3600	33.56	0.10	7.32	70.67	0.96
	#3	21203	3600	34.08	0.10	5.89	56.91	0.77
	#4	26105	3600	35.45	0.10	7.25	70.06	0.95
	#5	26057	3600	32.10	0.10	7.24	69.93	0.95
Average FWHM				35.39	Average Yield			0.91
STD				3.76	STD			0.08

Table Z. Data used for determining the FWHM and yield for 25 μL of cerium concentration with 1000 μL of HF for 20 minutes precipitation time at room temperature.

Detector	Trial #	Counts	Lifetime (sec)	FWHM (keV)	Detector Efficiency (% decimal)	Count rate (cps)	Corrected Counts (dps)	Yield (% decimal)
1A	#1	26257	3600	31.97	0.10	7.29	70.47	0.95
	#2	26107	3600	33.45	0.10	7.25	70.07	0.95
	#3	26334	3600	31.32	0.10	7.32	70.68	0.95
	#4	22578	3600	39.52	0.10	6.27	60.60	0.82
	#5	26377	3600	34.98	0.10	7.33	70.79	0.96
	#6	25948	3600	37.88	0.10	7.21	69.64	0.94
Average FWHM				34.85	Average Yield			0.93
STD				3.28	STD			0.05

Table AA. Data used for determining the FWHM and yield for 25 μL of cerium concentration with 1000 μL of HF for 45 minutes precipitation time at room temperature.

Detector	Trial #	Counts	Lifetime (sec)	FWHM (keV)	Detector Efficiency (% decimal)	Count rate (cps)	Corrected Counts (dps)	Yield (% decimal)
1B	#1	25529	3600	25.35	0.10	7.091	68.52	0.93
	#2	26388	3600	30.41	0.10	7.330	70.82	0.96
	#3	26083	3600	30.99	0.10	7.245	70.00	0.95
	#4	26076	3600	24.51	0.10	7.243	69.98	0.95
	#5	26277	3600	30.51	0.10	7.299	70.52	0.96
Average FWHM				28.36	Average Yield			0.95
STD				3.15	STD			0.01

Table BB. Data used for determining the FWHM and yield for 25 μL of cerium concentration with 1000 μL of HF for 50 minutes precipitation time at room temperature.

Detector	Trial #	Counts	Lifetime (sec)	FWHM (keV)	Detector Efficiency (% decimal)	Count rate (cps)	Corrected Counts (dps)	Yield (% decimal)
2A	#1	24322	3600	29.41	0.10	6.76	65.28	0.88
	#2	23503	3600	30.20	0.10	6.53	63.08	0.85
	#3	26073	3600	25.20	0.10	7.24	69.98	0.95
	#4	26302	3600	27.16	0.10	7.31	70.59	0.96
	#5	26457	3600	25.98	0.10	7.35	71.01	0.96
Average FWHM				27.59	Average Yield			0.92
STD				2.15	STD			0.05

Table CC. Data used for determining the FWHM and yield for 25 μL of cerium concentration with 1000 μL of HF for 1 hour precipitation time at room temperature.

Detector	Trial #	Counts	Lifetime (sec)	FWHM (keV)	Detector Efficiency (% decimal)	Count rate (cps)	Corrected Counts (dps)	Yield (% decimal)
2B	#1	25999	3600	34.22	0.10	7.22	69.78	0.95
	#2	26108	3600	34.65	0.10	7.25	70.07	0.95
	#3	26452	3600	31.70	0.10	7.35	70.99	0.96
	#4	26026	3600	33.57	0.10	7.23	69.85	0.95
	#5	26051	3600	32.77	0.10	7.24	69.92	0.95
Average FWHM				33.38	Average Yield			0.95
STD				1.18	STD			0.01

Table DD. Data used for determining the FWHM and yield for 25 μL of cerium concentration with 1000 μL of HF for 2 hour precipitation time at room temperature.

Detector	Trial #	Counts	Lifetime (sec)	FWHM (keV)	Detector Efficiency (% decimal)	Count rate (cps)	Corrected Counts (dps)	Yield (% decimal)
3A	#1	25480	3600	28.92	0.10	7.08	68.38	0.93
	#2	25483	3600	33.61	0.10	7.08	68.39	0.93
	#3	25498	3600	28.61	0.10	7.08	68.43	0.93
	#4	25280	3600	35.37	0.10	7.02	67.85	0.92
Average FWHM				31.63	Average Yield			0.92
STD				3.39	STD			0.003

Table EE. Data used for determining the FWHM and yield for 25 μL of cerium concentration with 1000 μL of HF for 4 hour precipitation time at room temperature.

Detector	Trial #	Counts	Lifetime (sec)	FWHM (keV)	Detector Efficiency (% decimal)	Count rate (cps)	Corrected Counts (dps)	Yield (% decimal)
1B	#1	26202	3600	33.85	0.10	7.28	70.32	0.95
	#2	25773	3600	29.97	0.10	7.16	69.17	0.93
	#3	26288	3600	30.75	0.10	7.30	70.55	0.95
	#4	26262	3600	30.90	0.10	7.30	70.48	0.95
	#5	24922	3600	31.70	0.10	6.92	66.89	0.90
	#6	25907	3600	29.25	0.10	7.20	69.53	0.94
Average FWHM				31.07	Average Yield			0.94
STD				1.60	STD			0.02

Table FF. Data used for determining the FWHM and yield for 25 μL of cerium concentration with 1000 μL of HF for 8 hour precipitation time at room temperature.

Detector	Trial #	Counts	Lifetime (sec)	FWHM (keV)	Detector Efficiency (% decimal)	Count rate (cps)	Corrected Counts (dps)	Yield (% decimal)
2A	#1	26028	3600	36.34	0.10	7.23	69.86	0.94
	#2	26377	3600	37.37	0.10	7.33	70.79	0.96
	#3	26134	3600	36.36	0.10	7.26	70.14	0.95
	#4	26351	3600	36.00	0.10	7.32	70.72	0.96
	#5	25983	3600	36.75	0.10	7.22	69.73	0.94
	#6	25920	3600	48.48	0.10	7.20	69.57	0.94
Average FWHM				38.55	Average Yield			0.95
STD				4.88	STD			0.01

Table GG. Data used for determining the FWHM and yield for 25 μL of cerium concentration with 1000 μL of HF for 16 hour precipitation time at room temperature.

Detector	Trial #	Counts	Lifetime (sec)	FWHM (keV)	Detector Efficiency (% decimal)	Count rate (cps)	Corrected Counts (dps)	Yield (% decimal)
2B	#1	26386	3600	39.14	0.10	7.32	70.82	0.89
	#2	26617	3600	39.05	0.10	7.39	71.44	0.90
	#3	26816	3600	42.07	0.10	7.45	71.97	0.91
	#4	26389	3600	41.35	0.10	7.33	70.82	0.89
	#5	25331	3600	40.79	0.10	7.04	67.98	0.86
Average FWHM				40.48	Average Yield			0.89
STD				1.34	STD			0.02

Table HH. Data used for determining the FWHM and yield for 25 μL of cerium concentration with 1000 μL of HF for 24 hour precipitation time at room temperature.

Detector	Trial #	Counts	Lifetime (sec)	FWHM (keV)	Detector Efficiency (% decimal)	Count rate (cps)	Corrected Counts (dps)	Yield (% decimal)
3A	#1	26046	3600	37.18	0.10	7.24	69.90	0.89
	#2	25750	3600	39.31	0.10	7.15	69.11	0.88
	#3	20245	3600	38.79	0.10	5.62	54.33	0.69
	#4	25874	3600	37.84	0.10	7.19	69.44	0.88
	#5	26334	3600	33.20	0.10	7.31	70.68	0.90
	#6	25845	3600	36.32	0.10	7.18	69.36	0.88
Average FWHM				37.11	Average Yield			0.86
STD				2.20	STD			0.08

Table II. Data used for determining the FWHM and yield for 5 μL of lanthanum concentration with 1000 μL of HF for 30 minute precipitation time at room temperature.

Detector	Trial #	Counts	Lifetime (sec)	FWHM (keV)	Detector Efficiency (% decimal)	Count rate (cps)	Corrected Counts (dps)	Yield (% decimal)
1A	#1	25519	3600	29.14	0.10	7.09	68.49	0.92
	#2	25797	3600	30.99	0.10	7.17	69.24	0.93
	#3	25724	3600	30.47	0.10	7.15	69.04	0.92
	#4	24980	3600	29.95	0.10	6.94	67.04	0.90
	#5	25817	3600	28.64	0.10	7.17	69.29	0.93
	#6	25983	3600	27.46	0.10	7.22	69.73	0.93
Average FWHM				29.44	Average Yield			0.92
STD				1.29	STD			0.01

Table JJ. Data used for determining the FWHM and yield for 10 μL of lanthanum concentration with 1000 μL of HF for 30 minute precipitation time at room temperature.

Detector	Trial #	Counts	Lifetime (sec)	FWHM (keV)	Detector Efficiency (% decimal)	Count rate (cps)	Corrected Counts (dps)	Yield (% decimal)
1B	#1	25114	3600	25.37	0.10	7.00	67.40	0.90
	#2	25656	3600	28.38	0.10	7.13	68.86	0.92
	#3	25403	3600	26.66	0.10	7.06	68.18	0.91
	#4	25702	3600	26.22	0.10	7.14	68.98	0.92
	#5	25378	3600	26.77	0.10	7.05	68.11	0.91
	#6	24280	3600	23.82	0.10	6.74	65.16	0.87
Average FWHM				26.20	Average Yield			0.91
STD				1.53	STD			0.02

Table KK. Data used for determining the FWHM and yield for 25 μL of lanthanum concentration with 1000 μL of HF for 30 minute precipitation time at room temperature.

Detector	Trial #	Counts	Lifetime (sec)	FWHM (keV)	Detector Efficiency (% decimal)	Count rate (cps)	Corrected Counts (dps)	Yield (% decimal)
2A	#1	25937	3600	28.36	0.10	7.21	69.61	0.93
	#2	24515	3600	34.87	0.10	6.81	65.79	0.88
	#3	25602	3600	29.12	0.10	7.11	68.71	0.92
	#4	26174	3600	26.52	0.10	7.27	70.25	0.94
	#5	25893	3600	26.31	0.10	7.19	69.49	0.93
	#6	25800	3600	25.97	0.10	7.17	69.24	0.93
Average FWHM				28.52	Average Yield			0.92
STD				3.35	STD			0.02

Table LL. Data used for determining the FWHM and yield for 50 μL of lanthanum concentration with 1000 μL of HF for 30 minute precipitation time at room temperature.

Detector	Trial #	Counts	Lifetime (sec)	FWHM (keV)	Detector Efficiency (% decimal)	Count rate (cps)	Corrected Counts (dps)	Yield (% decimal)
2B	#1	25865	3600	33.52	0.10	7.19	69.42	0.94
	#2	26533	3600	32.03	0.10	7.37	71.21	0.96
	#3	26031	3600	30.85	0.10	7.23	69.86	0.95
	#4	26351	3600	30.80	0.10	7.32	70.72	0.96
	#5	26692	3600	30.53	0.10	7.41	71.64	0.97
	#6	24201	3600	34.46	0.10	6.72	64.95	0.88
Average FWHM				32.03	Average Yield			0.94
STD				1.63	STD			0.03

Table MM. Data used for determining the FWHM and yield for 100 μL of lanthanum concentration with 1000 μL of HF for 30 minute precipitation time at room temperature.

Detector	Trial #	Counts	Lifetime (sec)	FWHM (keV)	Detector Efficiency (% decimal)	Count rate (cps)	Corrected Counts (dps)	Yield (% decimal)
3A	#1	24937	3600	42.05	0.10	6.93	66.93	0.91
	#2	25751	3600	49.64	0.10	7.15	69.11	0.94
	#3	24755	3600	43.41	0.10	6.88	66.44	0.90
	#4	25734	3600	47.60	0.10	7.15	69.07	0.94
	#5	25853	3600	41.83	0.10	7.18	69.39	0.94
	#6	26003	3600	52.33	0.10	7.22	69.79	0.95
Average FWHM				46.14	Average Yield			0.93
STD				4.37	STD			0.02

Table NN. Data used for determining the FWHM and yield for 5 μL of neodymium concentration with 1000 μL of HF for 30 minute precipitation time at room temperature.

Detector	Trial #	Counts	Lifetime (sec)	FWHM (keV)	Detector Efficiency (% decimal)	Count rate (cps)	Corrected Counts (dps)	Yield (% decimal)
3A	#1	24730	3600	28.63	0.10	6.87	66.37	0.92
	#2	25490	3600	27.96	0.10	7.08	68.41	0.94
	#3	25510	3600	28.98	0.10	7.09	68.46	0.95
	#4	25317	3600	27.01	0.10	7.03	67.95	0.94
	#5	25777	3600	29.41	0.10	7.16	69.18	0.96
	#6	25804	3600	30.13	0.10	7.17	69.25	0.96
Average FWHM				28.69	Average Yield			0.94
STD				1.10	STD			0.01

Table OO. Data used for determining the FWHM and yield for 10 μL of neodymium concentration with 1000 μL of HF for 30 minute precipitation time at room temperature.

Detector	Trial #	Counts	Lifetime (sec)	FWHM (keV)	Detector Efficiency (% decimal)	Count rate (cps)	Corrected Counts (dps)	Yield (% decimal)
2B	#1	26223	3600	31.09	0.10	7.28	70.38	0.97
	#2	26785	3600	30.06	0.10	7.44	71.89	0.99
	#3	26874	3600	33.24	0.10	7.47	72.13	1.00
	#4	26726	3600	31.98	0.10	7.42	71.73	0.99
	#5	23510	3600	34.00	0.10	6.53	63.10	0.87
	#6	26471	3600	31.78	0.10	7.35	71.04	0.98
Average FWHM				32.02	Average Yield			0.97
STD				1.43	STD			0.05

Table PP. Data used for determining the FWHM and yield for 25 μL of neodymium concentration with 1000 μL of HF for 30 minute precipitation time at room temperature.

Detector	Trial #	Counts	Lifetime (sec)	FWHM (keV)	Detector Efficiency (% decimal)	Count rate (cps)	Corrected Counts (dps)	Yield (% decimal)
2A	#1	25761	3600	36.86	0.10	7.16	69.14	0.95
	#2	25503	3600	35.20	0.10	7.08	68.45	0.95
	#3	24933	3600	36.79	0.10	6.93	66.92	0.92
	#4	26145	3600	35.18	0.10	7.26	70.17	0.97
	#5	25843	3600	36.11	0.10	7.18	69.36	0.96
	#6	25889	3600	31.31	0.10	7.19	69.48	0.96
Average FWHM				35.24	Average Yield			0.95
STD				2.06	STD			0.02

Table QQ. Data used for determining the FWHM and yield for 50 μL of neodymium concentration with 1000 μL of HF for 30 minute precipitation time at room temperature.

Detector	Trial #	Counts	Lifetime (sec)	FWHM (keV)	Detector Efficiency (% decimal)	Count rate (cps)	Corrected Counts (dps)	Yield (% decimal)
1B	#1	25637	3600	30.061	0.10	7.121	68.80569	0.9209
	#2	25269	3600	31.141	0.10	7.019	67.81804	0.9077
	#3	25906	3600	31.42	0.10	7.196	69.52764	0.9306
	#4	24102	3600	31.233	0.10	6.695	64.68599	0.8658
	#5	25063	3600	31.861	0.10	6.962	67.26516	0.9003
Average FWHM				31.143	Average Yield			0.905
STD				0.6654	STD			0.0249

Table RR. Data used for determining the FWHM and yield for 100 μL of neodymium concentration with 1000 μL of HF for 30 minute precipitation time at room temperature.

Detector	Trial #	Counts	Lifetime (sec)	FWHM (keV)	Detector Efficiency (% decimal)	Count rate (cps)	Corrected Counts (dps)	Yield (% decimal)
	#1	25535	3600	40.70	0.10	7.09	68.53	0.92
	#2	26057	3600	38.60	0.10	7.24	69.93	0.94
	#3	25949	3600	40.75	0.10	7.21	69.64	0.93
	#4	25877	3600	39.95	0.10	7.19	69.45	0.93
	#5	26084	3600	38.67	0.10	7.25	70.01	0.94
Average FWHM				39.84	Average Yield			0.93
STD				0.97	STD			0.01

Table SS. Data used for determining the FWHM and yield for 5 μL of cerium concentration with 1000 μL of HF and the addition of 20mL of HCl for 30 minute precipitation time at room temperature.

Detector	Trial #	Counts	Lifetime (sec)	FWHM (keV)	Detector Efficiency (% decimal)	Count rate (cps)	Corrected Counts (dps)	Yield (% decimal)
3A	#1	3607	510915.9	48.82	0.10	0.007	0.07	0.0009
	#2	1117	510907.6	46.14	0.10	0.002	0.02	0.0003
	#3	614	510891.8	32.94	0.10	0.001	0.01	0.0002
	#4	361	510884.5	46.11	0.10	0.001	0.007	9.4E-05
	#5	353	510899.4	48.55	0.10	0.001	0.007	9.2E-05
Average FWHM				44.514	Average Yield			0.0003
STD				6.59505	STD			0.0004

Table TT. Data used for determining the FWHM and yield for 10 μL of cerium concentration with 1000 μL of HF and the addition of 20mL of HCl for 30 minute precipitation time at room temperature.

Detector	Trial #	Counts	Lifetime (sec)	FWHM (keV)	Detector Efficiency (% decimal)	Count rate (cps)	Corrected Counts (dps)	Yield (% decimal)
2B	#1	966	519515.5	70.18	0.10	0.002	0.02	0.0003
	#2	537	519560.9	44.70	0.10	0.001	0.01	0.0001
	#3	795	519573.1	52.49	0.10	0.002	0.01	0.0002
	#4	2430	519596.4	65.34	0.10	0.005	0.05	0.0006
	#5	670	519620.7	48.43	0.10	0.001	0.01	0.0002
Average FWHM				56.23	Average Yield			0.0003
STD				11.01	STD			0.0002

Table UU. Data used for determining the FWHM and yield for 25 μL of cerium concentration with 1000 μL of HF and the addition of 20mL of HCl for 30 minute precipitation time at room temperature.

Detector	Trial #	Counts	Lifetime (sec)	FWHM (keV)	Detector Efficiency (% decimal)	Count rate (cps)	Corrected Counts (dps)	Yield (% decimal)
2A	#1	29312	432119.9	46.24	0.10	0.07	0.66	0.01
	#2	23152	432136.1	41.25	0.10	0.05	0.52	0.01
	#3	18955	432133.1	55.29	0.10	0.04	0.42	0.01
	#4	5287	432071.5	40.45	0.10	0.01	0.12	0.002
	#5	69136	432067.7	44.16	0.10	0.16	1.55	0.02
Average FWHM				45.48	Average Yield			0.00899
STD				5.95	STD			0.0074

Table VV. Data used for determining the FWHM and yield for 50 μL of cerium concentration with 1000 μL of HF and the addition of 20mL of HCl for 30 minute precipitation time at room temperature.

Detector	Trial #	Counts	Lifetime (sec)	FWHM (keV)	Detector Efficiency (% decimal)	Count rate (cps)	Corrected Counts (dps)	Yield (% decimal)
1B	#1	26261	433629.3	51.86	0.10	0.06	0.59	0.008
	#2	12833	433623.4	39.64	0.10	0.03	0.29	0.004
	#3	13165	433597.5	43.44	0.10	0.03	0.29	0.004
	#4	42559	433579.4	46.39	0.10	0.10	0.95	0.01
	#5	3875	433663.4	35.94	0.10	0.01	0.09	0.001
Average FWHM				43.45	Average Yield			0.01
STD				6.13	STD			0.005

Table WW. Data used for determining the FWHM and yield for 100 μL of cerium concentration with 1000 μL of HF and the addition of 20mL of HCl for 30 minute precipitation time at room temperature.

Detector	Trial #	Counts	Lifetime (sec)	FWHM (keV)	Detector Efficiency (% decimal)	Count rate (cps)	Corrected Counts (dps)	Yield (% decimal)
1A	#1	403944	119991.6	43.65	0.10	3.37	32.53	0.45
	#2	238769	119988.3	71.46	0.10	1.99	19.23	0.26
	#3	381330	119985.6	50.43	0.10	3.18	30.71	0.42
	#4	331396	119986.7	57.93	0.10	2.76	26.69	0.37
	#5	414659	119987	41.28	0.10	3.46	33.39	0.46
Average FWHM				52.95	Average Yield			0.39
STD				12.21	STD			0.08

Table XX. Data used for determining the FWHM and yield for 200 μL of cerium concentration with 1000 μL of HF and the addition of 20mL of HCl for 30 minute precipitation time at room temperature.

Detector	Trial #	Counts	Lifetime (sec)	FWHM (keV)	Detector Efficiency (% decimal)	Count rate (cps)	Corrected Counts (dps)	Yield (% decimal)
3A	#1	88965	26666.37	108.06	0.10	3.34	32.23	0.41
	#2	113576	26644.27	71.79	0.10	4.26	41.19	0.53
	#3	114883	26537.57	54.40	0.10	4.33	41.83	0.53
	#4	125030	26627.02	57.05	0.10	4.70	45.37	0.58
	#5	102459	26617.6	91.05	0.10	3.85	37.19	0.48
Average FWHM				76.47	Average Yield			0.51
STD				22.89	STD			0.064

Table YY. Data used for determining the FWHM and yield for 400 μL of cerium concentration with 1000 μL of HF and the addition of 20mL of HCl for 30 minute precipitation time at room temperature.

Detector	Trial #	Counts	Lifetime (sec)	FWHM (keV)	Detector Efficiency (% decimal)	Count rate (cps)	Corrected Counts (dps)	Yield (% decimal)
2B	#1	47755	9837.02	59.97	0.10	4.86	46.90	0.60
	#2	57578	9843.32	62.18	0.10	5.85	56.52	0.72
	#3	46750	9728.91	55.85	0.10	4.80	46.43	0.59
	#4	55442	9744.79	58.41	0.10	5.69	54.97	0.70
	#5	52618	9744.57	56.74	0.10	5.40	52.17	0.67
Average FWHM				58.63	Average Yield			0.66
STD				2.54	STD			0.06

Table ZZ. Data used for determining the FWHM and yield for 600 μL of cerium concentration with 1000 μL of HF and the addition of 20mL of HCl for 30 minute precipitation time at room temperature.

Detector	Trial #	Counts	Lifetime (sec)	FWHM (keV)	Detector Efficiency (% decimal)	Count rate (cps)	Corrected Counts (dps)	Yield (% decimal)
2A	#1	78916	7200	76.04	0.10	10.96	105.90	0.70
	#2	77434	7200	74.50	0.10	10.76	103.91	0.69
	#3	72996	7200	73.71	0.10	10.14	97.95	0.65
	#4	80947	7200	79.81	0.10	11.24	108.62	0.72
	#5	77156	7200	77.24	0.10	10.72	103.54	0.69
Average FWHM				76.26	Average Yield			0.69
STD				2.41	STD			0.03

Table AAA. Data used for determining the FWHM and yield for 800 μL of cerium concentration with 1000 μL of HF and the addition of 20mL of HCl for 30 minute precipitation time at room temperature.

Detector	Trial #	Counts	Lifetime (sec)	FWHM (keV)	Detector Efficiency (% decimal)	Count rate (cps)	Corrected Counts (dps)	Yield (% decimal)
	#1	92739	7200	93.74	0.10	12.88	124.45	0.83
	#2	92355	7200	91.58	0.10	12.83	123.93	0.82
	#3	91515	7200	91.55	0.10	12.71	122.81	0.82
	#4	94754	7200	88.79	0.10	13.16	127.15	0.85
	#5	92205	7200	95.23	0.10	12.81	123.73	0.82
Average FWHM				92.18	Average Yield			0.83
STD				2.45	STD			0.01

Table BBB. Data used for determining the FWHM and yield for 1000 μL of cerium concentration with 1000 μL of HF and the addition of 20mL of HCl for 30 minute precipitation time at room temperature.

Detector	Trial #	Counts	Lifetime (sec)	FWHM (keV)	Detector Efficiency (% decimal)	Count rate (cps)	Corrected Counts (dps)	Yield (% decimal)
1A	#1	49036	3600	103.38	0.10	13.62	131.60	0.90
	#2	48735	3600	108.83	0.10	13.54	130.80	0.89
	#3	48551	3600	103.56	0.10	13.49	130.30	0.89
	#4	47348	3600	98.31	0.10	13.15	127.07	0.87
Average FWHM				103.52	Average Yield			0.89
STD				4.30	STD			0.01

Table CCC. Data used for determining the FWHM and yield for 1200 μL of cerium concentration with 1000 μL of HF and the addition of 20mL of HCl for 30 minute precipitation time at room temperature.

Detector	Trial #	Counts	Lifetime (sec)	FWHM (keV)	Detector Efficiency (% decimal)	Count rate (cps)	Corrected Counts (dps)	Yield (% decimal)
	#1	49145	3600	118.05	0.10	13.65	131.90	0.90
	#2	50704	3600	129.42	0.10	14.08	136.08	0.93
	#3	48296	3600	120.99	0.10	13.42	129.62	0.88
	#4	48369	3600	115.74	0.10	13.44	129.81	0.89
	#5	44536	3600	107.92	0.10	12.37	119.53	0.82
Average FWHM				118.42	Average Yield			0.90
STD				7.83	STD			0.02

Table DDD. Data used for determining the FWHM and yield of ^{241}Am in a multinuclide solution using 5 μL of cerium concentration with 1000 μL of HF for 30 minute precipitation time at room temperature.

Detector	Trial #	Counts	Lifetime (sec)	FWHM (keV)	Detector Efficiency (% decimal)	Count rate (cps)	Corrected Counts (dps)	Yield (% decimal)
1A	#1	15678	2700	26.972	0.10	5.807	56.10306	0.8437
1B	#2	17244	2700	26.195	0.10	6.387	61.70692	0.9279
2A	#3	16942	2700	25.431	0.10	6.275	60.62623	0.9117
2B	#4	17341	2700	26.094	0.10	6.423	62.05403	0.9332
Average FWHM				26.173	Average Yield			0.9041
STD				0.63131	STD			0.0413

Table EEE. Data used for determining the FWHM and yield of ^{239}Pu in a multinuclide solution using 5 μL of cerium concentration with 1000 μL of HF for 30 minute precipitation time at room temperature.

Detector	Trial #	Counts	Lifetime (sec)	FWHM (keV)	Detector Efficiency (% decimal)	Count rate (cps)	Corrected Counts (dps)	Yield (% decimal)
1A	#1	17877	2700	32.37	0.10	6.62	63.97	0.85
1B	#2	19544	2700	30.91	0.10	7.24	69.94	0.93
2A	#3	19536	2700	31.60	0.10	7.24	69.91	0.93
2B	#4	19587	2700	30.69	0.10	7.25	70.09	0.93
Average FWHM				31.39	Average Yield			0.91
STD				0.76	STD			0.04

Table FFF. Data used for determining the FWHM and yield of ^{241}Am in a multinuclide solution using 10 μL of cerium concentration with 1000 μL of HF for 30 minute precipitation time at room temperature.

Detector	Trial #	Counts	Lifetime (sec)	FWHM (keV)	Detector Efficiency (% decimal)	Count rate (cps)	Corrected Counts (dps)	Yield (% decimal)
1A	#1	13456	2700	31.42	0.10	4.98	48.15	0.72
	#2	17120	2700	31.17	0.10	6.34	61.26	0.92
	#3	17060	2700	31.14	0.10	6.32	61.05	0.92
	#4	17138	2700	34.05	0.10	6.35	61.33	0.92
Average FWHM				32.12	Average Yield			0.92
STD				1.67	STD			0.002

Table GGG. Data used for determining the FWHM and yield of ^{239}Pu in a multinuclide solution using 10 μL of cerium concentration with 1000 μL of HF for 30 minute precipitation time at room temperature.

Detector	Trial #	Counts	Lifetime (sec)	FWHM (keV)	Detector Efficiency (% decimal)	Count rate (cps)	Corrected Counts (dps)	Yield (% decimal)
1A	#1	15609	2700	30.26	0.10	5.78	55.86	0.74
2A	#2	19763	2700	30.97	0.10	7.32	70.72	0.94
2B	#3	19645	2700	30.34	0.10	7.28	70.30	0.94
3A	#4	19411	2700	36.10	0.10	7.19	69.46	0.93
Average FWHM				32.47	Average Yield			0.93
STD				3.16	STD			0.009

Table HHH. Data used for determining the FWHM and yield of ^{241}Am in a multinuclide solution using 25 μL of cerium concentration with 1000 μL of HF for 30 minute precipitation time at room temperature.

Detector	Trial #	Counts	Lifetime (sec)	FWHM (keV)	Detector Efficiency (% decimal)	Count rate (cps)	Corrected Counts (dps)	Yield (% decimal)
1A	#1	24455	3600	29.09	0.10	6.79	65.63	0.99
1B	#2	23814	3600	28.31	0.10	6.62	63.91	0.96
2A	#3	11975	1800	29.46	0.10	6.65	64.28	0.97
2B	#4	10423	1800	27.71	0.10	5.79	55.95	0.84
3A	#5	22090	3600	28.53	0.10	6.14	59.29	0.89
Average FWHM				28.62	Average Yield			0.93
STD				0.68	STD			0.061

Table III. Data used for determining the FWHM and yield of ^{239}Pu in a multinuclide solution using 25 μL of cerium concentration with 1000 μL of HF for 30 minute precipitation time at room temperature.

Detector	Trial #	Counts	Lifetime (sec)	FWHM (keV)	Detector Efficiency (% decimal)	Count rate (cps)	Corrected Counts (dps)	Yield (% decimal)
1A	#1	27284	3600	32.29	0.10	7.58	73.23	0.92
1B	#2	26640	3600	32.46	0.10	7.40	71.50	0.90
2A	#3	13477	1800	32.45	0.10	7.49	72.34	0.91
2B	#4	11555	1800	33.07	0.10	6.42	62.02	0.78
3A	#5	24467	3600	34.35	0.10	6.80	65.67	0.82
Average FWHM				32.92	Average Yield			0.86
STD				0.85	STD			0.061

Table JJJ. Data used for determining the FWHM and yield of ^{241}Am in a multinuclide solution using 50 μL of cerium concentration with 1000 μL of HF for 30 minute precipitation time at room temperature.

Detector	Trial #	Counts	Lifetime (sec)	FWHM (keV)	Detector Efficiency (% decimal)	Count rate (cps)	Corrected Counts (dps)	Yield (% decimal)
1A	#1	25034	3600	29.53	0.10	6.95	67.19	1.01
1B	#2	24626	3600	29.79	0.10	6.84	66.09	0.99
2A	#3	24767	3600	26.66	0.10	6.88	66.47	1.00
2B	#4	23617	3600	28.06	0.10	6.56	63.38	0.95
3A	#5	23671	3600	30.51	0.10	6.58	63.53	0.96
Average FWHM				28.91	Average Yield			0.98
STD				1.54	STD			0.03

Table KKK. Data used for determining the FWHM and yield of ^{239}Pu in a multinuclide solution using 50 μL of cerium concentration with 1000 μL of HF for 30 minute precipitation time at room temperature.

Detector	Trial #	Counts	Lifetime (sec)	FWHM (keV)	Detector Efficiency (% decimal)	Count rate (cps)	Corrected Counts (dps)	Yield (% decimal)
1A	#1	27340	3600	32.94	0.10	7.59	73.38	0.92
1B	#2	27489	3600	31.80	0.10	7.64	73.78	0.92
2A	#3	27558	3600	31.52	0.10	7.66	73.96	0.93
2B	#4	27574	3600	32.48	0.10	7.66	74.00	0.93
3A	#5	27586	3600	33.24	0.10	7.66	74.04	0.93
Average FWHM				32.39	Average Yield			0.92
STD				0.73	STD			0.003

Table LLL. Data used for determining the FWHM and yield of ^{241}Am in a multinuclide solution using 100 μL of cerium concentration with 1000 μL of HF for 30 minute precipitation time at room temperature.

Detector	Trial #	Counts	Lifetime (sec)	FWHM (keV)	Detector Efficiency (% decimal)	Count rate (cps)	Corrected Counts (dps)	Yield (% decimal)
1A	#1	24134	3600	35.22	0.10	6.70	64.77	0.97
1B	#2	24290	3600	36.60	0.10	6.75	65.19	0.98
2A	#3	12452	1800	34.49	0.10	6.92	66.84	1.01
2B	#4	24167	3600	34.73	0.10	6.71	64.86	0.98
3A	#5	24295	3600	32.77	0.10	6.75	65.20	0.98
Average FWHM				34.76	Average Yield			0.98
STD				1.38	STD			0.013

Table MMM. Data used for determining the FWHM and yield of ^{239}Pu in a multinuclide solution using 100 μL of cerium concentration with 1000 μL of HF for 30 minute precipitation time at room temperature.

Detector	Trial #	Counts	Lifetime (sec)	FWHM (keV)	Detector Efficiency (% decimal)	Count rate (cps)	Corrected Counts (dps)	Yield (% decimal)
1A	#1	26514	3600	38.56	0.10	7.37	71.16	0.89
1B	#2	26352	3600	39.12	0.10	7.32	70.72	0.89
2A	#3	13292	1800	37.11	0.10	7.38	71.35	0.89
2B	#4	26965	3600	38.35	0.10	7.49	72.37	0.91
3A	#5	26529	3600	36.95	0.10	7.37	71.20	0.89
Average FWHM				38.02	Average Yield			0.89
STD				0.95	STD			0.008

Table NNN. Data used for determining the FWHM and yield of ^{241}Am in a multinuclide solution with 20mL of HCl and 5 μL of cerium concentration with 1000 μL of HF for 30 minute precipitation time at room temperature.

Detector	Trial #	Counts	Lifetime (sec)	FWHM (keV)	Detector Efficiency (% decimal)	Count rate (cps)	Corrected Counts (dps)	Yield (% decimal)
1A	#1	1385	333562.7	49.763	0.10	0.004	0.040117	0.00053
1B	#2	14455	333560.6	86.273	0.10	0.043	0.4187	0.00552
2A	#3	6838	333536.4	79.162	0.10	0.021	0.198082	0.00261
2B	#4	1775	333544.9	65.876	0.10	0.005	0.051417	0.00068
3A	#5	6831	333554.6	66.91	0.10	0.020	0.197869	0.00261
Average FWHM				69.597	Average Yield			0.0024
STD				14.00	STD			0.002

Table OOO. Data used for determining the FWHM and yield of ^{239}Pu in a multinuclide solution with 20mL of HCl and 5 μL of cerium concentration with 1000 μL of HF for 30 minute precipitation time at room temperature.

Detector	Trial #	Counts	Lifetime (sec)	FWHM (keV)	Detector Efficiency (% decimal)	Count rate (cps)	Corrected Counts (dps)	Yield (% decimal)
1A	#1	908	333562.7	37.86	0.10	0.003	0.026	0.00035
1B	#2	2403	33560.61	46.55	0.10	0.072	0.69	0.0092
2A	#3	1395	333536.4	45.04	0.10	0.0042	0.04	0.00054
2B	#4	657	33544.88	40.44	0.10	0.020	0.19	0.0025
3A	#5	2869	333554.6	44.20	0.10	0.0086	0.08	0.0011
Average FWHM				42.82	Average Yield			0.0027
STD				3.57	STD			0.0037

Table PPP. Data used for determining the FWHM and yield of ^{241}Am in a multinuclide solution with 20mL of HCl and 10 μL of cerium concentration with 1000 μL of HF for 30 minute precipitation time at room temperature.

Detector	Trial #	Counts	Lifetime (sec)	FWHM (keV)	Detector Efficiency (% decimal)	Count rate (cps)	Corrected Counts (dps)	Yield (% decimal)
1A	#1	462	178105.3	46.88	0.10	0.003	0.03	0.00032
1B	#2	653	178101.9	62.68	0.10	0.004	0.04	0.00045
2A	#3	3289	178088.1	73.12	0.10	0.018	0.18	0.0023
2B	#4	2641	178093.2	66.77	0.10	0.015	0.14	0.0018
3A	#5	749	178099.5	61.43	0.10	0.004	0.04	0.00052
Average FWHM				62.17	Average Yield			0.0012
STD				9.69	STD			0.0009

Table QQQ. Data used for determining the FWHM and yield of ^{239}Pu in a multinuclide solution with 20mL of HCl and 10 μL of cerium concentration with 1000 μL of HF for 30 minute precipitation time at room temperature.

Detector	Trial #	Counts	Lifetime (sec)	FWHM (keV)	Detector Efficiency (% decimal)	Count rate (cps)	Corrected Counts dps	Yield (% decimal)
1A	#1	530	178105.3	36.92	0.10	0.003	0.029	0.00038
1B	#2	244	178101.9	45.53	0.10	0.0014	0.013	0.00018
2A	#3	831	178088.1	47.74	0.10	0.0047	0.045	0.0006
2B	#4	855	178093.2	47.57	0.10	0.0048	0.046	0.00062
3A	#5	427	178099.5	35.32	0.10	0.0024	0.023	0.00031
Average FWHM				42.62	Average Yield			0.00042
STD				6.02	STD			0.00019

Table RRR. Data used for determining the FWHM and yield of ^{241}Am in a multinuclide solution with 20mL of HCl and 25 μL of cerium concentration with 1000 μL of HF for 30 minute precipitation time at room temperature.

Detector	Trial #	Counts	Lifetime (sec)	FWHM (keV)	Detector Efficiency (% decimal)	Count rate (cps)	Corrected Counts (dps)	Yield (% decimal)
1A	#1	170	47628.75	33.88	0.10	0.004	0.034	0.00044
1B	#2	199	47844.28	37.63	0.10	0.004	0.04	0.00051
2A	#3	74	47885.5	28.82	0.10	0.002	0.015	0.00019
2B	#4	186	47987.05	113.52	0.10	0.004	0.037	0.00048
3A	#5	240	48055.62	35.46	0.10	0.005	0.048	0.00061
Average FWHM				49.86	Average Yield			0.00044
STD				35.73	STD			0.00016

Table SSS. Data used for determining the FWHM and yield of ^{239}Pu in a multinuclide solution with 20mL of HCl and 25 μL of cerium concentration with 1000 μL of HF for 30 minute precipitation time at room temperature.

Detector	Trial #	Counts	Lifetime (sec)	FWHM (keV)	Detector Efficiency (% decimal)	Count rate (cps)	Corrected Counts (dps)	Yield (% decimal)
1A	#1	1888	47628.75	33.91	0.10	0.040	0.38	0.0051
1B	#2	1698	47844.28	36.63	0.10	0.035	0.34	0.0046
2A	#3	608	47885.5	40.28	0.10	0.013	0.12	0.0016
2B	#4	425	47987.05	41.48	0.10	0.0089	0.086	0.0012
3A	#5	666	48055.62	39.81	0.10	0.014	0.13	0.0018
Average FWHM				38.42	Average Yield			0.0029
STD				3.10	STD			0.0019

Table TTT. Data used for determining the FWHM and yield of ^{241}Am in a multi-nuclide solution with 20mL of HCl and 50 μL of cerium concentration with 1000 μL of HF for 30 minute precipitation time at room temperature.

Detector	Trial #	Counts	Lifetime (sec)	FWHM (keV)	Detector Efficiency (% decimal)	Count rate (cps)	Corrected Counts (dps)	Yield (% decimal)
1A	#1	231	7200	44.93	0.10	0.032	0.31	0.004
1B	#2	1516	7200	30.69	0.10	0.211	2.03	0.026
2A	#3	177	7200	24.42	0.10	0.025	0.24	0.003
2B	#4	213	7200	39.08	0.10	0.030	0.29	0.0036
3A	#5	166	7200	23.85	0.10	0.023	0.22	0.0028
Average FWHM				32.59	Average Yield			0.0078
STD				9.24	STD			0.01

Table UUU. Data used for determining the FWHM and yield of ^{239}Pu in a multi-nuclide solution with 20mL of HCl and 50 μL of cerium concentration with 1000 μL of HF for 30 minute precipitation time at room temperature.

Detector	Trial #	Counts	Lifetime (sec)	FWHM (keV)	Detector Efficiency (% decimal)	Count rate (cps)	Corrected Counts (dps)	Yield (% decimal)
1A	#1	2352	7200	35.49	0.10	0.33	3.16	0.042
1B	#2	17212	7200	33.59	0.10	2.39	23.10	0.31
2A	#3	2363	7200	36.08	0.10	0.33	3.17	0.042
2B	#4	2686	7200	34.23	0.10	0.37	3.60	0.048
3A	#5	1558	7200	41.88	0.10	0.22	2.09	0.028
Average FWHM				36.25	Average Yield			0.093
STD				3.3	STD			0.12

Table VVV. Data used for determining the FWHM and yield of ^{241}Am in a multi-nuclide solution with 20mL of HCl and 100 μL of cerium concentration with 1000 μL of HF for 30 minute precipitation time at room temperature.

Detector	Trial #	Counts	Lifetime (sec)	FWHM (keV)	Detector Efficiency (% decimal)	Count rate (cps)	Corrected Counts (dps)	Yield (% decimal)
1A	#1	6948	2400	38.32	0.10	2.9	27.97	0.35
1B	#2	8819	2400	35.21	0.10	3.68	35.50	0.45
2A	#3	5002	2400	60.44	0.10	2.08	20.14	0.26
2B	#4	7059	2400	43.68	0.10	2.94	28.42	0.36
3A	#5	8827	2400	36.39	0.10	3.68	35.54	0.45
Average FWHM				42.81	Average Yield			0.37
STD				10.38	STD			0.08

Table WWW. Data used for determining the FWHM and yield of ^{239}Pu in a multinuclide solution with 20mL of HCl and 100 μL of cerium concentration with 1000 μL of HF for 30 minute precipitation time at room temperature.

Detector	Trial #	Counts	Lifetime (sec)	FWHM (keV)	Detector Efficiency (% decimal)	Count rate (cps)	Corrected Counts (dps)	Yield (% decimal)
1A	#1	12407	2400	41.44	0.10	5.17	49.95	0.67
1B	#2	13294	2400	38.55	0.10	5.54	53.59	0.71
2A	#3	10525	2400	63.56	0.10	4.39	42.37	0.56
2B	#4	12325	2400	43.09	0.10	5.14	49.62	0.66
3A	#5	13296	2400	38.81	0.10	5.54	53.53	0.71
Average FWHM				45.09	Average Yield			0.66
STD				10.49	STD			0.06

BIBLIOGRAPHY

- Eichrom. "Analytical Procedures." Eichrom Industries, Inc. April 22, 2000.
- Eichrom Technologies, Inc. Cerium Fluoride Microprecipitation for Alpha Spectrometry Source Preparation of Actinides. Analytical Procedures, 2004.
- Friedlander, G. Nuclear and Radiochemistry. John Wiley & Son, Inc. New York; 1981.
- Hindman, F.D. "Neodymium Fluoride Mounting for Alpha Spectrometric Determination of Uranium, Plutonium, and Americium." *Analyt. Chem.* 59, 2556; 1983.
- Jia, Guo Gang. "Determination of Gross Alpha-Activity in Urine by Microprecipitation with LaF₃ and Alpha Spectrometry." *Journal of Radioanalytical and Nuclear Chemistry, Articles*, Vol. 178. No. 1: 11-18; 1994.
- Joshi, S.R. "Lanthanum Fluoride Coprecipitation Technique for the Preparation of Actinides for Alpha Particle Spectrometry." *J. Radioanal. Nuclear. Chem.-Art.* 90,409; 1985.
- Kristo, Michael. "U.S. and Russian Collaboration in the area of Nuclear Forensics." *Future of the Nuclear Security Environment in 2015: Proceedings of a Russian-U.S. Workshop.* 179-202; 2009.
- Lozano, J.C. "Preparation of Alpha-Spectrometric Sources by Coprecipitation with Fe(OH)₃: Application to Actinides." *Appl. Radiat. Isot.* Vol. 48, No. 3, pp. 383-389; 1997.
- "Millipore: 1225 Sampling Manifold." Millipore Corporation. 2000.
- Moody, Kenton James. Nuclear Forensic Analysis. Taylor & Francis Group, LLC. Boca Raton; 2005.
- Multi-Agency Radiological Laboratory Analytical Protocols (MARLAP); 2000.
- Pollanen, R. "Direct Alpha Spectrometry for Characterising Hot Particle Properties." *Radiation Measurements.* 42: 1667-1673; 2007.
- Raccio, Jeanne. "Cyclone Plus Storage Phosphor Screen Performance and Application Guide." PerkinElmer Life and Analytical Sciences. PerkinElmer, Inc. 2006.
- Sill, Claude W. "Preparation of Actinides for Alpha Spectroscopy without Electrodeposition." *Analytical Chemistry.* 53, 412-415; 1981.

Sill, Claude W. "Precipitation of Actinides as Fluorides or Hydroxides for High-Resolution Alpha Spectrometry." *Nuclear and Chemical Waste Management*. 7, 201-215; 1987.

Stock, Sherry. "Quantitative Comparison of Sample Preparation Methods for Low-Level Alpha Spectrometry." Master's Thesis. University of Nevada—Las Vegas. 2007.

VITA

Graduate College
University of Nevada, Las Vegas

Lyndsey Renee Kelly

Degrees: Bachelor of Science, Physics, 2007
Louisiana State University

Thesis Title: Optimization of the Microprecipitation Procedure for Nuclear Forensics
Applications

Thesis Examination Committee:
Chairperson, Ralf Sudowe, Ph.D.
Committee Member, Steen Madsen, Ph.D.
Committee Member, Phillip Patton, Ph. D.
Graduate Faculty Representative, Vernon Hodge, Ph. D.